

**EFFECT OF SEASONAL WATER FLUCTUATION UPON SOLUTE MOVEMENT  
WITHIN A POROUS MEDIA**

**A Thesis**

**Submitted to the College of Graduate Studies and Research  
in Partial Fulfillment of the Requirements  
for the Degree of**

**Masters of Science**

**in the**

**Department of Agricultural and Bioresource Engineering  
University of Saskatchewan  
Saskatoon, Saskatchewan, CANADA**

**By**

**Sleem Ali Kreba**

## **PERMISSION TO USE**

In presenting this thesis in partial fulfillment of the requirements for a Postgraduate degree from the University of Saskatchewan, I agree that the Libraries of this university may make it freely available for inspection. I further agree that permission for copying of this thesis in any manner, whole or in part, for scholarly purposes may be granted by the professor who supervised my thesis work, or in his absence, by the head of the department or the dean of the college in which my thesis work was done. It is understood that any copying or publication or use of this thesis or parts thereof for financial gain shall not be allowed without my written permission. It is also understood that due recognition shall be given to me and to the University of Saskatchewan in any scholarly use which may be made of any material in my thesis.

Requests for permission to copy or to make other use of material in this thesis in whole or part should be addressed to:

Head of the Department of Agricultural and Bio-resource Engineering  
University of Saskatchewan  
Saskatoon, Saskatchewan, S7N5A9, Canada

## ABSTRACT

Tracer methods are commonly used for estimation of soil water and groundwater recharge flux especially in arid and semiarid regions. These tracer methods are based on the solute profile shape (distribution of concentration with depth) and peak position. For soils of semi-arid to sub-humid climates, vertical water movement may seasonally vary in direction due to climate conditions and vegetative demands. The first objective of this thesis was to show that TDR (time domain reflectometry) can be a useful tool for estimation of soil water fluxes using tracer methods. The second objective was to study the effects of repeated cycles of directionally-varying flow upon solute profile shape and position used by tracer methods under controlled laboratory conditions. Three soil columns with a KCl tracer and Beaver Creek sand were used for this study. Rain and evaporative systems were used to cause the downward and upward soil water movements in the column, respectively. Soil moisture content and solute concentration were measured using TDR.

The result for the first objective was that the peak migration and the soil water balance methods gave similar average upward and downward soil water fluxes. This result indicates that the TDR method can be recommended for determination of soil water fluxes with tracer methods in fields or in laboratory studies for sufficient time and depth.

In the second objective, three different seasonal flow regimes were studied using the sand columns, and each flow regime simulated climatic seasons that might occur in the field. Several apparent and statistical parameters were used to evaluate the change of the solute profile shape and position under cycling conditions of the three different flow regimes. These parameters showed that the solute profile shape and position clearly changed under the three different repeated regimes of downward and upward seasonal flows. It was concluded that climate (seasonality) can have significant impacts on the estimation of soil water fluxes using tracer methods. The result from this investigation shows that the profile shape and position after a number of cycles (years of fluctuations) can provide a description of the previous climatic effects on the concentration profile. Therefore, the

profile shape can be used as an indicator of the flow regime that has affected the solute profile shape. Moreover, if a reference of a solute profile is available (a solute profile before a period of time), it is easier to determine the flow regime affected the profile shape and position by determining the change of the profile shape and position using statistical parameters presented in this thesis.

## **ACKNOWLEDGMENTS**

I would like to express my deep sense of gratitude to my supervisor, Professor Charles Maulé, whose expertise, understanding, and patience, added considerably to my graduate experience. I appreciate his vast knowledge and skill in many areas, and his assistance, guidance, support, and encouragement during my academic program. He provided me with direction, technical support and became more of a mentor and friend, than a professor. I doubt that I will ever be able to convey my appreciation fully, but I owe him my eternal gratitude.

I would like to thank the other members of my advisory committee, Professor Lope Tabil and Professor Terry Fonstad for the assistance, suggestions, and advises they provided at all levels of the research project. Finally, I would like to thank Professor Bing Si from the Soil Science Department, University of Saskatchewan, for taking time out from his busy schedule to serve as my external reader.

My sincerest gratitude and gratefulness to my family and my friends for the support they provided me through my entire life and in particular, I must acknowledge my mother Om-alsaad Alshween and my father Ali Kreba, without whose love, encouragement, and editing assistance, I would not have finished this thesis.

In conclusion, I recognize that this research would not have been possible without the financial assistance of the Libyan General People Committee of High Education (the Libyan Ministry of High Education) (scholarship), the Libyan Embassy (Cultural Section) in Canada, and the Saskatchewan Agriculture Fund (material). Also, I would like to thank my friends Abd-alslam Swise and Ine Herzog for helping me with the laboratory set up.

*Dedicated to.....*

*the loving of my mother "Om-alsaad Alshween" whose unending love and sacrifices inspired and encouraged me, my father "Ali Kreba" who instilled in me the value of education, my sisters and my brothers Ali, Ahmad, and Milad who supported me in this endeavor.*

## TABLE OF CONTENTS

PERMISSION TO USE .....	i
ABSTRACT .....	ii
ACKNOWLEDGMENTS .....	iv
TABLE OF CONTENTS .....	v
LIST OF TABLES .....	ix
LIST OF FIGURES .....	xii
LIST OF ABBREVIATIONS AND SYMBOLS .....	xvi
1 INTRODUCTION .....	1
1.1 Background .....	1
1.2 Objectives .....	3
1.3 Thesis organization .....	6
2 LITERATURE REVIEW .....	8
2.1 Semi-arid environments .....	8
2.2 Methods to estimate soil water fluxes .....	11
2.3 Using TDR in soil column and field studies .....	13
2.4 Estimating groundwater and soil water fluxes .....	16
2.5 Estimating groundwater recharge from tracer profiles .....	18
2.6 Seasonal flow fluctuation within unsaturated groundwater regime .....	19
3 MATERIALS AND METHODS .....	22
3.1 Column construction .....	22
3.2 Soil used in columns .....	23
3.3 Rain, evaporative, and drainage systems .....	24
3.4 Instrumentation .....	24
3.5 Column preparation .....	25
3.6 Determination of hydraulic and physical sand properties .....	26
3.7 Estimation of soil water fluxes .....	27

3.7.1 Peak migration method .....	27
3.7.2 Soil water balance method .....	28
3.8 Using and calibrating TDR readings .....	29
3.9 Expressing EC data at a reference temperature .....	31
3.10 Correcting EC data and simulations .....	33
3.11 Evaluating changes of profile shape and position .....	34
3.12 Measurement and experimental errors .....	39
3.13 Methods for objectives .....	39
4 RESULTS AND DESICCATION .....	41
4.1 Sand properties .....	41
4.2 Estimating soil water fluxes with tracers under controlled laboratory conditions.	43
4.2.1 Changes of soil moisture under upward and downward flow conditions ...	44
4.2.2 Changes of concentration and mass of salts under upward and downward flow conditions .....	47
4.2.3 Estimation of upward and downward fluxes .....	51
4.2.3.1 Peak migration method .....	52
4.2.3.2 Soil water balance method .....	53
4.2.3.3 Comparing the two methods .....	54
4.2.4 Summary .....	57
4.3 Investigating the effect of repeated cycles of directionally-varying flow upon tracer solute profile shape and position .....	58
4.3.1 Soil moisture content .....	59
4.3.1.1 Initial soil moisture .....	60
4.3.1.2 Change of soil moisture under cycling conditions .....	61
4.3.2 Concentration and mass of salts .....	63
4.3.2.1 Initial concentration and mass of salts .....	63
4.3.2.2 Change of concentration under cycling conditions .....	65
4.3.2.3 Change of dissolved salts under cycling conditions .....	66
4.3.2.4 Contribution of dissolved salts .....	68

4.3.3 Change of concentration profile shape and position under cycling conditions .....	69
4.3.3.1 The change of the solute profile shape and position under cycling of three different flow regimes .....	70
4.3.3.1.1 Downward flow = upward flow .....	70
4.3.3.1.2 Downward flow > upward flow .....	72
4.3.3.1.3 Upward flow > downward flow .....	74
4.3.3.2 Comparing the change of profile shape among the three columns and Summary .....	77
4.3.4 Estimating soil water fluxes under different regimes .....	81
4.3.4.1 Soil water fluxes in column 1 (downward flow = upward flow) .....	81
4.3.4.2 Soil water fluxes in column 2 (downward flow > upward flow).....	83
4.3.4.3 Soil water fluxes in column 3 (upward flow > downward flow) .....	85
4.3.4.4 Comparison of estimated fluxes among the three regimes and summary .....	87
5 SUMMARY AND CONCLUSIONS .....	91
5.1 Recommendations for future work .....	94
6 REFERENCES .....	97
APPENDIXES .....	108
Appendix A Calibration curves .....	108
Appendix B Estimating porosity under flow conditions .....	110
B.1 Estimating porosity under upward flow conditions .....	110
B.2 Estimating porosity under downward flow conditions .....	111
Appendix C Change of some soil water properties under upward and downward flow conditions .....	112
Appendix D Change of soil temperature, room temperature, and humidity during the cycling period .....	115
Appendix E The contribution of salt from the sand .....	116

Appendix F The change of some soil water properties under cycling conditions .....	121
Appendix G The change of the concentration profile shape and position under cycling conditions .....	124
Appendix H Correcting the solute profile shape .....	130
Appendix I Estimated upward and downward fluxes under different flow regimes ...	131

## LIST OF TABLES

Table 3.1	The variations of scenario, number of cycles, and experiment time for each column .....	40
Table 4.1	Physical and hydraulic sand proprieties among the three sand columns ....	43
Table 4.2	Conditions used for the first objective of evaluating the tracer method accuracy .....	44
Table 4.3	Changes in soil temperature (depth of 20 mm), evaporation rate and soil moisture before and during the evaporation period .....	45
Table 4.4	Peak location, peak concentration, average concentration and total mass of salts under upward and downward flow conditions .....	49
Table 4.5	Estimated upward and downward fluxes using the peak migration method	52
Table 4.6	Estimated upward and downward soil water fluxes using the soil water balance method .....	54
Table 4.7	The minimum, maximum and total soil moisture contents at initial conditions (before starting the cycles) .....	60
Table 4.8	The minimum, maximum, and change in total soil moisture contents during the study period and under the cycling conditions .....	62
Table 4.9	Comparing the three columns in term of peak concentration, peak depth, and total concentration and mass in the column before and after adding the tracer .....	64
Table 4.10	The variation and the change of average concentration under the cycling conditions in the three columns .....	65
Table 4.11	The variation and the change of total mass of salts under the cycling conditions in the three columns .....	67
Table 4.12	Change of the profile shape at completion of cycles for column 1 (downward seasonal flow = upward seasonal flow) .....	71
Table 4.13	Change of the profile shape at completion of cycles for column 2 (downward seasonal flow > upward seasonal flow) .....	73
Table 4.14	Change of the profile shape at completion of cycles for column 3 (downward seasonal flow < upward seasonal flow) .....	75

Table 4.15	Change of the profile shape at completion of cycles for the three columns (different regimes) .....	78
Table 4.16	Average upward and downward flows estimated using the peak migration method and the water balance method under the regime of downward flow = upward flow (column1) .....	82
Table 4.17	The variation of upward and downward flows estimated using the peak migration method and the water balance method under the regime of downward flow > upward flow (column 2) .....	84
Table 4.18	The variation of upward and downward flows estimated using the peak migration method and the water balance method under the conditions of upward flow > downward flow .....	86
Table 4.19	Average net soil water flux using the peak migration and the water balance methods in the three sand columns .....	88
Table B.1	The variation of estimated porosity under the upward flow conditions ...	110
Table B.2	The estimated porosity under the downward flow conditions using the peak location method .....	111
Table E.1	Total dissolved salts and the daily contribution rate of dissolved salts in each Sand column .....	117
Table E.2	The contribution of salts from sand to the solution measured in column 1 when it was left covered (no loss by evaporation or drainage) for a period of time .....	119
Table E.3	The contribution of salts from sand to the solution measured in column 2 when it was left covered (no loss by evaporation or drainage) for a period of time .....	120
Table E.4	The contribution of salts from sand to the solution measured in column 3 when it was left covered (no loss by evaporation or drainage) for a period of time .....	120
Table F.1	The change of total soil moisture, average concentration, and total mass of salts during the cycling period (taken after the evaporation period of each cycle) in column 1 (upward flow = downward flow) .....	121
Table F.2	The change of total soil moisture, average concentration, and total mass	

of salts during the cycling period (taken after the evaporation period of each cycle) in column 2 (upward flow < downward flow) .....	122	
<b>Table F.3</b>	The change of total soil moisture, average concentration, and total mass of salts during the cycling period (taken after the evaporation period of each cycle) in column 3 (upward flow > downward flow) .....	123
<b>Table H.1</b>	The observed and corrected concentration values in different depths in each column .....	130
<b>Table I.1</b>	The estimated upward fluxes (in each cycle) using the peak migration and soil water balance methods under the regime of equal upward and downward flows (column 1) .....	131
<b>Table I.2</b>	The estimated downward fluxes (in each cycle) using the peak migration and soil water balance methods under the regime of equal upward and downward flows (column 1) .....	132
<b>Table I.3</b>	The estimated upward fluxes (in each cycle) using the peak migration and soil water balance methods under the regime of downward flow greater than upward flow (column 2) .....	133
<b>Table I.4</b>	The estimated downward fluxes (in each cycle) using the peak migration and soil water balance methods under the regime of downward flow greater than upward flow (column 2) .....	134
<b>Table I.5</b>	The estimated upward fluxes (in each cycle) using the peak migration and soil water balance methods under the regime of upward flow greater than downward flow (column 3) .....	135
<b>Table I.6</b>	The estimated downward fluxes (in each cycle) using the peak migration and soil water balance methods under the regime of upward flow greater than downward flow (column 3) .....	136

## LIST OF FIGURES

Figure 1.1	Soil and groundwater definitions .....	2
Figure 1.2	KCl peak shape and location with three conditions of seasonal .....	5
Figure 3.1	The column with the rain, evaporation, and the draining systems with the TDR and the temperature loggers .....	23
Figure 3.2	Some parameters used to evaluate the change of the concentration profile shape .....	36
Figure 3.3	Skewed profiles to positive and negative values compared to standard normal distribution .....	37
Figure 3.4	Positive (peaked) and negative (flat) kurtosis distributions compared to standard normal distribution in term of kurtosis .....	38
Figure 4.1	The distribution of soil moisture as a function of depth under evaporative conditions .....	45
Figure 4.2	The distribution of soil moisture as a function of depth during the raining period .....	47
Figure 4.3	The change of distribution of concentration with depth under evaporation conditions .....	48
Figure 4.4	The change of the concentration distribution as a function of depth and time under the downward flow conditions (raining conditions) .....	51
Figure 4.5	Comparing the peak migration method and the water balance method in term of upward fluxes as a function of evaporation time .....	55
Figure 4.6	Comparing the estimated downward soil water flux using the peak migration method and the water balance method .....	56
Figure 4.7	The variation of average weekly room temperature and soil temperature (0.02 m depth) during the study period .....	59
Figure 4.8	The distribution of initial soil moisture before starting the cycles in the three columns .....	60
Figure 4.9	The variation of total soil moisture under the cycling conditions (time) in the three columns .....	62
Figure 4.10	The distribution of concentration as a function of depth in the three columns	

after adding the tracer followed by controlled flushing with distilled water to desired starting depth, before seasonal cycling began .....	64
Figure 4.11 The average concentration (not corrected for salt contribution by sand) as a function of time (cycles) for the three columns .....	66
Figure 4.12 Total mass of salts as a function of time (cycles) for the three columns ....	67
Figure 4.13 Shape of concentration profiles, corrected by subtracting the dissolved salts from soil, at different cycles for the regime of upward flow = downward flow (column 1) .....	72
Figure 4.14 The change of the concentration profile shape under the cycling condition of upward flow >downward flow (column 2) .....	74
Figure 4.15 The change of the concentration profile shape under the cycling condition of upward flow > downward flow (column 3) .....	76
Figure 4.16 Upward soil water flux using peak migration method and soil water balance method under the cycling conditions of upward flow being equal to downward flow (column 1) .....	82
Figure 4.17 Downward soil water flux using peak migration method and soil water balance method under the cycling condition of upward flow being equal to downward flow (column 1) .....	83
Figure 4.18 Upward soil water flux for each cycle under conditions of downward flow being greater than upward flow (column 2). The absence of values refers to zero flux .....	84
Figure 4.19 Downward soil water flux for each cycle under conditions of downward flow being greater than upward flow (column 2). The absence of values refers to zero flux .....	85
Figure 4.20 Upward soil water flux for each cycle under cycling conditions of upward flow being greater than downward flow (column 3). The absence of values refers to zero flux .....	86
Figure 4.21 Estimated downward soil water flux for each cycle under cycling conditions of upward flow being greater than downward flow (column 3). The absence of values refers to zero flux .....	87
Figure 4.22 Estimated upward flux using the peak migration method under each	

condition of upward and downward flows (under the condition of downward flow > upward flow, only 16 cycles were done). The absence of values refers to “zero” flux .....	89
Figure 4.23 Estimated downward flux using the peak migration method under each condition of upward and downward flows (under the condition of downward flow > upward flow, only 16 cycles were done). The absence of values refers to “zero” flux .....	89
Figure A.1 Calibration curve obtained using EC meter and TDR readings in order to calibrate the TDR readings .....	108
Figure A.2 Calibration curve obtained using EC meter and concentrations in order to calibrate the EC meter readings .....	108
Figure A.3 Observed and simulated change of concentration obtained using the SPSS .....	109
Figure C.1 The change of total soil moisture as a function of time in column 1 under the evaporation conditions (first objective) .....	112
Figure C.2 The change of total soil moisture with time in column 1 under the raining condition (first objective) .....	112
Figure C.3 The soil temperature (0.02 m depth) and evaporation rate as a function of evaporation time in column1 (first objective) .....	113
Figure C.4 Concentration profiles under the evaporation conditions in column 1 used to estimate the upward flux in the first objective .....	114
Figure D.1 Average soil temperature in different depths from the sand surface during the study period in column 1 .....	115
Figure D.2 Average room temperature and humidity during the study period .....	115
Figure E.1 Concentration in columns 1, 2 and 3 as a function of depth before (initial) and after (end) leaving the columns stagnant for 100, 94 and 96 days respectively .....	117
Figure E.2 Dissolved salt concentration as a function of time and depth in column 2 during 77 days of stagnant conditions .....	118
Figure E.3 The rate of dissolved mass of salts contributed by soil to the solution as a function of depth in the three columns .....	119

Figure G.1	The change of the solute profile shape under the cycling conditions of equal upward and downward flows (column 1) .....	124
Figure G.2	The change of the solute profile shape under the cycling conditions of equal upward and downward flows (column 1) .....	125
Figure G.3	The change of the solute profile shape under the cycling conditions of downward flow is greater than upward flow (column 2) .....	126
Figure G.4	The change of the solute profile shape under the cycling conditions of downward flow is greater than upward flow (column 2) .....	127
Figure G.5	The change of the solute profile shape under the cycling conditions of upward flow being greater than downward flow (column 3) .....	128
Figure G.6	The change of the solute profile shape under the cycling conditions of upward flow being greater than downward flow (column 3) .....	129

## LIST OF ABBREVIATIONS AND SYMBOLS

C	Concentration
CEC	Cation Exchange Capacity
CMI	Climate Moisture Index
dC	Change of concentration
dV	Change of voltage measured by TDR
EC <sub>t</sub>	EC at the measured temperature
EC	Electrical Conductivity
E	Evaporation
$\varepsilon_w$	Water dielectric coefficient
f <sub>t</sub>	Temperature-coefficient
Kurt.	Kurtosis
K <sub>sat</sub>	Saturated hydraulic conductivity
L	Column length
Max.	Maximum
Min.	Minimum
N	Number of observations
n	Porosity
PE	Potential Evaporation
P	Precipitation or rate of added water to the system
Q	Upward or downward soil water flux
R <sup>2</sup>	Coefficient of determination
SD	Standard Deviation
SEK	Standard Error of Kurtosis
SES	Standard Error of Skewness
Skew.	Skewness
TDR	Time Domain Reflectometry
t	Time
T	Temperature
V <sub>f</sub>	Constant voltage approached by the TDR signal

$V_0$	TDR input signal
$W$	Amount of water added to the system
WT	Water Table
Y	Observed value
$\bar{Y}$	Mean
Z	Depth from the sand surface
$\theta$	Volumetric water content
$\rho_b$	Bulk density
$\rho_p$	Particle density
$\Delta h$	Change of the hydraulic head across the system
$\Delta S$	Rate of the change of total soil moisture (storage)

## CHAPTER 1: INTRODUCTION

This chapter establishes the relevance of the subject area and provides a brief background and the importance of the research. The background includes the effect of climate on vertical soil water movement, the causes and the magnitude of unsaturated soil water fluxes beneath the root zone, and the definition of seasonality. The objectives of the study are also listed and explained. Thesis organization is provided in the end of the chapter to lay out the structure of the thesis in order to facilitate the task of understanding the presented material.

### 1.1 Background

For soils of semi-arid to sub-humid climates, vertical water movement may seasonally vary in direction due to climate conditions and vegetative demands. Canadian prairies, with its long cold winters, wet spring with snowmelts and warm dry summers with intense convective storms, can have distinct seasonal effects on water movement in the vadose zone between the bottom of the root zone (1.2 m depth) and a deep water table (>3 m depth) (Maule et al. 1993). Upward movement of vadose zone water can occur due to winter freezing (during winter, the ground may be frozen up to two meters in depth) (Maclean 1974) or due to summer drying caused by evaporation and plant transpiration. On the other hand, wet rain periods and/or spring snowmelt, will result in excess water moving downward through the soil and into the vadose zone.

Due to low precipitation and high evaporative conditions of the Canadian prairies, downward water flow past the root zone on agricultural fields is low, between 2 and 20 mm yr<sup>-1</sup> (Christie et al. 1985; Zebarth and de Jong 1989; Joshi and Maule 2000). Transported with these vadose zone water fluxes are nutrients (e.g., nitrates), dissolved salts (e.g., Mg<sup>+2</sup>, Na<sup>+</sup>, Cl<sup>-</sup>, SO<sub>4</sub><sup>-2</sup>), or various potential pollutants (excess nutrients, dissolved organics, insecticides). The rate of transport and the accumulation of nutrients, salts, and potential pollutants are of concern for any agricultural soil-groundwater system. In general, the groundwater zone is defined as the region below the root zone (1.2 m

depth); it includes the saturated and the unsaturated soils (Figure 1.1). The study of the process of flow and the solute transport within the vadose zone of semi-arid to sub-humid climates is difficult due to the unsaturated conditions and the slow rate of transport, relative to humid regions.

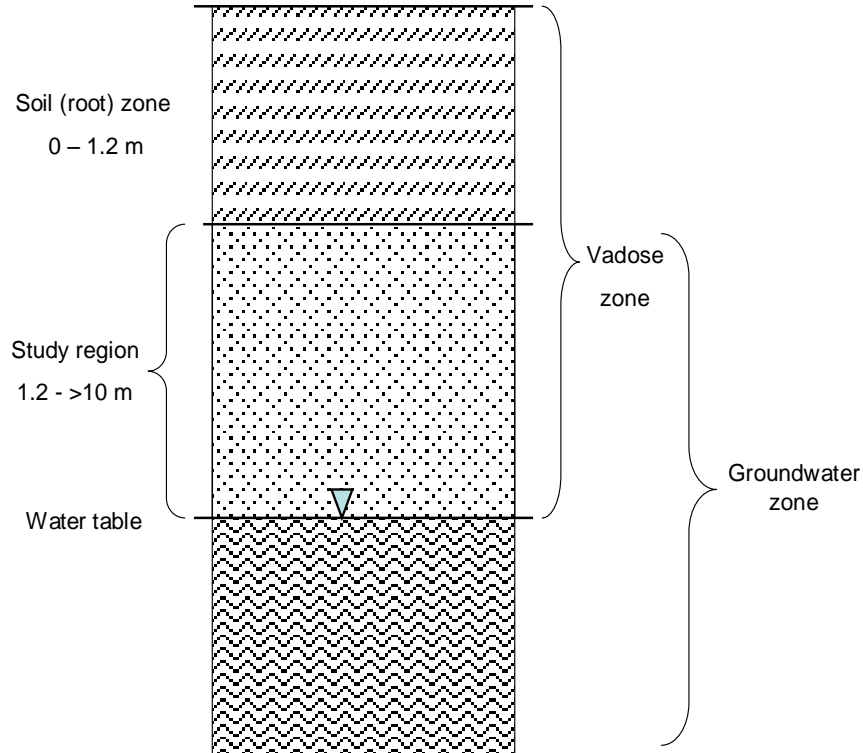


Figure 1.1: Soil and groundwater definitions.

One approach towards the quantification of unsaturated flow and solute transport in dry regions is the use of tracer profiles (Allison et al. 1994; Scanlon et al. 1997). The rate of downward movement is determined by the position of the tracer peak relative to time, concentration, and depth. As the Canadian prairies have distinctly upward and downward flow regimes that vary with seasons and annual climate variation (Maule et al. 1993), it is hypothesized that this seasonality will affect not only the net transport rate of tracers, but also the shape and concentration of the tracer profile. To date no literature has considered the effect of flow, seasonally varying in direction, upon tracer profiles. As this might not

only affect correct calculations of recharge rates but could perhaps enable further interpretation of tracer profiles, the study is focused upon this. The primary focus of this study is the seasonality of flow and flow direction and its affect upon solute concentration with depth. The method used for investigation of this study was time domain reflectrometry (TDR). Although TDR has been used to determine and investigate soil hydraulic properties (Ward et al. 1994; Buttle and Leigh 1995; Wang et al. 1998; Si et al. 1999; Lee et al. 2001; Noborio et al. 2006), no literature has been found that shows the application of TDR for estimation of soil water flux using tracer methods.

Studying the seasonal effects on deep unsaturated water movement in the vadose zone (i.e., that between the bottom of the root zone and the top of the water table) will improve understanding about the contribution and loss of water and solutes from the root zone, the process of soil salinization, and potential long term pollutant movement from prairie soils to the groundwater zone. Groundwater inflow and outflow can also strongly affect the water quality of wetlands. Wetlands recharging groundwater have low salinity water and can be easily distinguished from discharge wetlands that have high salinity water. As tracer profiles have become a more common way of studying recharge in deep unsaturated regimes (Allison et al. 1994; Scanlon et al. 1997; Dyck et al. 2003; Si and Kachanoski 2003), it is hoped that such a study will enable greater interpretation of field data. Also, understanding the relationship between the seasonal effects and soil water movement gives an opportunity to better determine the seasonal contribution of precipitation and snowmelt to the soil water and ground water systems and to evaluate the ground water recharge or to understand the effects of climate on the ground water recharge and discharge.

## **1.2 Objectives**

The primary purpose for this thesis was to study the effect of different seasonal flow regimes upon the distribution of the solute concentration with depth of the vadose portion of the groundwater zone (Figure 1.1) under controlled laboratory conditions. Although a laboratory study cannot simulate all field conditions, it does offer the

advantage of isolating a few important parameters and changing a complex system into something that can be easily studied. Some field conditions that can affect seasonal flow are climate variability, textural variability, plants, land use, and preferential flow paths. Additionally, solute transport from the soil to the groundwater vadose zone may take decades to occur or reach equilibrium given a land use change that affects water or solute input. As an initial study, it was proposed to focus upon a sandy soil (no preferential flow paths) of homogeneous density with depth and under controlled conditions of upward and downward fluxes that would enable 20 years of seasonal effects to be simulated within four months.

The general objective of the thesis is to study the effect of different flow regimes that seasonally vary in direction (upward vs downward) upon the tracer ‘profile’ shape and position (Figure 1.2). Profile shape refers to how solute concentration varies with soil depth. The seasonal flow regime can be defined as a number of different climatic seasons that occur within one year or ‘cycle’. In this study there are two different climatic seasons within each cycle, one of upward flow (caused by evaporation) and one of downward flow that occurs due to excess rain.

The study assumes that at depth within the soil profile (0.6 m for the lab columns, 1.5 to 5 m within field situations), there is a peak concentration that has occurred as the result of at least 20 years of seasonal flow regimes upon the profile shape.

The specific objectives of this study are:

1. To show that TDR (time domain reflectrometry) and tracer methods, used for field studies, can be successfully used for determination of hydraulic fluxes; and
2. To investigate the effect of repeated cycles (15-20) of directionally-varying flow upon solute profile shape and position used by tracer methods. This objective will help to investigate the following questions that occur with field data:
  - Can profile shape and/or profile position be used to indicate whether flow is dominantly upward or dominantly downward?
  - Do profile shape and/or position change with repeated cycles?

- What is the accuracy of the tracer method in determining long-term net flux values in deep unsaturated systems under directionally varying flow?

To meet the second objective of investigating the effect of numerous cycles of directionally-varying flow upon solute profiles using tracer methods, the following different seasonal flow regimes were studied:

- Downward seasonal flow = upward seasonal flow (15-20 ‘years’ where each year consists of two seasons, one of downward flow and another of upward at similar flow amounts);
- Downward seasonal flow > upward seasonal flow (15-20 ‘years’, where the downward flow is greater than the upward flow); and
- Downward seasonal flow < upward seasonal flow (15-20 dry ‘years’, where upward flow is greater than the downward flow).

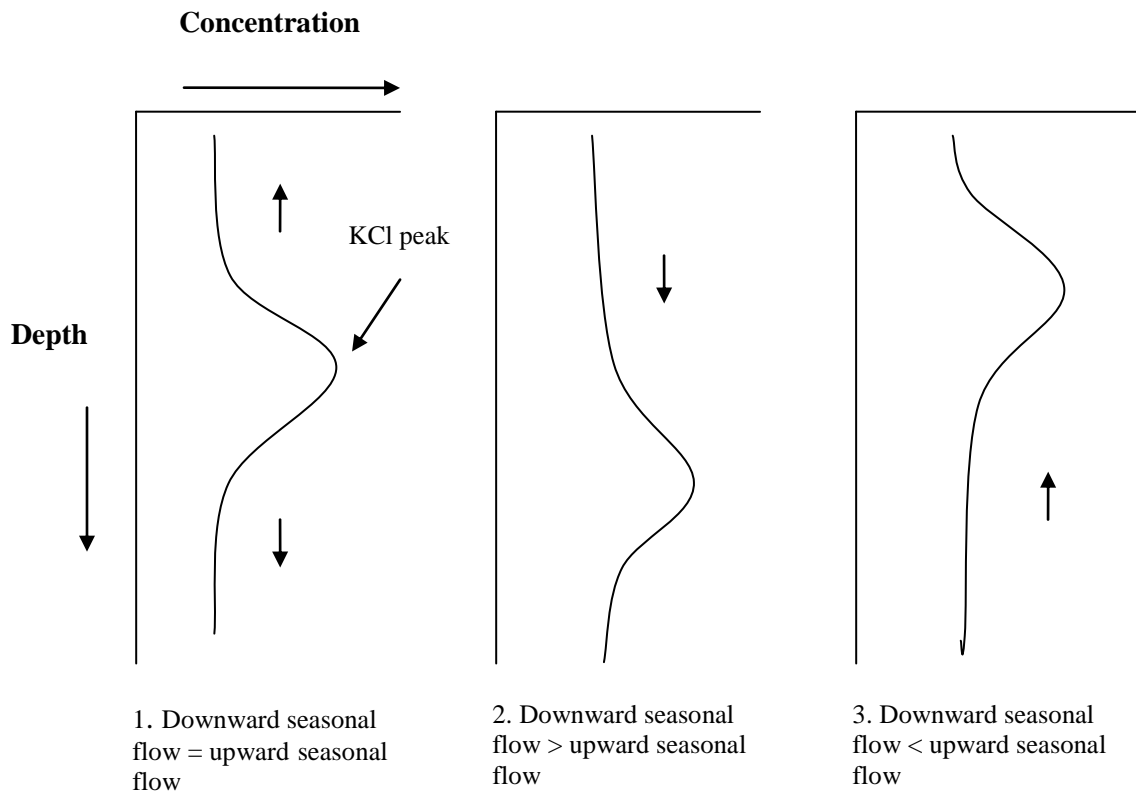


Figure 1.2: Hypothetical KCl peak shape and location with three conditions of seasonal flow.

The objectives were studied in the context of 1.05 m deep sand columns with KCl used as a tracer. The columns were maintained at moisture contents between saturation and field capacity. Water and the KCl solution were added using a drop sprinkler such that water or the solution were added evenly across the surface. Seasons involved small amounts of water added or removed over short periods of time; e.g. 60 mm depth in soil of rain (distilled water) added over several hours was the ‘wet’ season and 60 mm depth in soil of evaporation was the dry season. Thus ‘one year’ took between three to four days. TDR instrumentation installed in the column measured the moisture content and the electrical conductivity (EC) concentration ‘profile’ (Figure 1.2) at 20 mm depth intervals.

### **1.3 Thesis organization**

The thesis’ structure is summarized and listed below in order to facilitate the task of understanding the material presented subsequently:

- 1) Chapter 1: Introduction: This chapter shows the background of the subject area and presenting the importance of the research. The objectives of the study are also listed and explained.
- 2) Chapter 2: Literature Review: This chapter provides a broad overview of the available literature. The literature presented is related to specific topics including: classification of semi-arid environments, a review of methods for estimation of soil water fluxes, the use of TDR, tracer methods, and the fluctuation of seasonal flow below the soil root zone.
- 3) Chapter 3: Materials and Methods: This chapter describes the laboratory procedures for soil column construction and setup, and the analytical methods that were used in the study to investigate and measure solute flow in the soil columns.
- 4) Chapter 4: Results and Discussion: This chapter includes three sections: the physical, chemical, and hydraulic properties of the sand columns; determination and comparison of soil water fluxes; and investigation of the effect of repeated cycles of directionally-varying flow upon tracer profile shape and position. The third section provides a comprehensive discussion about: the change of soil

- moisture and concentration under cycling conditions; an evaluation of the change of the solute profile shape and position under cycling conditions, and estimation of soil water fluxes under cycling conditions.
- 5) Chapter 5: Summary and Conclusions: This chapter provides a summary of the major results and important conclusions. Some suggestions for recommendations and future work are also listed.

## CHAPTER 2: LITERATURE REVIEW

This chapter gives a broad overview of the available literature. The literature covers specific topics related to the application of unsaturated soil water fluxes. These topics include: classification of semi-arid environments, a review of methods for the estimation of soil water fluxes, using TDR in soil columns and field studies, using tracer techniques for determination of groundwater recharge, and seasonal flow fluctuation within unsaturated groundwater regime.

### 2.1 Semi-arid environments

Due to this study being based on soil water movement under semiarid climate conditions, a description of different climate regimes is provided. Some classifications of arid, semiarid, humid regions have been based on mean annual precipitation (Lloyd 1986):

- hyper-arid, 0-50 mm;
- arid, 50-200 mm;
- semiarid, 200-500 mm; and
- humid, > 500 mm.

Climate regimes may also be classified on the basis of precipitation/potential evaporation ratios (Potter 1992):

- arid is < 0.5;
- semiarid is 0.5-1.0; and
- humid is > 1.0.

Semiarid areas have been classified by Allison (1987) as receiving less than 700 mm per year of precipitation, and where native vegetation has often developed such extensive root systems that most of the precipitation is consumed by evapotranspiration.

The Canadian Soil System classifies the soil moisture regime as (Soil Classification Working Group 1998):

- Humid, slight soil water deficits in the growing season (25 to < 65 mm) or a CMI (Climate Moisture Index) of 74-84%;
- Sub-humid, significant deficits in the growing season having soil water deficit of 65 to < 130 mm or a CMI of 59 to 73%; and
- Semiarid, moderately severe deficits in the growing season, having a soil water deficit of 130 to < 190 mm or a CMI of 16% to 58%; (PET-P is 130-190 mm).

The CMI is defined as:

$$\text{CMI} = 100 * P / PE \quad (2.1)$$

The Canadian prairies, which account for about 80% of Canada's farmland, have the shortest frost-free period of any of the major agricultural dry land areas in North America.

To study the seasonal effects on soil water movement in the Canadian prairies, it is necessary to consider using a water balance method. The water balance method may be considered as similar to an accounting procedure where water inputs and outputs to the soil are algebraically added. It assumes that air temperature and day-length represent the energy required for evaporation and transpiration. Precipitation represents the water input and the soil moisture storage is regulated by assuming a maximum capacity based on the soil texture. Other operations regulate the water through the cycle for example, snowmelt, runoff, infiltration, and vegetative interception.

In the Canadian prairies, the average annual precipitation varies from 300 to 500 mm, being the lowest in the southwest near Lethbridge, Alberta, and the greatest in the eastern and northern extremities with approximately half of the yearly precipitation occurring during the growing season. Generally, two thirds of the precipitation is in the form of rain

with the remainder as snow (Steppuhn 1980; Dey 1982). Most of the rains occur between May and August (Bonsal et al. 1999). Much of the growing season rain is in the form of light showers although heavy rainstorms occur occasionally from mid June to early July and can wet much of the root zone (Bonsal et al. 1999).

During much of winter the ground is frozen often to depths surpassing 2 m (Maclean 1974) and any accumulated snow cover melting may not completely infiltrate due to reduced infiltrability of the frozen soil (Granger et al. 1984; Gray et al. 1986).

The observed snowfall and the accumulation of the snow cover throughout a particular area differ due to the physical nature of the receiving surface. Variability in the snow cover of a particular area can be caused by interception evaporation and wind action. The density of the vegetative cover can cause variability of the amount of intercepted snow. Snowmelt occurs when there is sufficient heat transfer from external sources, for example, observed solar radiation, net long wave radiation, convection, release of latent heat transfer conduction, and heat from rain water. The characteristics of the snowpack can also be important. However, the air temperature can serve as an index of the many heat transfer processes, and melting is dependent on all terms of the energy complex, not just air temperature, and the average air temperature at which melting begins varies seasonally (Ripley 1988).

Estimated potential evapotranspiration over the prairies ranges from 500 to 900 mm annually and gives the region its semiarid character. Extreme temperatures vary between 43°C in summer and -48°C in winter (Dregne and Willis 1983). Most of the region has between 80 and 100 frost-free days. January is generally the coldest month with average daily temperatures ranging from -15°C to -10°C and July the warmest with average daily temperatures of 16°C to 20°C. Therefore, the prairie climate is distinctly seasonal, consisting of cold winters and warm summers.

As a consequence of this climatic pattern in the Canadian prairies, soil moisture accumulates from about September to May and is then rapidly lost, along with summer

rains, by evapotranspiration between May and September (van Der Kamp and Maathuis 1991).

## 2.2 Methods to estimate soil water fluxes

In arid and semiarid regions, both physical and chemical methods have been used to estimate the soil water fluxes. Chemical methods are more accurate than physical methods (water balance and Darcy flux approaches) in determining the groundwater recharge in dry regions (Gee and Hillel 1988; Allison et al. 1994; Scanlon et al. 1997). Physical methods, which are based on hydrological parameters, are problematic because in arid and semiarid regions, the fluxes are low and very variable in both time and space, and changes in hydrological parameters are small and difficult to detect (Gaye and Edmunds 1996; Salle et al. 2001). The downward water movement in arid and semiarid regions is low because of low precipitation rates and high evapotranspiration rates, so the ratio of annual recharge to total volume of the aquifer is often small. The disadvantage with physical methods under these conditions is that measurements are required for several years to obtain a reliable estimate of mean values, and a large number of sampling locations are required to assess recharge variability due to variation in topography and soil texture (Allison et al. 1994).

Both natural (environmental) and applied chemical tracers have been used in obtaining quantitative estimates of soil water fluxes. Marshall and Holmes (1979) described natural tracers as tracers that are not added artificially to the aquifer or soil water, but occur naturally as a peculiar feature of the hydrological cycle. Applied tracers are those injected into the aquifer or soil water system for purpose of experiments. Since natural systems are voluminous and travel times are long, applied tracers may not always be the best method (Joshi 1997). Therefore, the use of natural tracers has been more common in estimating soil water fluxes. Stable oxygen and hydrogen isotopes have been used in groundwater studies to investigate recharge, mixing, ground water/surface water interaction, advective-diffusive transport, paleohydrogeologic interactions, and to estimate groundwater ages (Harvey 2001).

Scanlon et al. (1997) stated that using environmental tracers to quantify unsaturated flow is more appropriate than physical approaches because hydraulic conductivity can vary over orders of magnitude. However, both approaches should be used because physical data provide information on current processes, whereas environmental tracers provide information on longer term net water fluxes. A variety of environmental tracers should also be used because some are restricted to liquid phase flow (chloride and chlorine-36), whereas others are found in liquid and vapor phases (tritiated water). Bekele et al. (2006) studied the effects of changing the vegetation cover on groundwater recharge and also stated that several recharge estimation techniques are required for better understanding of recharge processes and evaluation of recharge.

Natural tracers can represent a spatially uniform input to the soil water and groundwater system. The most commonly used natural tracers in recharge studies are tritium, carbon-14, chlorine-36, nitrogen-15, oxygen-18, deuterium, carbon-13, and chloride. Deuterium, tritium, and oxygen-18 may be expected to simulate water movement more accurately since they are form part of the water molecule itself. Tritium may be subject to vaporization under very dry conditions (Allison 1987). In most soils, chloride and nitrate move as the water does but anion exclusion may be a problem in soils with high clay content. Chlorine-36 may be useful for studying low recharge rates due to its long half life (300,000 years), though it has not been employed frequently due to lack of analytical facilities (Allison 1987). An advantage of tracers is that they integrate all of the processes that combine to effect water flow in the unsaturated zone. A tracer's behavior is generally a much more robust indicator of water movement in a porous medium than is the solutions of the equations of water flow, especially when soils are relatively dry (Allison et al. 1994). Gaye and Editor (2001) suggest that isotope techniques are particularly effective for identifying the sources of salinity and the inflow of fresh groundwater. Allison and Hughes (1978) and Gaye and Edmunds (1996) both state that the agreement between estimates of recharge using chloride and tritium suggests that both tracers' behavior represents a very good indicator of water movement in unsaturated porous media, and the chloride method represents the most widely applicable and most reliable

technique for recharge estimation in semiarid regions. Compared with tritium, chloride has the advantage of simple analysis, but information about fallout and land use changes at the sampling sites is essential. Danquigny et al. (2004) used NaCl in laboratory experiments to define effective hydraulic conductivity and macrodispersivity.

Hsieh et al. (1998) stated that the oxygen isotopic composition of soil water provides an extra quantitative dimension in water balance analysis which allows separation of evaporation from transpiration. Landon et al. (1999) used stable oxygen and hydrogen isotopes to compare two different methods, suction lysimeters and wick samplers, of collecting soil water in the unsaturated zone of sand and gravel aquifer.

As a summary, both physical and tracer methods have been used to determine and study the groundwater and soil water fluxes; however, tracer methods are recommended especially in arid and semiarid environments because the soil water fluxes are low, very variable, and chemical methods are easier to use. Other advantages of using tracer methods are that natural tracers can represent a spatially uniform input to the soil water and groundwater systems and some tracers are part of the water molecule or travel with water. However, there are several disadvantages of using tracer methods. For example, changing land use can effect the determination of the soil water and groundwater fluxes. Also, using some of the tracers may face the problem of anion exchange or exclusion in soils with high clay content. Using natural tracers requires long-term records of rainfall chemistry and/or of landuse. Determining the groundwater recharge using tracer methods may be influenced by seasonality because seasonality may affect the downward flow rates and shape and concentration of the tracer profile; therefore, the purpose of this study is to study these seasonal effects on soil water movement under laboratory conditions.

### **2.3 Using TDR in soil columns and field studies**

TDR has been used by previous researchers to simultaneously measure both soil water content and electrical conductivity (EC). There are several traditional techniques for measuring the soil water content. Although gravimetric sampling for water content is

the most accurate method, soil samples must be removed from a soil mass. Widely accepted in situ methods to measure soil water content are radioactive methods such as the neutron scattering method and the gamma ray attenuation method. However, these methods require some calibration and special caution to avoid possible health hazards.

Time domain reflectometry has become an established method to measure both soil volumetric water content and bulk soil electrical conductivity. It is based on measuring the travel time and the attenuation of the amplitude of an electromagnetic pulse launched along a transmission line of unknown length embedded in the soil. Time domain reflectometry is a less-destructive and more cost-effective method enabling continuous readings at different soil depths (Vanclooster et al. 1996). According to Robinson et al. (2003), the underlying success of these techniques can be considered in two parts. First of all, the equipment's ability can accurately measure the bulk dielectric permittivity and electrical conductivity of a material. Second, there is a close relationship between the measured dielectric permittivity and the volumetric water content, and between the ionic concentration and the bulk electrical conductivity of the material. Using TDR, water content measurement is only slightly susceptible to changes in soil bulk density, temperature, and salinity (Topp et al. 1980). Sabburg et al. (1997) found a dependency for volumetric water content on soil bulk density for swelling clay soils, but not for non-swelling soils. Wraith and Baker (1991) suggested that TDR usually does not require site-specific calibration because it is nearly insensitive to variations in bulk density, mineral composition, and salinity. Nadler et al. (1991) used time domain reflectometry for simultaneous measurement of soil water content and bulk soil electrical conductivity for uniform and layered soil profiles in the laboratory. They stated that volumetric soil water contents were found to be accurately determined by the TDR method except in the case of very dry soil overlying very wet soil. This may be attributed to the difficulty in interpreting the TDR trace and not to the basic principles of the TDR technique. Zhang and van Geel (2007) studied the use of TDR to measure vertical moisture content profile in a soil column. They found a good agreement between moisture content measurements taken by vertical and horizontal TDR probes in the soil column under various drainage conditions.

In addition, the TDR has been widely used to measure soil salinity (Ward et al. 1994; Ferre et al. 1998; Amente et al. 2000; Vogeler et al. 2000). To measure salinity, TDR provides a simpler method of monitoring than traditional methods involving soil extracts. Traditional techniques for solute concentration measurements (e.g., soil coring and solution extractors) are usually inappropriate for obtaining high quality data with good spatiotemporal resolution. For this reason, time domain reflectometry (TDR) has become increasingly popular as it allows for continuous and simultaneous measurements of the soil water content and the electrical conductivity of the soil solution (Ritter et al. 2005).

“When the tracer is a saline solute, and for certain temperature conditions and low background salinities, changes in EC can be linearly related to changes in the solute concentration” (Ritter et al. 2005). Ritter et al. (2005) used TDR and bromide as a tracer to analyze solute transport in volcanic soils. They stated that bromide resident concentrations were monitored successfully with TDR technology. They also stated that one limitation with TDR is in accurately measuring electrolyte concentrations at low soil moisture conditions, which may be observed in sandy profiles. This should be less problematic for finer textured soils, but these soils generally have much larger anion-exchange capacity, which may limit the usefulness of independently derived functions relating solute concentration and TDR-measured electrical conductivity. Jury and Roth (1990) stated that solute concentration can be classified as resident concentration and flux concentration. They defined the resident concentration as “the mass of solute per unit volume of soil” and the flux concentration for one dimensional flow as “the ratio of solute mass flux to the water flux”. Si and Kachanoski (2003) stated that the solute concentration measured by soil coring or horizontally installed TDR probes is the resident concentration, and the outflow concentration from a soil column is the flux concentration.

Moreover, TDR can be used to determine other soil hydraulic properties such as solute transport. Ward et al. (1994) stated that measurement of solute transport at different depths in layered soil columns using TDR and KCl as a tracer, provides more information

than traditional outflow measurements. They found that the measurement of volumetric water content and subsequent calculation of bulk soil electrical conductivity are sufficient to obtain transport parameters for homogeneous soils and packed columns or multidimensional flow cells. Buttle and Leigh (1995) used  $^{18}\text{O}$  and Cl with TDR and laboratory columns to study the influence of macropores on meltwater infiltration through the unsaturated zone. Hart and Lowery (1998) suggest that instantaneous loading may be estimated using TDR with a relative error of about 10 to 30% if the flow fields are correctly identified. Wang et al. (1998) used TDR and tensiometers during field tension infiltrometer experiments to provide simultaneous measurements of soil water content, tension, and transient infiltration rate.

As a summary, TDR has been used widely in laboratory and field studies to measure the soil water content, electrical conductivity, and other soil hydraulic properties. TDR has the advantage of allowing for continuous and simultaneous measurements of the soil water content and the electrical conductivity, and it usually does not require site-specific calibration. However, TDR is not accurate for measuring soil water content in very dry overlying very wet soils, and there is a limitation with measuring electrolyte concentration at low soil moisture conditions and large CEC.

## 2.4 Estimating groundwater and soil water fluxes

TDR and/or tracers have been used to determine and study groundwater and soil water fluxes. Groundwater is increasingly being used as a water source. As the world's population is growing, concerns are being raised about the overall health of this water and the possibility of contamination. The term "recharge" has been generally used to describe downward water movement in the unsaturated zone; however, in thick unsaturated sections where water is moving slowly, it may be impossible to determine whether downward moving water in shallow depths will recharge the aquifer at deep depths. To avoid the problem of using the "recharge" term, "infiltration" can be used to refer to water movement from the surface into the subsurface and "percolation" or "drainage" to refer to penetration of water below the shallow subsurface, where most

evapotranspiration occurs. “Recharge” is restricted to situations where it is likely that the water reaches the water table. Although the terms “percolation” and “recharge” imply downward water movement, determining short-term direction of water movement is often difficult. In these situations, “water flux” is better because it implies no particular direction.

To estimate local recharge, some techniques rely on measurements in the unsaturated zone and others in the saturated zone. In semiarid areas, measurements in the unsaturated zone need to be made below the zone where uptake of water by roots is significant. Different tracers have been used to determine the groundwater recharge. Gaye and Edmunds (1996) used environmental chloride, deuterium, oxygen-18, and tritium in deep sand profiles in Senegal to estimate their relative value for measuring groundwater recharge. They reported that chloride has the advantage over tritium of simple analysis and of being conserved during the recharge process so that a mass balance approach can be used. However, the chloride technique is limited by the need to have long-term records of rainfall chemistry. They found that using the three-year average data for rainfall, a mean value of  $31.7 \text{ mm yr}^{-1}$  for the two profiles based on chloride is slightly higher than the average for the two tritium profiles ( $24 \text{ mm yr}^{-1}$ ). Nakayama et al. (1973) studied the movement and accumulation of chloride at shallow depths in a bare soil following irrigation under field conditions. Gee and Hillel (1988) stated that lysimetry and tracer tests offer the best hope for evaluating recharge at arid and semiarid sites, and tracer tests using long-lived tracers as  $^{36}\text{Cl}$  or stable isotopes ( $^{18}\text{O}$ , deuterium) can provide qualitative estimates of recent recharge at a given site.

Tracers and/or TDR have been widely used to study the factors which can influence the groundwater recharge in semiarid regions. TDR and tracers can be used to determine the effect of preferential solute transport on groundwater recharge. For example, Magesan et al. (2003) used TDR with Br and Cl as tracers with undisturbed soil columns to determine the extent of preferential solute transport in the topsoil. They suggested that the TDR data also can be used to look at the depth dependence of the transport properties. The effect of changing land use on the groundwater recharge can be studied using tracers. Allison and

Hughes (1983) used chloride, tritium, oxygen-18, and deuterium to study the effect of changing land use from Eucalyptus scrub to cropping with wheat on the mechanism of the movement of soil water and the amount of deep drainage in semiarid area of southern Australia. Tracers and TDR has been used to determine the recharge from depressions. Derby and Knighton (2001) used granular potassium chloride and TDR to investigate depression-focused recharge and to monitor solute movement through the vadose zone into the shallow groundwater in southeastern North Dakota. Seasonal contribution of precipitation, also, was investigated using tracers. Maule et al. (1992) used deuterium and oxygen-18 to study the seasonal contribution of precipitation (snow and rain) to soil water and groundwater in the Canadian prairies. Edmunds et al. (2002) used stable isotopes, radiocarbon, and major and trace elements to determine the natural baseline conditions, the extent of any contamination and the effectiveness of the overlying aquitard seal; they were capable of determining the groundwater age. Onodera and Kobayashi (1995) investigated the seasonal variation in the transport of Br<sup>-</sup> through macropores, mesopores, and micropores in a forest soil. They found that the flux estimated by using the water balance was similar to the results by the tracer method.

The upward movement of the soil water under semiarid conditions has been also studied and in some of these studies, TDR and/or tracers has been used. Marshall and Gurr (1954) studied the movement of chlorides in soil packed in shallow cups from which water was allowed to evaporate. They found that chlorides moved from the lower to the upper halves of the cups in soils that were as dry as the wilting percentage. Also, they concluded that water can move in the liquid phase throughout the whole range in which it is available to plants. Stephens (1993) suggested that where soil water fluxes are very low, upward vapor phase transport may be significant in quantifying recharge. Warner et al. (1997) used TDR to study the upward movement of water into the root zone from shallow water tables, and they concluded that upward fluxes are a significant contribution to soil water available for plant growth and should not be ignored.

## **2.5 Estimating groundwater recharge from tracer profiles**

Three techniques have been suggested (Allison et al. 1994) for estimating recharge rate from tracer profiles in the unsaturated zone: 1) from the total amount of tracer stored in the profile; 2) from the shape of the tracer profile in the soil; and 3) from the position of the tracer peak (the peak migration method). For this column study, it was not possible to determine the soil water fluxes using the first technique; there is insufficient information within the literature for the second technique and thus, just the peak migration method is considered in this review.

The peak migration method is based on the argument that a volume of water equal to that present above the peak at the time of sampling has been displaced. This method relies on steady-state flow and spatially uniform solute input assumptions (Joshi and Maule 2000). The peak method has been used mostly to estimate recharge fluxes from tritium data (Smith et al. 1970; Allison and Hughes 1974; Gaye and Edmunds 1996) because the number of years elapsed since 1963 is known. Piston flow through the unsaturated zone is assumed (Daniels et al. 1991). Annual precipitation is assumed to be infiltrating as a slug and that it vertically displaces residual precipitation from the preceding year. Since tritium originates in the atmosphere and is deposited with precipitation, a low-high-low tritium profile will be recognized in the field. This reflects the movement of peak tritium concentration in the soil through time. The moisture content is taken as the average moisture content from the ground surface to the peak depth (Wood et al. 1997). However, most studies do not specify how the moisture content was calculated (Ward 2003). Potential problems with this method are the violation of the piston flow assumption and the absence of a distinct tritium peak (Allison et al. 1994).

## **2.6 Seasonal flow fluctuation within unsaturated groundwater regime**

In semiarid regions, annual groundwater fluctuations have been monitored, and they are commonly considered as evidence of recharge. The water-table fluctuation method may be the most widely used technique for estimating recharge; it requires

knowledge of specific yield and changes in water levels over time (Healy and Cook 2002). However, groundwater levels may change as a result of natural causes other than recharge such as changes of barometric pressures, lunar and solar tides, and other factors. ZebARTH et al. (1989) stated that the annual fluctuation of the water table in the sloughs in Saskatchewan, Canada, is in the order of 2 m. Fullerton et al. (1987) studied the seasonal salt and water fluxes into black Solonetz soils at two sites in east-central Alberta, Canada, and they described the groundwater dynamics in Canadian prairies. They reported that groundwater recharged from May to August, discharged from September to December and was lateral from January to March. Therefore, in general, the water tables were closest to the soil surface during or immediately following periods of high precipitation, under recharging or lateral groundwater flow conditions when all horizons had temperatures above 0°C (May to November). They also suggested that the addition of salt and moisture into the soil zone resulted from capillary movement from the water table, and values for moisture content and soil salinity are related. They concluded that capillary movement and evaporation were the major means by which the salt became transported, concentrated, and deposited during the warmer months. Moreover, from December to March when soil temperatures were below 0°C, maximum moisture content and salt concentrations were recorded in the soil pedons. Water moved upwards from the water table towards the freezing zone depositing salts upon freezing.

As another example of annual groundwater fluctuation studies, Armstrong et al. (1996) studied the seasonal changes in the distribution of salt and water in fields of both arable and grassland saline sodic clay soils under rainfed conditions, and they used soil columns to investigate leaching of topsoils during winter rains. They concluded that during winter rains, the water moving through the macropores uniformly leached salt from the soil profile to a depth of 1.2 m, but in late summer the salt content of the grassland and arable soils had increased again by 11% and 35%, respectively compared with their early spring salinity levels. Therefore, they stated that the salt leached in winter was not lost, but leached below 1.2 m, only to rise again as the soil profile dried in the summer.

Annual groundwater fluctuations are not always related to groundwater recharge. For instance, van Der Kamp and Maathuis (1991) studied the long term hydrographs for deep confined aquifers in southern Saskatchewan, Canada. They found that annual fluctuations were characterized by a gradual rise in head from October to May/June and a rapid drop from May/June to October. They stated that these fluctuations are distinctly different from the seasonal fluctuations observed in surficial and shallow semi-confined aquifers which reflect the response of these aquifers to recharge derived from snowmelt and early spring rains. This pattern of hydraulic head fluctuations observed for the deep confined aquifers and theoretical considerations do not reflect recharge to the aquifer by transient flow through the confining layer, but instead it reflects changes of the total mechanical load on the aquifer-aquitard system, mainly because of changes in total soil moisture, snow, and groundwater storage at the water table. They concluded that the loading effects have to be taken into account in any analysis of seasonal changes in groundwater levels.

In summary, the annual soil water fluctuation has been investigated in field studies and it was taken as evidence of groundwater recharge. However, some literatures have shown that the water table fluctuation does not reflect the groundwater recharge. Also, the effect of seasonality on the soil water movement under laboratory conditions of different upward and downward regimes has not been considered and it needs to be studied.

## CHAPTER 3: MATERIALS AND METHODS

This chapter provides detailed description on the laboratory procedures for soil column construction and setup including; fabrication and use of rain, drainage, and evaporative systems, instrumentation, and column preparation. It also gives a description on the analytical methods that were used in this study to carry out the conclusions. These methods include: determination of sand properties, estimation of soil water fluxes, using and calibrating TDR readings, correcting and simulating EC data, and evaluating changes of the solute profile shape and position. In the end of the chapter the expected measurement and experimental errors are discussed.

### 3.1 Column construction

The research of this thesis is entirely based upon solute transport in a sand column within controlled laboratory conditions. Three (PVC pipes) columns were used for this study. Each column was 1.2 m length, and 0.25 m in diameter. Each column was sealed in the bottom except a hole for drainage. The columns were set on stands, so the bottom was approximately 0.43 m high from the floor. The sand at the upper end was exposed to allow water addition by a sprinkler system or losses by evaporation. Approximately 50 pairs of TDR probes were installed in each column spaced at 20 mm intervals with depth. The TDR probes were inserted through pre-drilled holes in the plastic of the column. The holes were 3.2 mm in diameter and the horizontal distance between each rod in a pair was 12 mm. The holes were made on helical form on the column to avoid the influence of each other with regards to water and solute flow. The horizontal offset angle between each successive pairs was 10 degrees. Several large holes (30 mm in diameter) were made in the top 100 mm of each column, above the sand surface, to allow the air to enter above the soil surface to better enhance evaporation from the sand surface (Figure 3.1).

### 3.2 Soil used in columns

Beaver Creek sand was chosen for this study. Beaver Creek sand has been widely used for laboratory studies at the University of Saskatchewan, Canada (Wilson 1990; Bruch 1993). This sand was so chosen to better control soil porosity and pore size distribution and to avoid cracks and aggregates, such as would occur with soils with any clay content. This sand was located southeast of Saskatoon, Saskatchewan, Canada. This olive brown oxidized fine to medium sand was dried for several days then sieved using a 2 mm screen (sieve).

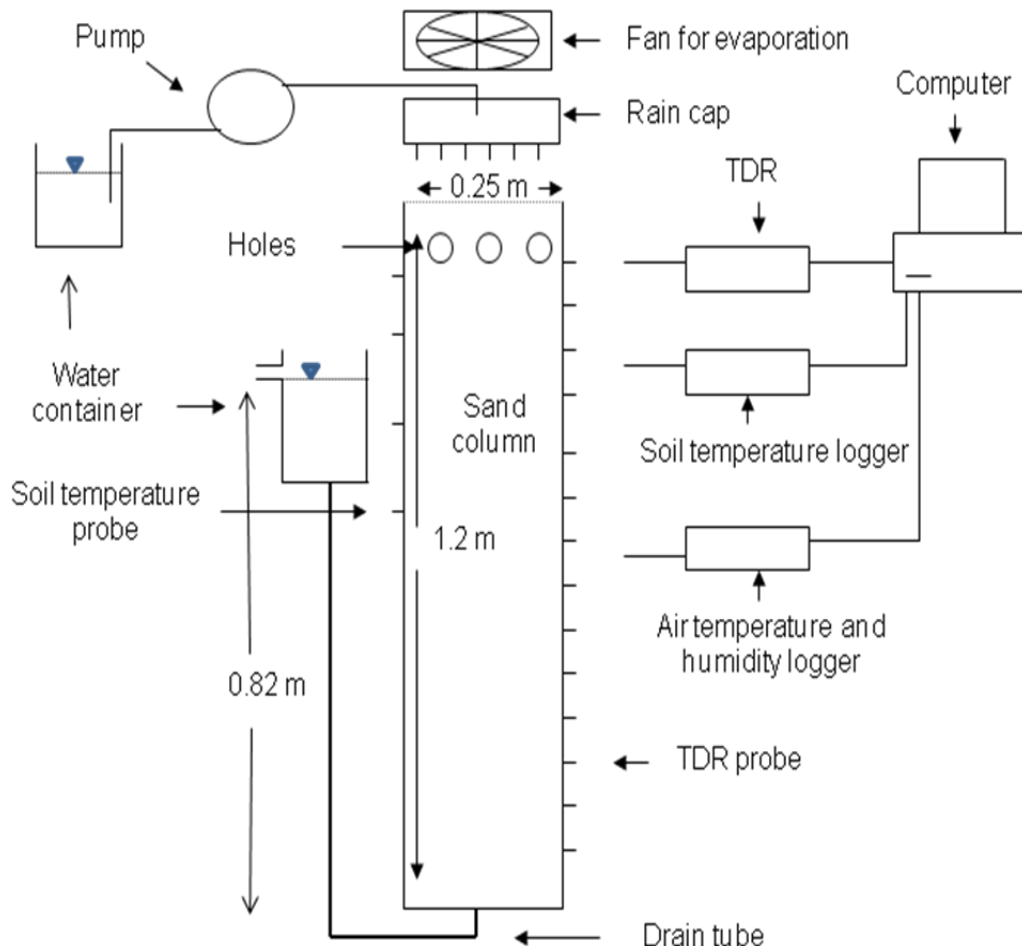


Figure 3.1: The column with the rain, evaporation, and the drainage systems with the TDR and the temperature loggers.

### **3.3 Rain, evaporative, and drainage systems**

Rain, evaporative, and drainage systems were made and used with the columns (Figure 3.1). For ‘rain’ water, a tube pump was used to supply the water to a rain cap. The rain rate was set by controlling the speed of the pump. The rain cap was designed to add the water equally distributed to the sand surface of the column. The rain cap was 0.25 m in diameter with water received in a top inlet and water outflow through numerous equally spaced 0.5 mm (i.d.) needles. The tube pump insured a constant rate of water application through the needles.

Evaporation was used to cause upward movement of soil water. To evaporate the water from the sand surface, a 90 mm diameter fan placed within a 0.25 m diameter plastic dish was located on top of each column. Fan speed could be controlled and varied between 380 and 3270 RPM.

A tygon tube of 9.5 mm diameter was used for draining the water from the columns. The tube outlet was maintained in a container of water located beside the sand column. This tube was used to initially saturate the sand columns from the bottom, and to control the water level in the sand columns at a height of 0.32 m.

### **3.4 Instrumentation**

Four soil temperature probes were located at depths of 20, 50, 200, and 500 mm. The soil temperature was recorded every hour using a soil temperature logger. Later these values were used to correct TDR measurements and helped with evaporation interpretation. The air temperature and relative humidity in the room were also recorded hourly by another logger with two probes. One of these probes was located immediately above the sand surface during the evaporation period, and the other probe was located in the centre of the room.

Soil moisture content and solute concentration were measured using time domain reflectometry (TDR) with a MP917 Moisture Point (Environmental Sensors, Victoria, British Columbia) TDR instrument. The length of the TDR probes was 0.21 m with approximately 0.19 m of the probe inserted into the sand of the column. A computer program was set up to analyze data which was collected by the TDR. After packing the sand to the column, the 50 pairs of the TDR probes were inserted into the sand horizontally through the column wall. Thirteen millimeter of each probe was left outside the column for the TDR's cable connection. Glue (contact adhesive and sealant glue) was used to seal the gap between each probe and the column's wall.

### 3.5 Column preparation

To pack the sand to the columns, all probe holes were sealed by tape. A piece of metal screen (screen opening of 1.2 mm), with three layers of cloth above the metal screen were located at the bottom of the column to prevent loss of sand during draining the column. Approximately 0.05 m depth of high hydraulic conductivity sand (no silt or clay particles) was packed first. Approximately 100 mm depth of Beaver Creek sand was packed each time, by a funnel connected to a 30 mm diameter plastic tube, with shaking and tapping the column with a rubber mallet and moving around the plastic tube inside the column. The procedure was repeated until the top of the column.

TDR measurements were obtained of the dry sand and of saturated sand for later probe calibration and soil description. A 20 liter container, located beside each column, was used as a water source to saturate the column from the bottom by connecting the drainage tube. After saturating the column, it was covered for one day before TDR measurements were taken. All sand columns were leached with a pore volume of 7 dS m<sup>-1</sup> KCl to avoid the tracer interaction in the sand column. Then the columns were leached with distilled water several times to reduce background salinity. Initial exfiltrate from this sand was 1.4 dS m<sup>-1</sup> after saturating column 1 from the bottom using distilled water.

### 3.6 Determination of hydraulic and physical sand properties

The saturated hydraulic conductivity ( $K_{sat}$ ) was calculated using Darcy's law (Equations 3.1a and 3.1b) for each sand column using two different methods; upward flow and downward flow conditions. Darcy's law is discussed and presented in a number of soil physics books (Kirkham and Powers 1972; Marshall and Holmes 1979; Hillel 1980; Jury et al. 1991; Hillel 1998).

$$K_{sat} = \frac{QZ}{\Delta h} \quad (3.1a)$$

$$Q = \frac{\bar{Q}}{A} \quad (3.1b)$$

Where:

$K_{sat}$  is the saturated hydraulic conductivity ( $\text{m s}^{-1}$ ),

$Q$  is the water flux calculated from cumulative outflow volume as a function of time ( $\text{m}^3 \text{ m}^{-2} \text{ s}^{-1}$ ),

$\Delta h$  is the change of the total hydraulic head across the system (m),

$Z$  is the sand column length (m),

$\bar{Q}$  is the water flow (cumulative volume per time) from the sand column ( $\text{m}^3 \text{ s}^{-1}$ ), and

$A$  is the column area ( $\text{m}^2$ ).

The bulk density of sand was calculated using the mass method for each sand column during packing the columns. Three different methods were used to determine the porosity in the sand column. The first method calculated the sand porosity from the dry bulk density (Equation 3.2a) as it was described by Marshall and Holmes (1979), Maidment (1993), and Hillel (1998) assuming a particle density of  $2650 \text{ kg m}^{-3}$  (Marshall and Holmes 1979; Maidment 1993; Lehmann et al. 1998). The moisture content, which is measured by TDR, for the saturated sand (beneath the water table), can indicate the sand porosity because the moisture content for saturated sand is equal to the sand porosity

(Maidment 1993). Porosity was also estimated from the concentration data which was measured by TDR under upward or downward movement conditions of the concentration peak. Equation 3.2b can be used to determine the sand porosity from the concentration data.

$$n = 1 - \frac{\rho_b}{\rho_p} \quad (3.2a)$$

$$n = \frac{W}{Z} \quad (3.2b)$$

Where:

- n is the porosity ( $\text{m}^3 \text{ m}^{-3}$ ),
- $\rho_b$  is the bulk density ( $\text{kg m}^{-3}$ ),
- $\rho_p$  is the particle density ( $\text{kg m}^{-3}$ ),
- Z is the distance of upward or downward movement of the concentration peak (m),
- W is the amount of water added to the system to cause Z (m).

### 3.7 Estimation of soil water fluxes

Two methods were used to determine upward and downward soil water fluxes; the peak migration method and the soil water balance method. We chose these methods to estimate the soil water fluxes because these methods are applicable for data available in this research.

#### 3.7.1 Peak migration method

The peak migration method depends on the concentration peak in the sand column. The soil water fluxes can be estimated using this method by considering the movement of the concentration peak through time and the average water content for the distance which the peak moved. This method relies on steady-state flow, spatially

uniform solute input, and piston flow through the unsaturated zone assumptions. The soil water flux can be calculated by the peak migration method using the following equation used by Ward (2003).

$$Q = \frac{Z\theta}{t} \quad (3.3)$$

Where:

$Q$  is the upward or downward soil water flux ( $\text{m}^3 \text{ m}^{-2} \text{ s}^{-1}$ ),

$Z$  is the distance that the peak moved up or down (m),

$t$  is the time for the peak to move  $Z$  (s), and

$\theta$  is the average volumetric water content for  $Z$  ( $\text{m}^3 \text{ m}^{-3}$ ).

### 3.7.2 Soil water balance method

The soil water balance technique was used to estimate soil water fluxes for the sand columns. This method can give the actual upward and downward soil water fluxes under evaporative and rain conditions and considers the total amount of accumulated moisture in the sand column rather than the peak. This method was used to evaluate the performance of the peak migration method in determining soil water fluxes in a column study. Equation 3.4 can be used to estimate the soil water flux in a sand column using the soil water balance method. This equation is presented in a number of papers (Gee and Hillel 1988; Allison et al. 1994; Scanlon et al. 1997).

$$Q = P - E \pm \Delta S \quad (3.4)$$

Where:

$Q$  is the upward (-) or downward (+) soil water flux ( $\text{m s}^{-1}$ ),

$P$  is the rate of rain ( $\text{m s}^{-1}$ ),

$E$  is the rate of evaporation ( $\text{m s}^{-1}$ ), and

$\Delta S$  is the rate of the change of total soil moisture (storage) in the sand column, where a negative value means a loss, and a positive value a gain ( $m s^{-1}$ ).

Total soil water flux was calculated using both the peak migration and the water balance methods in each column and under each regime of directionally-varying flows. The estimated average net soil water flux using the peak migration method was calculated using the total peak movement during the study period and the average soil moisture in the depth where the peak moved. The estimated average net soil water flux using the water balance method was calculated using the total water evaporated from the sand column (as measured from the water container used to establish the water table), the total added water to the sand column as rain, and the total change of the total soil moisture (storage as measured with the TDR) during the study period.

### 3.8 Using and calibrating TDR readings

TDR was used to measure soil moisture content and concentrations at different depths in the sand columns. Measuring the soil water content using the TDR is based on the linear relationship between volumetric soil water content and the ratio between the travel time of radio frequency pulse in soil and air ( $T/T_{air}$ ) (Hook and Livingston 1995). The following equation, established by Hook and Livingston (1995) and described by Ebrahimi-Birang et al. (2006), was used to calculate the soil moisture from the TDR readings:

$$\theta_v = \frac{\frac{t}{t_s} - \frac{t_{air}}{t_{air}}}{\varepsilon_w^{0.5} - 1} \quad (3.5)$$

Where:

$\theta_v$  is the volumetric water content of soil ( $m^3 m^{-3}$ ),

$\varepsilon_w$  is water dielectric coefficient. It is 80.362 at 20°C (Weast 1986), and

$t$ ,  $t_s$ , and  $t_{air}$  are the travel time of a radio frequency pulse in soil, in oven-dried

soil, and in air, respectively (s).

The value of a constant voltage approached by the TDR signal ( $V_f$ ) and relative to the TDR input signal ( $V_0$ ) can be used to obtain the bulk electrical conductivity (EC) of the porous media (Ebrahimi-Birang et al. 2006). TDR readings were calibrated using the EC meter and a small column (0.102 m in diameter and 0.305 m length) with the sand (Beaver Creek sand) packed dry into the column. The column was sealed at the bottom except a hole for draining and saturating the sand column from the bottom. A piece of metal screen (a screen opening of 1.2 mm), and several layers of cloth were located above of the metal screen at the bottom of the column to prevent loss of sand during draining the column. The sand column was flushed three times (a pore volume each time) by distilled water before using it. A pair of TDR probes (0.21 m length) was inserted vertically into the sand in the column. Four KCl solutions (0.5, 1.0, 2.0, and 3.0 g L<sup>-1</sup>) were prepared and added, starting with the lowest concentration, to the sand column. The column was saturated with one of the solutions from the bottom and left for 24 h each time to allow for equilibrium. Each time the solution was added to the column, a TDR reading was taken. Also, EC readings were taken of the drainage waters using the EC meter. A polynomial relationship was observed and yielded a coefficient of determination ( $R^2$ ) of 0.95 between the TDR readings ( $dV$ ) and the EC measured in drainage by the EC meter. Equation 3.6 was developed from these readings and used to calculate the electrical conductivity (EC).

$$EC = 0.0002 dV^2 - 0.0467 dV + 3.0326 \quad (3.6)$$

Where:

EC is the electrical conductivity (dS m<sup>-1</sup>), and

$dV$  is the change of voltage measured by TDR (V).

The EC values measured by the EC meter also were calibrated. A solution of 2.2 g L<sup>-1</sup> KCl was prepared and diluted many times (22 times and the lowest concentration was 0.084 g L<sup>-1</sup>). EC measurements were taken using the EC meter each time the solution was

diluted. A polynomial relationship yielded a coefficient of determination ( $R^2$ ) of 0.99 between the EC readings and the concentration in the solution was obtained and equation 3.7 was developed and used to convert the EC readings to concentration.

$$C = 0.0465 EC^2 + 1.3513 EC + 0.1318 \quad (3.7)$$

Where:

C is the salt (KCl) concentration ( $\text{g L}^{-1}$ ), and

EC is the electrical conductivity ( $\text{dS m}^{-1}$ ).

The soil moisture content was not considered in calibrating the TDR readings because the sand columns were mostly saturated, and the only change of soil moisture was in the top part of the sand columns (e.g. 0 - 0.07 m depth under evaporative conditions) which was not considered in evaluating the profile shape and position.

### 3.9 Expressing EC data at a reference temperature

The EC data was expressed at a reference temperature using a method that was described and taken verbatim from Rhoades et al. (1999) with the exception of a few sentences as indicated by ‘....’:

*“Electrolytic conductivity (unlike metallic conductivity) increases at a rate of approximately 1.9% per degree centigrade increase in temperature.*

*Therefore, EC needs to be expressed at a reference temperature for purposes of comparison and accurate salinity expression; 25°C is most commonly used in this regard. ... For practical purposes of agricultural salinity appraisal, EC is measured at one known temperature other than 25°C and then adjusted to this latter reference using an appropriate temperature-coefficient ( $f_T$ ). This coefficient varies for different salt solutions but is usually based on sodium chloride solutions, since their temperature coefficients closely approximate those of most salt-affected surface, ground, and soil waters. Another limitation in the use of temperature coefficients to adjust EC readings to 25°C*

*is that they vary somewhat with solute concentration, the lower the concentration, the higher the coefficient, due to the effect that the temperature has upon the dissociation of water. However, for practical needs, this later limitation may be ignored and the value of ( $f_T$ ) may be assumed to single-valued. It may be estimated as:*

$$f_T = 1 - 0.20346 (T) + 0.03822 (T^2) - 0.00555 (T^3) \quad (3.8)$$

*Where:*

$$T = [\text{temperature in degrees Celsius} - 25] / 10$$

(The symbol “T” here is alternate to symbol used in the reference “t”)

*This relation was derived from data given in Table 15 of Handbook 60 (US Salinity Laboratory Staff 1954). In turn, the electrical conductivity at 25°C ( $EC_{25}$ ) can be calculated as:*

$$EC_{25} = f_T * EC_T \quad (3.9)$$

*Where:*

*$EC_T$  is the EC at the measured temperature ( $T$ ).*

*The above approach and  $f_T$ -temperature relation have been routinely used to reference soil electrical conductivities...The applicability of these  $f_T$  factors were tested for their appropriateness in this regard and concluded to be appropriate by McKenzie et al. (1989), Johnston (1994), and Heimovaara (1995)".*

### 3.10 Correcting EC data and simulations

High EC ( $1.4 \text{ dS m}^{-1}$  in exfiltrate) was monitored in this sand since the beginning of the experiment, and the contribution of dissolved salt from the sand to the solution was thus of concern. The dissolved salts from sand had to be determined because it could influence the evaluation of the change of the concentration profile shape. The measured EC by the TDR in this sand does not give the actual change of the concentration profile shape under the cycling conditions because part of the change of the concentration profile shape occurs due to the dissolved salt contribution from the sand. Therefore, measured EC by TDR had to be corrected by subtracting the contributed salts by sand (change of EC) from the measured EC data.

In the end of the experiment, and after the cycles were done for the thesis objectives, the three columns were flushed by distilled water (one pore volume), and then the three columns, 1, 2, and 3, were left covered with no loss by evaporation or drainage for 100, 94, and 96 days, respectively. TDR readings taken weekly for each column showed that the EC changed with depth and time. A general linear regression model (Equation 3.10) was developed (using SPSS) and was used to simulate the change of concentration as a function of time and depth in each column. This equation was then used to represent the contribution of the salts from the sand to the EC determined for the thesis objectives. This contribution was subtracted so the effect of the added KCl tracer could be properly determined.

$$dC = 0.04530 - 0.00064 Z + 0.00224 t \quad (3.10)$$

Where:

$dC$  is the change of salt concentration ( $\text{g L}^{-1}$ ),

$Z$  is the depth from the sand surface (cm), and

$t$  is time since column was first saturated (day).

### **3.11 Evaluating changes of profile shape and position**

The main purpose of this thesis (the second objective) is to investigate the effect of repeated cycles of directionally-varying flows upon solute profile shape and position used by tracer methods. It was hypothesized that there could be changes of the solute profile shape and position under cycling conditions of directionally-varying flow regimes depending on the seasonal net movement of the solute and soil water (Figure 1.2). The profile shape refers to the distribution of solute concentration with depth in the column (soil profile). The profile position refers to the peak location or “depth” in the column (soil profile). To evaluate the change of the concentration profile shape and position, several apparent parameters were developed and considered. These parameters are rising point, peak, falling point, and total mass above and below the peak depth (Figure 3.2). Moreover, several statistical parameters were considered to describe and determine the change of the profile shape and position under the cycling conditions. These statistical parameters are: mean, standard deviation, skewness, and kurtosis. These parameters were calculated so that profiles could be compared with time (within a flow regime) and among the three different regimes of upward and downward flows. Variation in readings due to unexpected differences in soil properties, or/and instrumental and measurement error was corrected so as to minimize their influence on the statistical parameters (Appendix H). The comparison amongst several profiles within one regime was done in terms of depth and concentration of the rising point, peak, and falling point for each profile. The rising point is the point where the concentration profile starts to rise up from the baseline; and the falling point is the point where the concentration profile falls down and meets the baseline (Figure 3.2). Comparing these parameters with time can describe the change of the concentration profile shape and position. The total mass of salts above and below the peak depth also was considered as an indicator of change of the profile shape (Figure 3.2).

The mean is defined as that measure of central tendency which is the average value of all values in a distribution of observations. The standard deviation is defined as the average amount by which observations in a distribution differ from the mean, with ignoring the

sign of the difference. The standard deviation can be calculated using the following formula as it was provided by Burford (1968) and Champion (1970):

$$SD = \sqrt{\frac{\sum_{i=1}^N (Y - \bar{Y})^2}{N - 1}} \quad (3.11)$$

Where:

- SD is the standard deviation,
- Y is the observed value,
- N is the number of observations, and
- $\bar{Y}$  is the mean.

Skewness is a method used to characterize the degree of asymmetry of a distribution around its mean. Skewness is used in this study to evaluate the changes of the solute profile shape and position caused by cycling conditions of directionally-varying flow regimes. Positive skewness indicates a distribution with an asymmetric tail extending towards more positive values, and negative skewness indicates a distribution with an asymmetric tail extending towards more negative values (Figure 3.3). Normal distributions produce a skewness statistic of about zero. Skewness can be calculated using the following formula as it was described by Burford (1968):

$$Skewness = \frac{\sum_{i=1}^N (Y - \bar{Y})^3}{(N - 1)SD^3} \quad (3.12)$$

Where:

- SD is the standard deviation,
- Y is the observed value,
- N is the number of observations, and

$\bar{Y}$  is the mean.

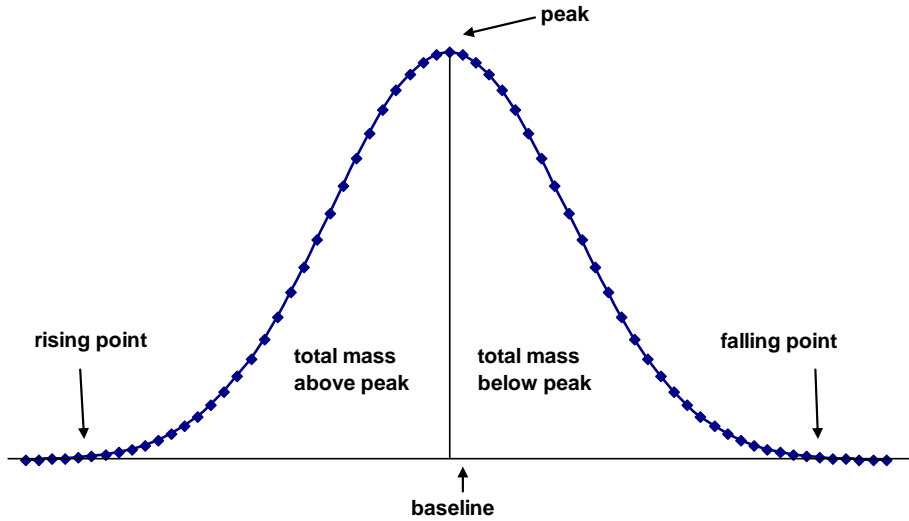


Figure 3.2: Some parameters used to evaluate the change of the concentration profile shape.

Kurtosis is another descriptive statistic that can be derived to describe a distribution and to characterize the relative peakedness or flatness of a distribution compared to the normal distribution. Kurtosis is used in this study to evaluate the change of the solute profile shape and position in term of peakedness. Positive (high) kurtosis indicates a relatively peaked distribution, and negative (low) kurtosis indicates a relatively flat distribution (Figure 3.4). Normal distributions produce a kurtosis statistic of zero if Equation 3.13 is used. The term platykurtic is used if the distribution is flatter than the normal distribution curve and leptokurtic is used if the distribution is more peaked than the normal distribution curve. Also, the term mesokurtic is used if the distribution is a normal distribution with kurtosis of zero. The following equation was described by Burford (1968):

$$\text{Kurtosis} = \frac{\sum_{i=1}^N (Y - \bar{Y})^4}{(N - 1)SD^4} - 3 \quad (3.13)$$

Where:

$SD$  is the standard deviation,

$Y$  is the observed value,

$N$  is the number of observations, and

$\bar{Y}$  is the mean.

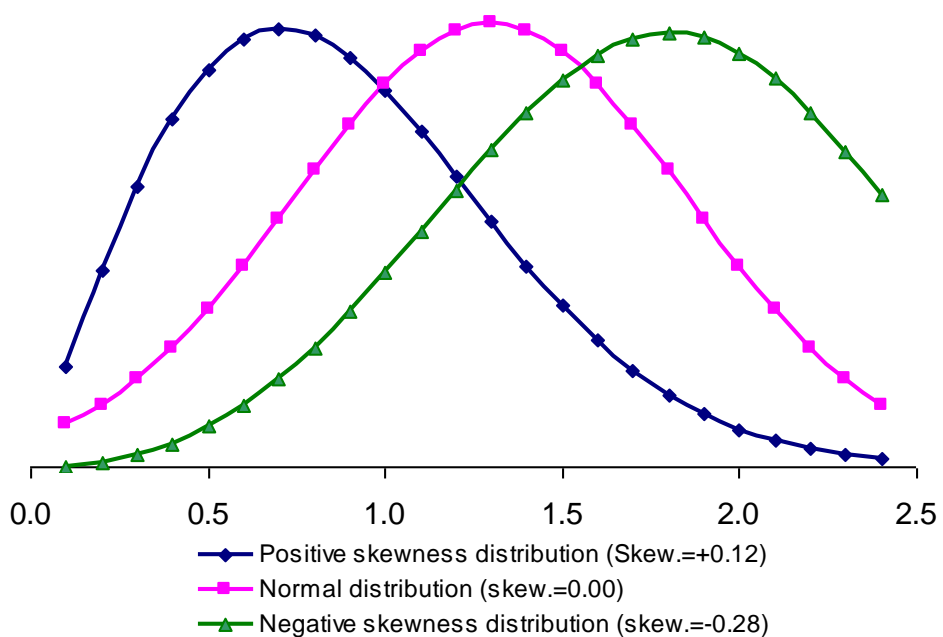


Figure 3.3: Skewed profiles to positive and negative values compared to standard normal distribution.

To determine if skewness and kurtosis are significantly non-normal, the method described by Price (2000) was used. For skewness, the calculated numerical value of skewness is compared to twice the standard error of skewness (SES) and including the range from minus twice the standard error of skewness to plus twice the standard error of skewness (Equations 3.14a and 3.14c). If the value for skewness falls within this range (range of normality) the skewness is considered not seriously violated and the distribution is normal. The same numerical process can be used to check if the kurtosis is significantly non-normal. The standard error of skewness and kurtosis can be calculated as described by Brown (2008):

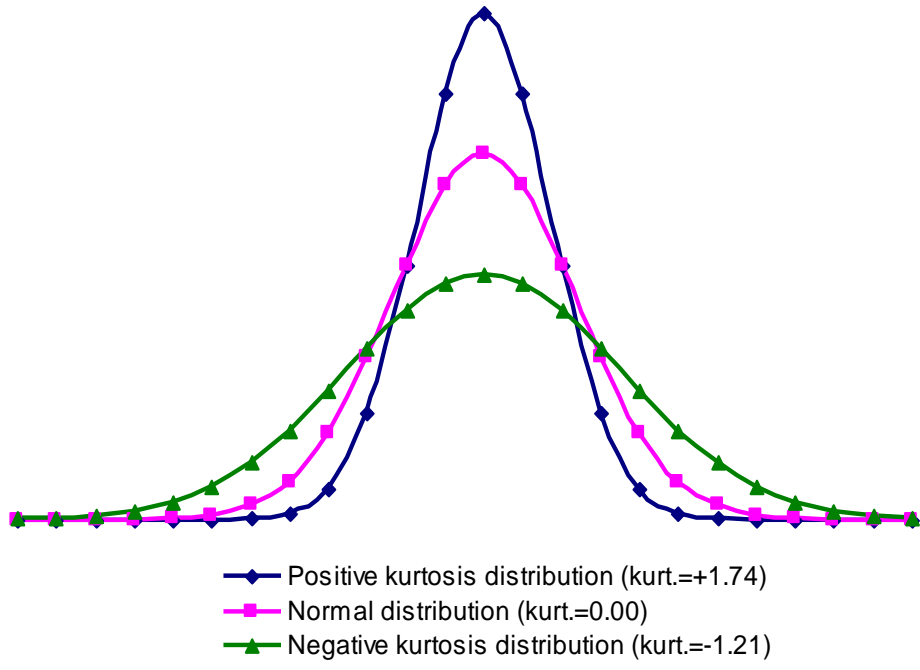


Figure 3.4: Positive (peaked) and negative (flat) kurtosis distributions compared to standard normal distribution in term of kurtosis.

$$SES = \sqrt{\frac{6N(N-1)}{(N-2)(N+1)(N+3)}} \quad (3.14a)$$

$$SEK = 2(SES) \sqrt{\frac{N^2 - 1}{(N-3)(N+5)}} \quad (3.14b)$$

$$-2(SES) < \text{range of skew. (normal distribution)} < +2(SES) \quad (3.14c)$$

Where:

SES is the standard error of skewness,

SEK is the standard error of kurtosis, and

N is the number of observations.

### **3.12 Measurement and experimental errors**

There were experimental and measurement errors associated with the methods and instruments used to meet the objectives. Measurement error of evaporation could occur based upon daily depth measurements of the water container located beside the column which might vary by  $\pm 0.5$  mm of evaporated water from the sand column. This error was a result of using ruler with millimeter marking which can measure something to nearest 0.5 mm; however, if the operator is shaking, then it could be  $\pm 3$  mm. Measured soil moisture content by TDR beneath the water table shows that there is a measurement error of  $\pm 0.016 \text{ m}^3 \text{ m}^{-3}$ . The tube pump was tested for a 24 hour period and it gave a relatively constant rate ( $89.6 \text{ mm d}^{-1}$ ); though, there might be a variation of rain from the rain cap during the rain period. EC data shows that there might be instrumental error for measuring the EC by TDR because the peak in some readings was not observed and some noise occurred on the solute profile. This error might be caused by the TDR probes or sand layers in the column caused by the backing method. Also, there might be error of estimation of the concentration peak depth due to the 20 mm vertical distance between each two pairs of the TDR probes, so the peak might be somewhere in this depth.

Some assumptions also were made to meet the objectives. It was assumed that there was no loss of water (evaporation) from the water container and the water lost from the sand column by evaporation was equal to the change in depth of the water container, so there were no storage gains or losses. Also, it was assumed that there was no water table fluctuation caused from dropping or rising the water level in the water container because of evaporation or adding water.

### **3.13 Methods for objectives**

Column 1 was selected to represent the first objective. The first objective of this thesis was to show that TDR can be a useful tool for estimation of soil water fluxes using tracer methods. The location and concentration of the starting peak were done by adding 20 mm (depth in soil column) of  $7 \text{ dS m}^{-1}$  KCl solution followed by 188.7 mm of distilled

water to the top of the sand column using the rain system. The upward flow was caused by evaporation and downward flow was caused by adding distilled water to the column (rain) using the rain system. Thirteen days was the evaporation period and TDR readings were taken every two days. Three days was the rain period and TDR readings were taken every day. Between the evaporation and the rain periods, the column was left (covered) for two days to allow for equilibrium to be established.

Each column focused on one of the sub-objectives of the second objective (Table 3.1). The second objective was investigating the effect of repeated cycles of directionally-varying flow upon solute profile shape and position used by tracer methods. The first sub-objective considers having a season of upward water flux the same as a season of downward water flux. This was accomplished by moving the peak down by a distance of approximately 60 mm through the addition of 22.2 mm of water in column 1 and 21.6 mm in columns 2 and 3, then evaporating the same amount of water for 3-4 days, so the peak returned to the same location. The second column considered having a season of downward water flux greater than a season of upward water flux. This was accomplished by moving the peak down for about 60 mm then moving the peak up for about 40 mm by evaporation for 2-3 days, so the peak will move down by about 20 mm each cycle. The third column considered having a season of upward soil water flux greater than that of downward soil water flux by moving the peak down for about 40 mm then moving it up for about 60 mm by evaporation.

Table 3.1: The variations of scenario, number of cycles, and experiment time for each column.

Column	Scenarios (total flow volume)	Downward/upward* (mm)	Number of cycles	Study period (day)
C1	Upward = downward	60/60	20	77
C2	Downward > upward	60/40	16	51
C3	Upward > downward	40/60	20	78

\* Downward/upward refers to change in vertical distance (down and up) of the concentration peak in the sand column in each cycle.

## CHAPTER 4: RESULTS AND DISCUSSION

This chapter presents data collected and discussed in order to carry out the conclusions. This chapter includes three sections: 1) presentation of the sand properties, 2) estimation of soil water fluxes using TDR with tracers under controlled laboratory conditions, and 3) investigation of the effect of repeated cycles of directionally-varying flow upon solute profile shape and position. The first section shows the collected data of physical, chemical, and hydraulic sand properties. The second section presents data collected and discussed to meet the first objective: the change of soil moisture under upward and downward flow conditions; the change of salt concentration and mass under upward and downward flow conditions; and estimation of upward and downward fluxes using both the peak migration and the soil water balance methods. The third section presents the second objective of this thesis. It includes a number of sub-sections discussing the effect of cycling conditions of three different flow regimes on: soil moisture content, concentration and mass of salts, and the change of concentration profile shape and position. Also, the estimation of soil water fluxes under three different flow regimes is provided in the third section.

### 4.1 Sand properties

Physical, chemical, and hydraulic sand properties were estimated and compared among the sand columns to investigate whether or not these three columns have similar base properties such that they would react similarly given the same flow and solute conditions. The particle size analyses showed that 95.5% of the material is sand size (0.074 to 2.0 mm) with only 3.5% silt and less than 1% clay ( $< 2 \mu\text{m}$ ). The bulk density was similar for columns 2 and 3 ( $1650 \text{ kg m}^{-3}$ ); however, it was  $1588 \text{ kg m}^{-3}$  for column 1 (Table 4.1). The variation of bulk density between column 1 and the other columns could possibly be due to the packing method because columns 2 and 3 were packed together, several weeks after column 1 was packed. Porosity as determined using saturated moisture showed that the average porosity (averaged from the 50 TDR probes spaced within each column) varied between  $0.36$  and  $0.37 \text{ m}^3 \text{ m}^{-3}$  among the three sand columns.

Organic and inorganic carbons were measured in the sand before starting the experiment and they were 0.33 and 0.46%, respectively. If assuming all the inorganic carbon is in the form of  $\text{CaCO}_3$ , then the calculated  $\text{CaCO}_3$  in this sand is 3.8%. The  $\text{CaCO}_3$  was indicated by light fizzing (Personal Communication, Charles Maule, Professor, Department of Agricultural and Bioresource Engineering, University of Saskatchewan, Canada) when a 7% HCl solution was applied. Acton and Ellis (1978) described soils in Saskatoon, Saskatchewan area, where the Beaver Creek sand was found, and stated that in this area “most glacial deposits contain moderate amounts of soluble lime-carbonate and salts”. Available data in this book shows that the  $\text{CaCO}_3$  in Saskatoon area varies between 0.1 and 33.5 equivalent %, and for soils near the location where the sand was found, it varies between 0.4 and 20.3 equivalent %. It indicates that the Beaver Creek sand used in this study contains salts (e.g.  $\text{KCl}$ ,  $\text{CaSO}_4$ , and  $\text{MgSO}_4$ ) and it is likely in the form of  $\text{CaCO}_3$ .

Saturated hydraulic conductivity for columns 2 and 3 was similar; however, it was slightly higher in column 1 (Table 4.1). The infiltration rate for the three sand columns 1, 2, and 3 was 0.36, 0.18, and  $0.18 \text{ mm min}^{-1}$ , respectively. The differences in saturated hydraulic conductivity ( $K_{\text{sat}}$ ) between column 1 and the other columns could be related to the lower bulk density in column 1. These differences among the three sand columns might be because of the variation of the packing method.

The same Beaver Creek sand (from the same location) used in this study also was used in studies by both Wilson (1990) and Bruch (1993). The particle size analysis, done by Wilson (1990), showed that 98% of the material was sand size with only 2% silt and clay size particles. Bruch (1993) showed that 96.5% of the material was sand and 3.5% was silt and clay. Also, Wilson (1990) reported that the saturated hydraulic conductivity for this sand was  $0.234 \text{ mm min}^{-1}$ . Bruch (1993) stated that the porosity for this sand (at 10 KPa load) was 0.347, and the saturated hydraulic conductivity  $K_{\text{sat}}$  (at 10 KPa load) was  $0.256 \text{ mm min}^{-1}$ . Both Wilson (1990) and Bruch (1993) did not show bulk density or particle density measurements. These two studies showed similar results to measurements done in this thesis in term of particle size and porosity. However, both studies showed

lower saturated hydraulic conductivity than that estimated in this study. This could be due to different packing methods and/or methods of measurement. Wilson showed that the total hardness as  $\text{CaCO}_3$  in Beaver Creek sand was  $14 \text{ mg L}^{-1}$ .

Table 4.1: Physical and hydraulic sand properties among the three sand columns.

Columns	Bulk density ( $\text{kg m}^{-3}$ )	Calculated porosity* ( $\text{m}^3 \text{ m}^{-3}$ )	Measured porosity** ( $\text{m}^3 \text{ m}^{-3}$ )	$K_{\text{sat}}$ (upward method) ( $\text{mm min}^{-1}$ )	$K_{\text{sat}}$ (downward method) ( $\text{mm min}^{-1}$ )
C1	1588	0.40	0.37	1.084	0.973
C2	1650	0.38	0.36	0.573	0.605
C3	1650	0.38	0.36	0.499	0.551

\* Calculated assuming particle density of  $2650 \text{ kg m}^{-3}$ .

\*\* Measured from saturated moisture content using TDR.

## 4.2 Estimating soil water fluxes using TDR with tracers under controlled laboratory conditions

The first objective of this thesis was to show that TDR can be used with tracer methods for estimation of soil water fluxes. This objective was met by comparing the estimated soil water fluxes determined using two methods; the peak migration and the soil water balance. Such a result is used to evaluate the accuracy of the tracer method in determination of flow rates, and to show that tracer methods, normally used for field studies, can be successfully used for determination of flow rates in a column setting.

Column 1 was used to test this objective. The water table (WT) was maintained at a depth of 0.32 m from the sand surface (Figure 3.1), in order to establish a sufficient evaporation rate from the sand surface. A deeper water table was tried and the evaporation rate was not high enough to have an amount equal to that of downward flow within less than two weeks. Yang and Yanful (2002) studied the effects of water table depth on the evaporation rate from a soil column using different soils. They stated that the water level affects evaporation from soil by inducing suction and hence limiting water supply.

Gardner (1958) showed that if the water table is located at a shallow depth, a steady evaporation rate will be attained and the greater the depth to the water table, the lower the steady state evaporation rate will be. The water container, located beside the sand column and connected to the bottom of the sand column, was used as a water source so the lost

water from the sand column by evaporation was gained from the water container (Figure 3.1). Upward flow by evaporation occurred first then downward flow by rain. The evaporation period was 13 days and TDR readings were taken every two days. The raining period was three days and TDR readings were taken every day. Actual average evaporation rate from the sand column calculated from change of moisture storage and lost water from the water container was  $11.3 \text{ mm d}^{-1}$ , and the rain rate was assumed constant at  $89.6 \text{ mm d}^{-1}$  (Table 4.2). The rate of water loss, measured from the water container during the drying period, of the study was  $10.3 \text{ mm d}^{-1}$ .

Table 4.2: Conditions used for the first objective of evaluating the tracer method accuracy.

Starting peak depth (m)	Water table depth (m)	Average* evaporation rate ( $\text{mm d}^{-1}$ )	Rain rate ( $\text{mm d}^{-1}$ )	Evaporation period (day)	Raining period (day)
0.51	0.32	11.3	89.6	13	3

\*Average evaporation rate refer to actual average evaporation rate from the sand column.

#### 4.2.1 Changes of soil moisture under upward and downward flow conditions

Determination of soil moisture under both upward and downward flow conditions was necessary in order to be used for correct estimation of upward and downward fluxes using the peak migration and the soil water balance methods. The soil moisture measured using TDR varied between  $0.36$  and  $0.38 \text{ m}^3 \text{ m}^{-3}$  beneath the depth of  $0.07 \text{ m}$  from the sand surface before and during the evaporation period (Table 4.3). Total, minimum, and maximum soil moisture in the sand column were calculated from all TDR readings for all TDR probes. The soil moisture beneath the water table indicates that the porosity for this sand column (column 1) is approximately  $0.37 \text{ m}^3 \text{ m}^{-3}$ . The soil moisture between the sand surface and the depth of  $0.07 \text{ m}$  varied between  $0.14$  and  $0.28 \text{ m}^3 \text{ m}^{-3}$  under evaporative conditions (Figure 4.1). Total soil moisture varied with time under evaporative conditions between  $366$  and  $382 \text{ mm}$  depth of water, decreasing with time until day 10 (Table 4.3; Figure 4.1). This decrease was largely due to variation of soil moisture between the sand surface and the depth of  $0.07 \text{ m}$ . The soil moisture beneath  $0.07 \text{ m}$  did not decrease under evaporative conditions because there was a source of water

Table 4.3: Changes in soil temperature (depth of 20 mm), evaporation rate and soil moisture before and during the evaporation period.

Days of evapo.	Aver. soil temperature (°C)	Evaporation rate <sup>1</sup> (mm d <sup>-1</sup> )	Min. moisture <sup>2</sup> beneath 0.07 m (m <sup>3</sup> m <sup>-3</sup> )	Max. moisture <sup>3</sup> beneath 0.07 m (m <sup>3</sup> m <sup>-3</sup> )	Total soil moisture <sup>4</sup> (mm)
0	21.5	na	0.36	0.38	382.4
2	21.9	9.1	0.36	0.38	380.9
4	21.3	10.3	0.36	0.38	na
6	21.7	na	0.36	0.38	375.7
8	20.7	11.5	0.36	0.38	370.1
10	20.9	8.7	0.36	0.38	365.8
13	21.4	12.2	0.36	0.38	368.8
Average	21.3	10.3	0.36	0.38	374.0

<sup>1</sup> Evaporation rate as measured from the water container and thus does not include changes in soil moisture.

<sup>2</sup> Min. moisture beneath 0.07 m refers to the minimum soil moisture beneath the depth of 0.07 m from the sand surface for any one TDR reading.

<sup>3</sup> Max. moisture beneath 0.07 m refers to maximum soil moisture beneath the depth of 0.07 m from the sand surface for any one TDR reading.

<sup>4</sup> Total soil moisture refers to total soil moisture in the column as a depth in the soil.

na = not available

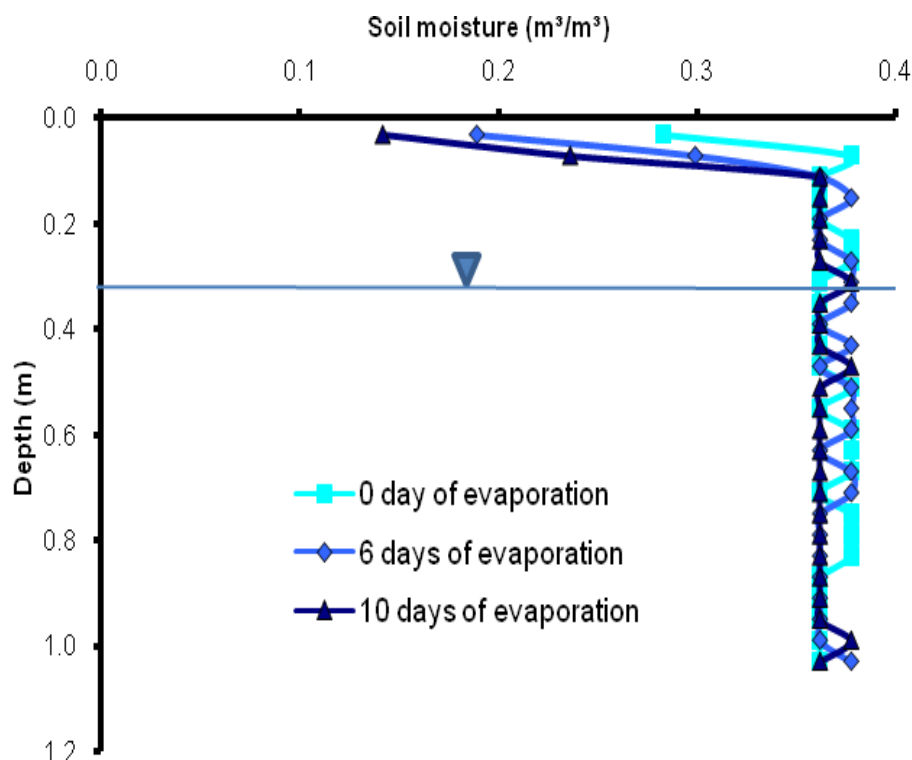


Figure 4.1: The distribution of soil moisture as a function of depth under evaporative conditions.

(water container connected to the bottom of the column) that replaced the water lost from the sand column due to evaporation. The amount of evaporation was measured daily from the water container and the evaporation rate varied between 8.7 and 12.2 mm d<sup>-1</sup> during the 13 days evaporation period (Table 4.3). The evaporation rate was maintained at this rate because higher evaporation rates can break down the capillary transfer (Idso et al. 1974). The variation of the evaporation rate did not seem to be related to soil temperature, but it could be due to measurement and experimental error. Soil temperature measured hourly for several depths (20, 50, 200, and 500 mm) beneath the sand surface and the average daily soil temperatures in the depth of 20 mm are shown in Table 4.3. The change in total soil moisture was due to drying in the top 0.07 m of the sand column where the sand is unsaturated (Figure 4.1). A total of 13.5 mm of soil moisture was the change of storage (lost from the sand column) after 13 days of evaporation (Table 4.3). The amount of lost water from the water container was 133.9 mm after 13 days, so 147.4 mm (13.5 mm + 133.9 mm) of water was evaporated from the sand column after 13 days of evaporation.

The same calculations of minimum, maximum, and total soil moisture were done for the TDR data measured under downward flow resulting from rain conditions. During the three days of rain, the soil moisture content remained constant with time at all depths (Figure 4.2) and also constant in value ( $0.36 \text{ m}^3 \text{ m}^{-3}$ ) beneath 0.11 m depth. The only change in moisture content was within the top 0.11 m because the soil in this depth was unsaturated. Total soil moisture varied between 369 and 371 mm of water in the sand column during the three days of rain.

The soil moisture distribution, under the evaporation conditions, was similar to that found in other studies. Konukcu et al. (2004) determined the water content of the evaporation front including the water content range in the transition zone from liquid to vapour under laboratory conditions. They used similar columns with high evaporative demand of 16.3 mm d<sup>-1</sup> and water table maintained at 1 m below the soil surface. They presented similar soil water content (with time) profiles for clay loam soils to soil moisture profiles

presented in this thesis (Figure 4.1). They stated that the water contents decreased towards the soil surface but the magnitude of change in the upper part of the soil profile dried out quickly to meet the evaporation demand of the atmosphere. Also, they found that the minimum water contents of a clay loam soil in the upper part of the soil profile were around  $0.12 \text{ m}^3 \text{ m}^{-3}$  under a fresh water table. Figures 4.1 and 4.2 show that soil moisture remained constant beneath a particular depth in the column that separated the moisture profile (vertically) to two parts. Chen et al. (2006) described the soil moisture profile in a soil column under evaporation conditions to three different moisture transfer regions: the moisture releasing zone, the transition zone, and the absorbing zone. This description of the soil moisture profile strongly depends on the soil structure and soil texture.

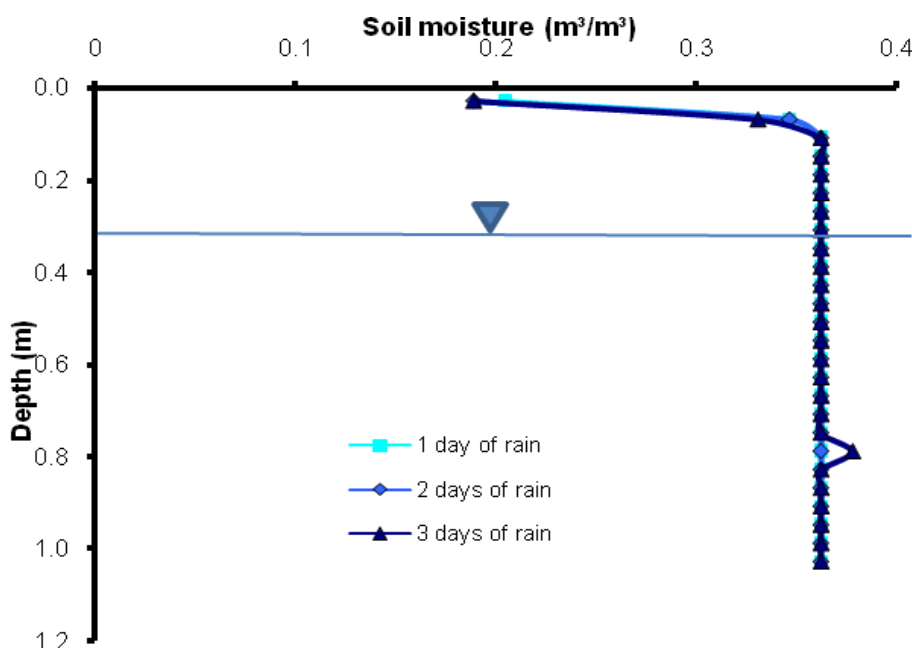


Figure 4.2: The distribution of soil moisture as a function of depth during the raining period.

#### 4.2.2 Changes of concentration and mass of salts under upward and downward flow conditions

Electrical conductivity (EC) was determined using the TDR as corrected to  $25^\circ\text{C}$ . The concentration profile in the sand column was used to calculate upward and

downward fluxes using the peak migration method. The changes of total salt mass and concentration in the sand column describe the effects of upward and downward flow conditions on the salt mass and concentration distributions in the solute profile. Before starting the experiment, the peak was located at a depth of 0.51 m from the sand surface and its concentration was  $1.76 \text{ g L}^{-1}$ . As described in the Materials and Methods chapter, the location and concentration of the starting peak were done by adding 20 mm (depth in soil column) of  $7 \text{ dS m}^{-1}$  KCl solution (4.5 g of salt) followed by 188.7 mm of distilled water to the top of the sand column using the rain system. Under the evaporative conditions, there was an upward movement for the concentration peak such that after 13 days of evaporation, the peak was 0.15 m from the sand surface and its concentration decreased to  $1.59 \text{ g L}^{-1}$  (Figure 4.3). Kowalik (2006) determined the amount of water coming from ground water to the topsoil by capillary rise in Poland and stated that in a dry year, the capillary supply can be 40–50% of the total supply for clay loamy soil.

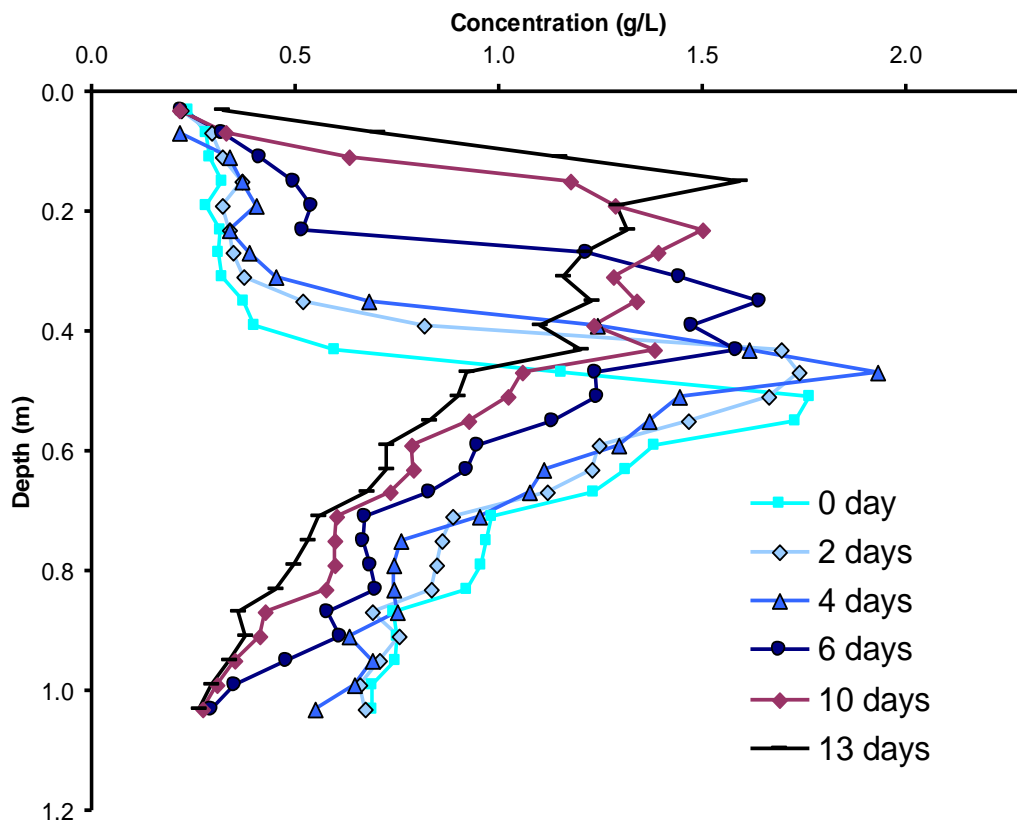


Figure 4.3: The change of distribution of concentration with depth under evaporation conditions.

At the bottom of the sand column, the concentration decreased by  $0.41 \text{ g L}^{-1}$  after 13 days of evaporation. The decrease of the concentration in the bottom of the sand column was due to the inflow of distilled water from the inlet at the column bottom. In the top of the sand column (0.03 m depth), the concentration increased by  $0.10 \text{ g L}^{-1}$  after 13 days of evaporation due to concentration by evaporation. Chen et al. (2006) stated that with the moisture upward transfer under evaporation conditions, the salts will be taken from the bottom of the column to the surface and accumulate there.

The total mass of dissolved salts was calculated from soil moisture and concentration data by multiplying concentration by soil moisture for each TDR probe reading (Table 4.4). The total mass of dissolved salts is used to determine the change of total salts (dissolved and solid) with time in the soil column. The total mass of salts in the sand column varied between 14.3 and 15.3 g during the evaporation period.

Table 4.4: Peak location, peak concentration, average concentration and total mass of salts under upward and downward flow conditions.

Flow direction	Period of time (day)	Peak depth (m)	Peak concentration ( $\text{g L}^{-1}$ )	Average* concentration ( $\text{g L}^{-1}$ )	Total mass of salts** (g)
Upward flow	0	0.51	1.76	0.76	14.3
	2	0.47	1.74	0.81	15.2
	4	0.43	1.93	0.82	15.2
	6	0.39	1.64	0.82	15.3
	8	0.31	1.46	0.82	15.1
	10	0.23	1.50	0.82	15.0
	13	0.15	1.59	0.80	14.6
Downward flow	1	0.43	1.60	0.79	14.5
	2	0.67	1.37	0.69	12.8
	3	0.91	1.44	0.53	9.8

\* Average concentration refers to average concentration in the sand column.

\*\* Total mass of salts refers to total mass of salts in the sand column.

Table 4.4 indicates that there were some salts added to the system during the evaporation period (13 days) because of dissolution of natural precipitated salts from the sand to the solution (see Appendix E for further discussion of this). The increase in dissolved salts could also be related to instrumental or measurement error because the change of total

mass of salts, from start to finish in the column calculated using Equation 3.9 was just 0.13 g. This variation of total mass of salts could also be due to variation of soil moisture and/or variation of concentration with time as both were used for calculations of the total mass of salts in the column. This variation also can be because of cumulative error occurred from measuring both soil moisture and concentration by TDR.

Concentration data for the downward flow conditions showed that the concentration peak moved downward under rain conditions. Figure 4.4 shows that the peak concentration did not change much with time and this supports the concept of the piston-flow model. In piston flow model, “annual precipitation is assumed to be infiltrating as a ‘slug’ and vertically displaces residual precipitation from the preceding year” (Ward 2003) as opposed to mixing with the residual soil water. Dahiya et al. (1984) stated that in most early studies (Warrick et al. 1971; Kirda et al. 1973; Ghuman et al. 1975; Balasubramanian et al. 1976; Ghuman and Prihar 1980), the movement of surface applied salts during infiltration was found to be explicable by a model based on piston-like displacement of initial water by the invading water. Smiles and Philip (1978), and Smiles et al. (1978, 1981) also observed the piston-like displacement of the initial water in soil columns by the absorbed water. Phillips (2004) described the upward soil water movement using the piston front model when he investigated KCl leaching in sandy columns. The average concentration under the downward flow conditions decreased with time (Table 4.4). The concentration in the sand surface (0.03 m depth) did not change; however, the concentration in the bottom of the sand column increased with time under the downward flow conditions (Figure 4.4). The exfiltrate concentration increased during the rain period from that of  $0.17 \text{ g L}^{-1}$  at the start to  $0.88 \text{ g L}^{-1}$  on the last day of rain, and it can explain the reason of decreasing the peak concentration with time.

The total mass of salts, calculated using soil moisture and concentration data, decreased with time under the downward flow conditions (Table 4.4). There was 4.75 g of salts lost from the system (column) during the rain period by drainage. The decrease of average concentration and total mass of salts with time and the increase of concentration in the

bottom of the sand column were caused by the downward peak movement and loss of salts with drainage.

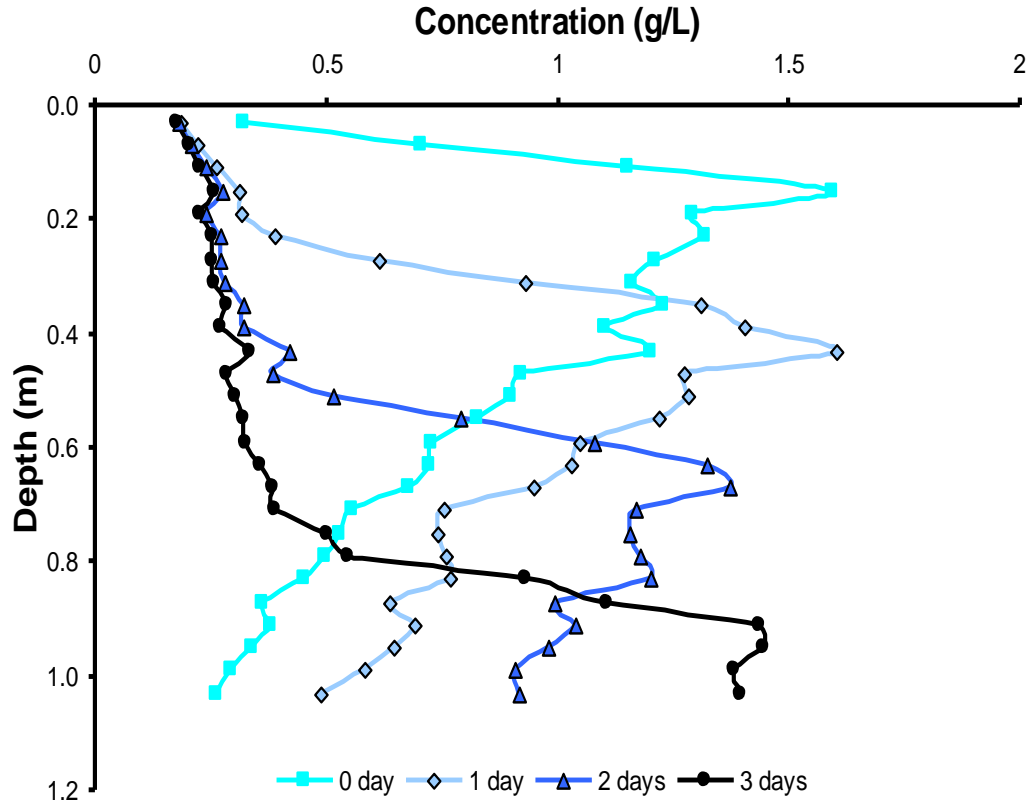


Figure 4.4: The change of the concentration distribution as a function of depth and time under the downward flow conditions (rain conditions).

#### 4.2.3 Estimation of upward and downward fluxes

Upward and downward soil water fluxes were estimated using two different methods; the peak migration method and the water balance method. Such comparison between two different methods can evaluate the capability of the TDR with tracer methods for estimation of soil water fluxes. Also, it can determine the accuracy of the tracer method in evaluating alternating direction flow and to estimate soil water fluxes in fields or in laboratory studies assuming that the soil water balance method gives the actual soil water fluxes in the column.

#### 4.2.3.1 Peak migration method

The upward and downward soil water fluxes were estimated using the peak migration method as described by Equation 3.2 in section 3.7.1. Peak movement with time was calculated from the concentration profiles estimated using the TDR. TDR also was used to measure the soil moisture in the depth where the peak moved. The average estimated upward flux, using the peak migration method, from the start to the end of the evaporation period (13 days) was  $10.2 \text{ mm d}^{-1}$  (depth in soil per time). The estimated upward flux varied with time and depth between  $7.4 \text{ mm d}^{-1}$ , during the first six days, to that of  $14.8 \text{ mm d}^{-1}$  in the following four days (Table 4.5). The increase of the upward flux in the period between the sixth and tenth days of evaporation could be related to the difficulty in determining the location (depth) of the concentration peak (e. g. 6 days of evaporation; Figure 4.3). It was because the peak became flat and its depth was difficult to determine in order to be used for estimation of soil water fluxes.

Table 4.5: Estimated upward and downward soil water fluxes using the peak migration method.

Flow direction	Period of time * (day)	Distance of peak movement (m)	Average soil moisture ( $\text{m}^3 \text{ m}^{-3}$ )	Estimated flux ( $\text{mm d}^{-1}$ )
Upward flow	0-2	0.51-0.47	0.37	-7.4
	2-4	0.47-0.43	0.37	-7.4
	4-6	0.43-0.39	0.37	-7.4
	6-8	0.39-0.31	0.37	-14.8
	8-10	0.31-0.23	0.37	-14.8
	10-13	0.23-0.15	0.36	-9.6
	0-13	0.51-0.15	0.37	-10.2
Downward flow	0-1	0.15-0.43	0.36	101.4
	1-2	0.43-0.67	0.36	86.9
	2-3	0.67-0.91	0.36	87.4
	0-3	0.15-0.91	0.36	91.9

\* Period of time refers to evaporation time (first 13 days) and raining time (last 3 days). The ‘zero’ day of the raining period (downward flow) refers to the last day of evaporation.

The peak migration method also was used to estimate the downward soil water flux. The last day of evaporation was considered as a “zero” day of the rain period. The average

estimated downward flux, using the peak migration method for the rain period (three days) was  $91.9 \text{ mm d}^{-1}$ . The downward soil water flux for the first day of the rain period was slightly high ( $101.4 \text{ mm d}^{-1}$ ), then it decreased to be relatively constant in the last two days of the rain period ( $86.9$  and  $87.4 \text{ mm d}^{-1}$ , respectively) (Table 4.5). The downward soil water flux was higher in the first day of the rain period because the soil was unsaturated in the top 0.11 m after the evaporation period, so increase of soil moisture resulted in an increase of estimated soil water flux.

#### 4.2.3.2 Soil water balance method

The water balance method was also used to estimate the upward and downward soil water fluxes under the upward (evaporative) and downward (rain) conditions. To estimate the upward and downward fluxes in the sand column, Equation 3.3 was used. Under evaporative conditions, daily rates of evaporated water from the sand column were measured from the water container located beside the sand column. The change of moisture “storage” was calculated from the total soil moisture using TDR measurements then the upward flux was calculated. The average upward flux determined using the soil water balance method for the evaporation period (13 days) was  $11.3 \text{ mm d}^{-1}$  and it varied between  $9.8$  and  $14.3 \text{ mm d}^{-1}$  (Table 4.6). Table 4.6 shows that the system lost water during the first ten days of evaporation; however, it gained water from the water container during the last three days of evaporation. The reason why the entering water, during the last three days, exceeded the evaporation rate cannot be explained.

Under downward flow condition, the change of total soil moisture (change of storage) at the first day of raining was slightly high (2.67 mm) compared to the other days. The change of total soil moisture was relatively high in the first day due to the soil depth between the sand surface and the water table not being saturated. The rain system was used to supply the distilled water to the top of the sand column and the rain rate was constant at  $89.6 \text{ mm d}^{-1}$  during the rain period. The average estimated downward soil water flux for the rain period (three days) using the soil water balance method was  $90.2 \text{ mm d}^{-1}$  varying between  $88.8$  and  $92.3 \text{ mm d}^{-1}$  (Table 4.6).

Table 4.6: Estimated upward and downward soil water fluxes using the soil water balance method.

Flow direction	Period of time (day)	Change of storage (mm)	Rate of change of storage ( $\text{mm d}^{-1}$ )	Aver. rate of evapo. or rain* ( $\text{mm d}^{-1}$ )	Estimated flux ( $\text{mm d}^{-1}$ )
Upward flow	0-2	-1.42	-0.71	-9.1	-9.8
	2-4	-3.23	-1.61	-10.3	-11.9
	4-6	-1.97	-0.98	-11.5	-12.5
	6-8	-5.66	-2.83	-11.5	-14.3
	8-10	-4.25	-2.12	-8.7	-10.8
	10-13	2.99	1.00	-12.2	-11.2
Downward flow	0-13	-13.53	-1.04	-10.3	-11.3
	0-1	2.67	2.67	89.6	92.3
	1-2	-0.79	-0.79	89.6	88.8
	2-3	0.00	0.00	89.6	89.6
	0-3	1.89	0.63	89.6	90.2

\* Average rate of evaporation or rain refers to average rate of evaporation (first 13 days) or average rate of rain (last three days).

#### 4.2.3.3 Comparing the two methods

Both the peak migration method and the soil water balance method gave similar average upward soil water fluxes ( $10.2$  and  $11.3 \text{ mm d}^{-1}$ , respectively) over the 13 day period (0-13 days, Figure 4.5). The difference between average estimated upward fluxes using both methods was 10% relative to the higher flux. The water balance method gave slightly higher values of upward fluxes than the peak migration method during the first six days of evaporation, but both methods gave relatively similar results in the following seven days (except for the period between 8 and 10 days). The difference between both methods during the first six days might be due to loss of water from soil storage rather than from the water supply container, so the flow was unsteady-state. That is because the movement of the solute peak might have been delayed (six days) due to loss of moisture from soil storage from above the peak without equivalent replacement from the water container. This assumes that the water balance method gives the actual flux. The variations of estimated upward flux using both methods can be also because of low flux values which can show higher variation with time than that with higher flux values.

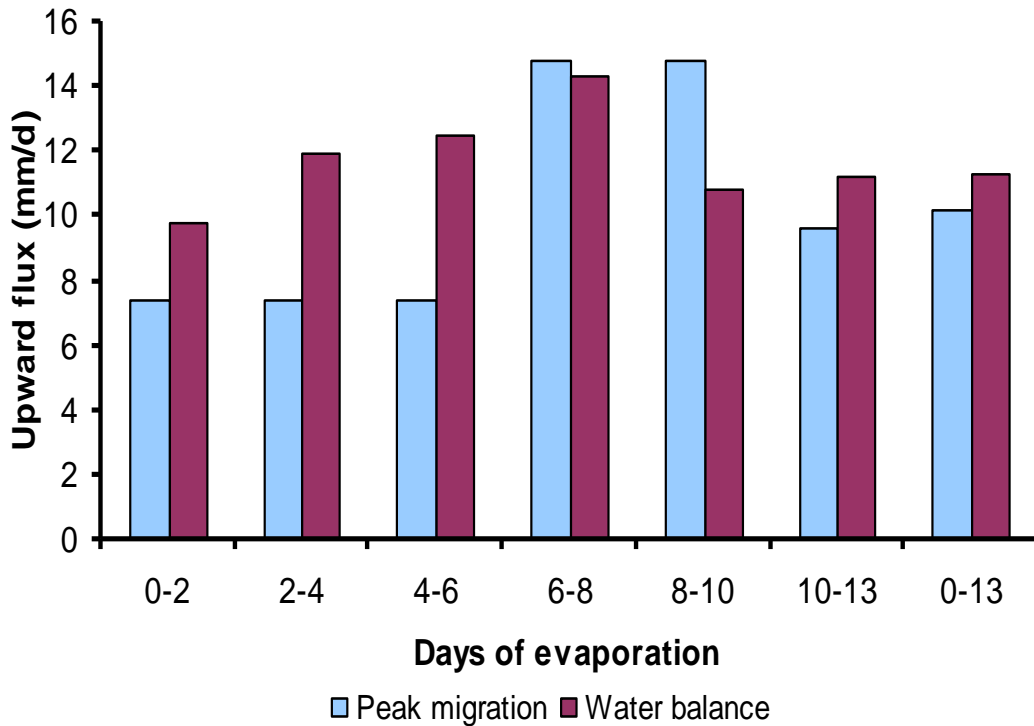


Figure 4.5: Comparing the peak migration method and the water balance method in term of upward fluxes as a function of evaporation time.

For downward soil water flow, both methods (peak migration and soil water balance) also provided similar results of average downward flux of  $91.9$  and  $90.2 \text{ mm d}^{-1}$ , respectively (Figure 4.6). The difference between average estimated downward fluxes using both methods was 2% relative to the higher flux. Both methods estimated a relatively high downward flux in the first day then decreased in the last two days. Both methods showed that the last day of evaporation did not represent the “zero” day of rain, and it seems that the system took one day to be established under the rain conditions. The estimated downward soil water flux by both methods was high in the first day because the sand was unsaturated in the top part of the sand column ( $0 - 0.11 \text{ m}$  depth). The variations of estimated soil water fluxes with time from both methods can be due to measurement or/and instrumental error (section 3.12). Even though, these measurement and instrumental errors cannot explain the differences of 20% which occurred during estimation of individual upward fluxes.

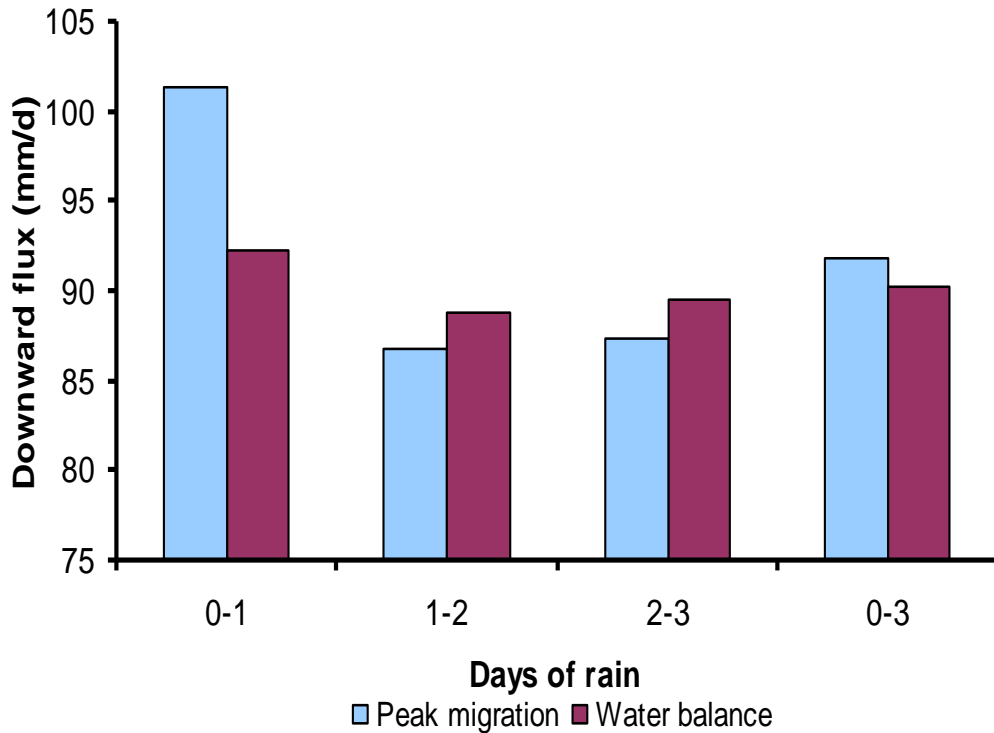


Figure 4.6: The estimated downward soil water flux using the peak migration and the soil water balance methods.

The greatest difficulty using the peak migration method was that of determining the exact peak location. This occurred because the peak became flatter in some depths in the sand column. The change of the peak's shape can be due to the possibility of changes in bulk density caused by sand packing. Also, it can be because the peak might have moved to the depth between two probe pairs (20 mm vertical distance) in the sand column. Ward (2003) stated that one of the potential problems with the peak migration method is the absence of a distinct peak. The result shows that the peak migration method gives the capability of estimating the soil water fluxes in spatial and temporal resolutions. By using the peak migration method, the soil water flux can be determined at a specific depth and time. This advantage cannot be realized with other methods, such as the soil water balance method, which gives the average soil water flux for the entire profile. The peak profile method can show the variations of soil water fluxes with depth due to variations of soil properties with depth.

The soil water balance method is commonly used for estimation of soil water fluxes and it is used in this study to determine the actual soil water flux in the sand column.

However, this approach has the disadvantage of possible cumulative error because it is based on several different parameters which are subject to measurement or/and experimental error. Gee and Hillel (1988) stated that the reliability of recharge estimated using the soil water balance depends on the accuracy and precision with which each of the water balance components is measured. Perhaps using soil columns minimizes the cumulative error because some of the soil water balance components did not occur (runoff, interception, and transpiration), and others were well controlled (e.g. rain rate).

Since the estimation of soil water fluxes is difficult in arid and semiarid environments, this investigation provides a simple approach using TDR with tracer methods. This investigation shows that measurements of soil moisture and electrical conductivity by TDR in different depths and time can be used for determination of soil water fluxes. Also, it shows that the peak migration method is a dependable approach for estimating soil water fluxes in field and laboratory studies, and it can be used in evaluating alternating direction flow under controlled laboratory conditions which is the subject of the second investigation of this thesis. The result of estimated soil water fluxes from this investigation was not compared with other results because no literature was found showing estimated soil water fluxes using peak migration or/and water balance methods in soil columns.

#### **4.2.4 Summary**

The first objective of this thesis was to show that TDR can be used for determination of soil water fluxes using tracer methods. Column 1 was used to estimate the upward and downward soil water fluxes using two methods: the peak migration and the soil water balance. The soil moisture measured by TDR under the upward and downward flow conditions was relatively constant beneath 0.07 m depth from the sand surface. However, in the depth between the sand surface and 0.07 m, it varied with time.

Under the downward flow conditions, the total mass of salts decreased with time and there was 4.75 g of salts lost from the system with drainage during the rain period.

The peak migration and the soil water balance methods gave similar average upward and downward soil water fluxes; however, the upward soil water fluxes varied with time when measured at short time periods (1 to 2 days), under the upward flow conditions. This result of estimated upward and downward fluxes indicates that TDR can be a useful tool for determination of soil water fluxes, and the tracer method can be recommended for determination of soil water fluxes in fields or in laboratory studies for sufficient time and depth. An advantage with the peak migration method is that it shows greater spatial and temporal resolution than that of the water balance method. Moreover, it indicates that the tracer method can be successfully used in evaluating alternating direction flow under controlled laboratory conditions.

#### **4.3 Investigating the effect of repeated cycles of directionally-varying flow upon tracer solute profile shape and position**

The second objective of this thesis is to investigate the effects of repeated cycles of directionally-varying flow upon solute profile shape and position used by tracer methods. The relevance of this objective is to determine the accuracy of the tracer method in determining long-term net flux values in deep unsaturated systems under directionally-varying flow. Three different seasonal flow regimes were simulated using three sand columns. Column 1 used a season of upward water flux of equal volume of flow as a season of downward water flux. The second column had a season of upward water flux less than a season of downward water flux, while the third column considered a season of upward water flux greater than that of downward water flux. Soil and room temperature data was needed to correct the TDR readings and to investigate the effect of temperature on soil water processes. The average column evaporation rate measured from the water container during the study period varied among the three columns between 5.0 and 6.0 mm d<sup>-1</sup>. Room and soil temperature (depths of 0.02, 0.06, 0.21, and 0.51 m) and humidity were recorded hourly using the air temperature and humidity logger and the soil

temperature logger (Appendix D). Average weekly soil temperature at the depth of 0.02 m varied between 18 and 23°C, and the average weekly room temperature varied between 23 and 26°C during the study period (Figure 4.7).

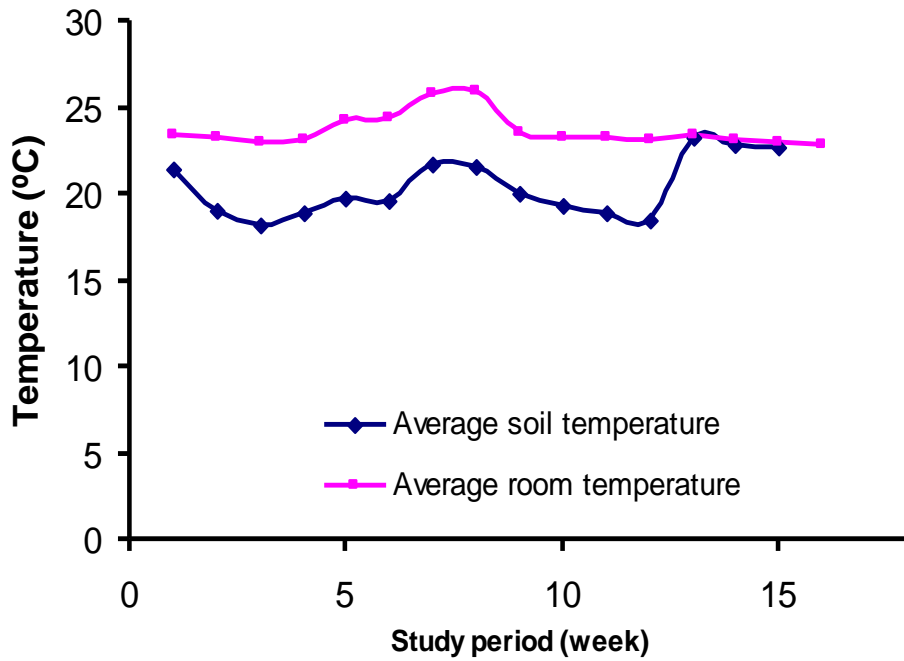


Figure 4.7: The variation of average weekly room temperature and soil temperature (0.02 m depth) during the study period.

#### 4.3.1 Soil moisture content

Soil moisture content was measured using the TDR. This sub-section provides soil moisture data collected before and during seasonal flow cycling at the end of the evaporation period of each cycle. This data shows the effects of the three different seasonal flow regimes on the change of the soil moisture content. Also, soil moisture data was used for estimating soil water fluxes using both the peak migration and soil water balance methods.

#### 4.3.1.1 Initial soil moisture

The initial soil moisture content, measured using TDR, was collected before starting the cycles (Table 4.7; Figure 4.8). The purpose of measuring the initial soil moisture was to determine the basic properties of soil moisture for the three sand columns and to estimate the effects of directionally-varying flow upon the initial soil moisture.

Table 4.7: The minimum, maximum, and total soil moisture contents at initial conditions (before starting the cycles).

Columns	Water table (WT) depth (m)	Minimum soil moisture* ( $\text{m}^3\text{m}^{-3}$ )	Maximum** soil moisture ( $\text{m}^3\text{m}^{-3}$ )	Total soil moisture (mm)
C1	0.325	0.25	0.38	372
C2	0.335	0.33	0.38	386
C3	0.375	0.17	0.39	380

\* Minimum soil moisture refers to the lowest moisture content of all the individual TDR probes.

\*\* Maximum soil moisture refers to the highest moisture content of all the individual TDR probes.

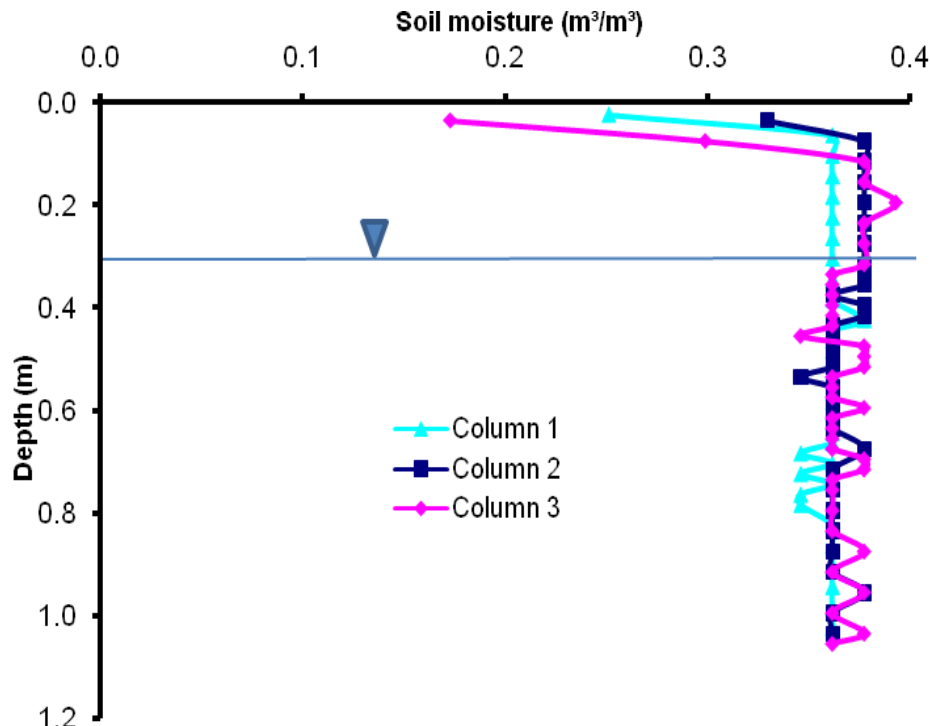


Figure 4.8: The distribution of initial soil moisture before starting the cycles in the three columns.

The water table in the three columns varied at 0.325, 0.335, and 0.375 m depth from the sand surface in columns 1, 2, and 3, respectively. The total soil moisture in columns 1, 2, and 3 was 372, 386, and 380 mm, respectively. The variation of total soil moisture among the three sand columns was caused by the distance of the water table from the sand surface and the resulting effect upon soil moisture in that region.

The minimum soil moisture in the three columns occurred at the depth of 0.025 m (sand surface) and the maximum soil moisture was in depths beneath the water table. Some of the variations of soil moisture in the depth between the sand surface and the water table were because the TDR measurements were not taken at the same time after adding the tracer and there was a slight difference of porosity among the sand columns. The high maximum soil moisture ( $0.39 \text{ m}^3 \text{ m}^{-3}$ ) in column 3 (Table 4.7) might be due to measurement error (approximately 0.20 m depth, Figure 4.8).

#### **4.3.1.2 Change of soil moisture under cycling conditions**

Total soil moisture (summed once per cycle at the end of each evaporation period and at the start of the precipitation period) was calculated as a depth of water in the sand column and used to determine the changes of the soil moisture under the cycling conditions. Total soil moisture in column 1 under the cycling conditions varied with time between 366 and 384 mm (Table 4.8). The total soil moisture (storage) in column 1 decreased by 7.3 mm after 20 cycles. The total soil moisture in column 2 did not change much between start and end (0.4 mm); however, it varied between 374 and 388 mm, with much of the change occurring in the last cycle (Figure 4.8). The minimum and maximum of total soil moisture in column 3 were 378 and 391 mm, respectively, with an overall increase of 2.9 mm after 20 cycles (Table 4.8, Figure 4.9). Moisture lost from storage (e.g. -7.3 mm in column 1, Table 4.8) represents this water going to evaporation, whereas moisture gained in storage (e.g. 2.9 mm in column 3) represents this water not going to evaporation.

Table 4.8: The minimum, maximum, and change in total soil moisture contents during the study period and under the cycling conditions.

Columns	Min. of total moisture <sup>1</sup> (mm)	Max. of total moisture <sup>2</sup> (mm)	Change in total moisture <sup>3</sup> (mm)	Standard deviation <sup>4</sup> (mm)
C1	366	384	-7.3	4.51
C2	374	388	0.4	4.59
C3	378	391	2.9	3.09

<sup>1</sup> Min. of total moisture refers to the minimum of total values measured within the entire column during the study period.

<sup>2</sup> Max. of total moisture refers to the maximum of total values measured within the entire column.

<sup>3</sup> Change in total moisture is the difference in moisture between the first and last cycles of the tests.

<sup>4</sup> Standard deviation refers to the standard deviation of the total soil moisture in the column during the cycling period.

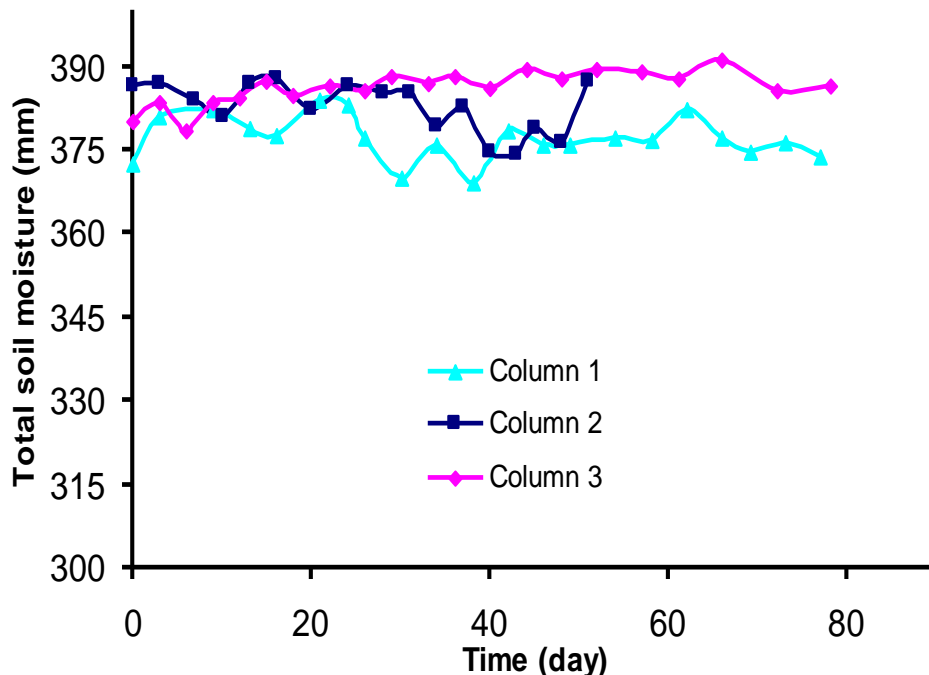


Figure 4.9: The variation of total soil moisture under the cycling conditions (time) in the three columns.

Column 1 had lower minimum and maximum total soil moisture values and column 3 had higher values than the other columns (Figure 4.9). It can be because of the difference in the water table depth among the three sand columns (Table 4.7) and slight differences in packing. The differences between minimum and maximum values are small, being

between 3 and 5% of the total soil moisture. This change of soil moisture under cycling conditions was not discussed in any literature reviewed within this thesis.

### **4.3.2 Concentration and mass of salts**

This sub-section presents and discusses estimated concentrations using TDR (corrected to 25°C but not corrected for salt contribution from the sand) and calculated mass of salt data. It shows the effect of three different seasonal flow regimes on concentration and dissolved salts in the sand columns. The contribution of precipitated salts in the sand to the solution is also discussed briefly. These concentration profiles are used to show the effect of three different seasonal flow regimes on the profile shape and position which is discussed in a later subsection. Concentration profiles are also used for estimation of soil water fluxes using the peak migration method.

#### **4.3.2.1 Initial concentration and mass of salts**

Electrical conductivity (EC corrected to 25°C) data was measured using the TDR after adding the tracer but before starting the cycles. Initial concentration and mass of salts were considered to determine the change of concentration and mass of salts under cycling conditions of different flow regimes. A concentration peak was developed at a depth between 0.4 and 0.6 m from the sand surface for initial conditions (Table 4.9, Figure 4.10). The concentration peak was developed by adding 20 mm of 7 dS m<sup>-1</sup> (4.5 g) KCl followed by a sufficient depth of distilled water using the rain system. The initial peak depth was different for each column dependent on the objectives. A shallower peak depth was set for column 2 as dominant flow was downward and it was not wished that after 16-20 cycles, an appreciable part of the tracer would be lost out the bottom of the sand column. There was variation among the three columns in terms of peak concentrations even though the same amount of tracer was added to each column using the same method (section 3.5). This variation could have been caused by soil layering which affected the distribution of the concentration with depth among the three columns (Figure 4.10).

Table 4.9: Comparing the three columns in term of tracer peak concentration, peak depth, and total concentration and mass in the column before and after adding the tracer.

Columns	Peak concentration ( $\text{g L}^{-1}$ )	Peak depth (m)	Average concentration after adding tracer ( $\text{g L}^{-1}$ )	Total dissolved salts before tracer (g)	Total dissolved salts after tracer (g)
C1	1.59	0.585	0.62	1.03	5.53
C2	1.04	0.435	0.52	1.28	5.78
C3	0.90	0.635	0.60	2.40	6.90

Mass of salt (g) was calculated by multiplying concentration ( $\text{g L}^{-1}$ ) with volume of water (L) in the column for each TDR probe reading.

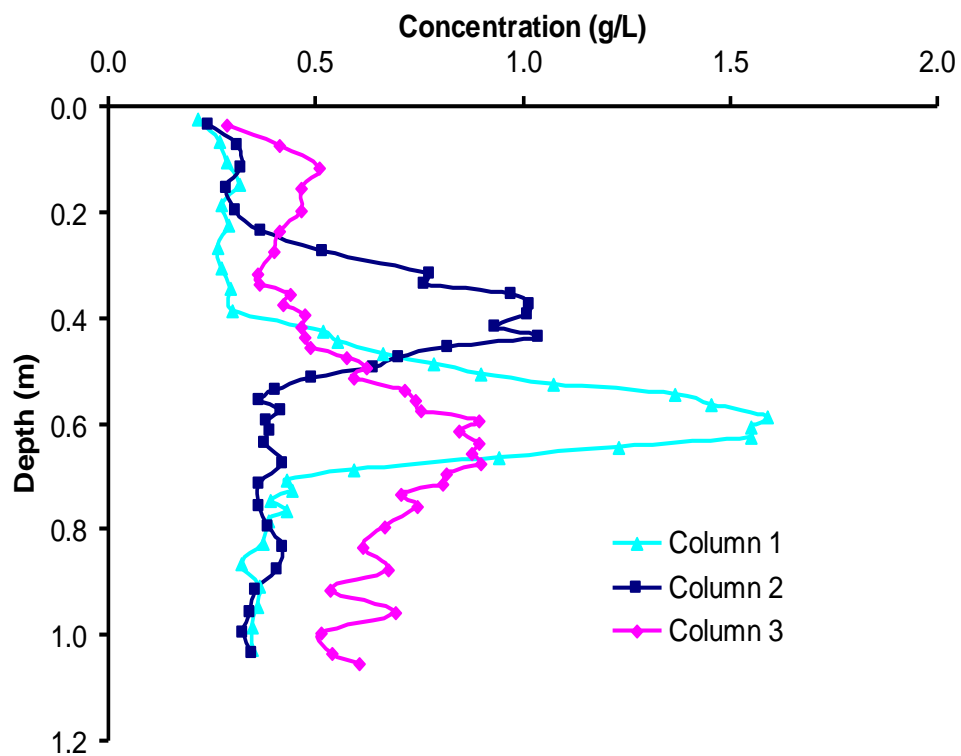


Figure 4.10: The distribution of concentration as a function of depth in the three columns after adding the tracer followed by controlled flushing with distilled water to desired starting depth, before seasonal cycling began.

Also, it can be due to the different concentration distribution (profile shape) was amongst the three sand columns, with a wider peak having a lower peak concentration. The average concentration in columns 1 and 3 was similar ( $0.62$  and  $0.60 \text{ g L}^{-1}$ , respectively); however, it was lower in column 2 ( $0.52 \text{ g L}^{-1}$ ).

The total mass of dissolved salts before and after adding the tracer also varied amongst the three columns (Table 4.9). The total mass of dissolved salts after adding the tracer shows that column 1 is the lowest. It can be because of variations of soil moisture content between the two sand columns (Table 4.8) and initial mass of salts (before adding the tracer) among the three columns. Also, the variation of initial total dissolved salts in the sand columns can be due to cumulative error because it was summed from the calculated mass of salts using soil moisture and concentration data estimated using TDR readings.

#### 4.3.2.2 Change of concentration under cycling conditions

The average concentration was calculated from TDR readings and not corrected for salt contribution from the sand. During the study period, the minimum average concentrations of the three columns varied from 0.52 to 0.60 g L<sup>-1</sup> with the maximum average varying between 0.63 and 0.77 g L<sup>-1</sup> (Table 4.10). All three columns had an increase in average concentration, ranging from 0.04 to 0.15 g L<sup>-1</sup> during the study period (Table 4.10, Figure 4.11).

Table 4.10: The variation and the change of average concentration under the cycling conditions in the three sand columns.

Columns	Min. average concentration <sup>1</sup> (g L <sup>-1</sup> )	Max. average concentration <sup>2</sup> (g L <sup>-1</sup> )	Change in average concentration <sup>3</sup> (g L <sup>-1</sup> )	Standard deviation <sup>4</sup> (g L <sup>-1</sup> )
C1	0.58	0.67	0.04	0.02
C2	0.52	0.63	0.11	0.03
C3	0.60	0.77	0.15	0.05

<sup>1</sup> Min. average concentration refers to minimum of average concentration in the column during the cycling period.

<sup>2</sup> Max. average concentration refers to maximum of average concentration in the column during the cycling period.

<sup>3</sup> Change in average concentration is the difference in average concentration between the start and the end of the period time.

<sup>4</sup> Standard deviation refers to the standard deviation of the average concentration in the column during the cycling period calculated from all averages of TDR readings in each cycle.

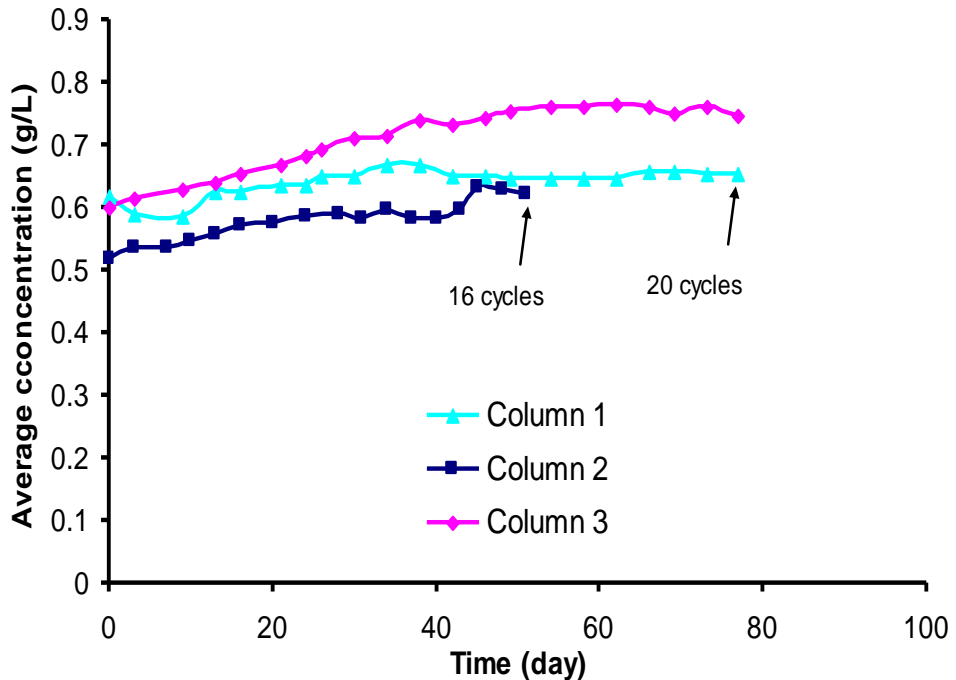


Figure 4.11: The average concentration (not corrected for salt contribution by sand) as a function of time (cycles) for the three columns.

Standard deviations were relatively low for the three columns, showing that the variations of average concentration in each column were relatively constant with time (cycles).

Column 3 had the highest average concentration of the three columns and column 2 had the lowest average concentration (Figure 4.11). This variation could be relative to change of soil moisture in the top part of the sand columns (unsaturated depth) because the TDR readings were calibrated based on saturated soil assuming that the three columns are mostly saturated. The increase of average concentration in each column was due to the contribution of salts from sand to the solution (Appendix E).

#### 4.3.2.3 Change of dissolved salts under cycling conditions

The mass of dissolved salts was calculated for each column using soil moisture and concentration information obtained from each probe reading and not corrected for salt contribution from the sand. The total mass of dissolved salts increased for the three columns (Table 4.11, Figure 4.12), due to dissolution of salts present in the sand. Over the same period, there was some mass loss of dissolved salts in the drainage waters

during the downward movement periods, and it was not measured. Due to this loss, it would be expected that a greater amount of salt would have been lost from column 2 than the others.

Table 4.11: The variation and the change of total mass of dissolved salts under the cycling conditions in the three columns.

Columns	Minimum <sup>1</sup> total mass of salts (g)	Maximum <sup>2</sup> total mass of salts (g)	Change <sup>3</sup> in total mass of salts (g)	Standard deviation (g)
C1	5.5	8.3	2.8	0.7
C2	5.8	8.1	1.8	0.7
C3	6.9	9.0	1.4	0.5

<sup>1</sup> Minimum total mass of salts refers to the lowest total mass of salts in the column.

<sup>2</sup> Maximum total mass of salts refers to the highest total mass of salts in the column.

<sup>3</sup> Change in total mass of salts refers to total change of total mass between the last day and before starting cycling.

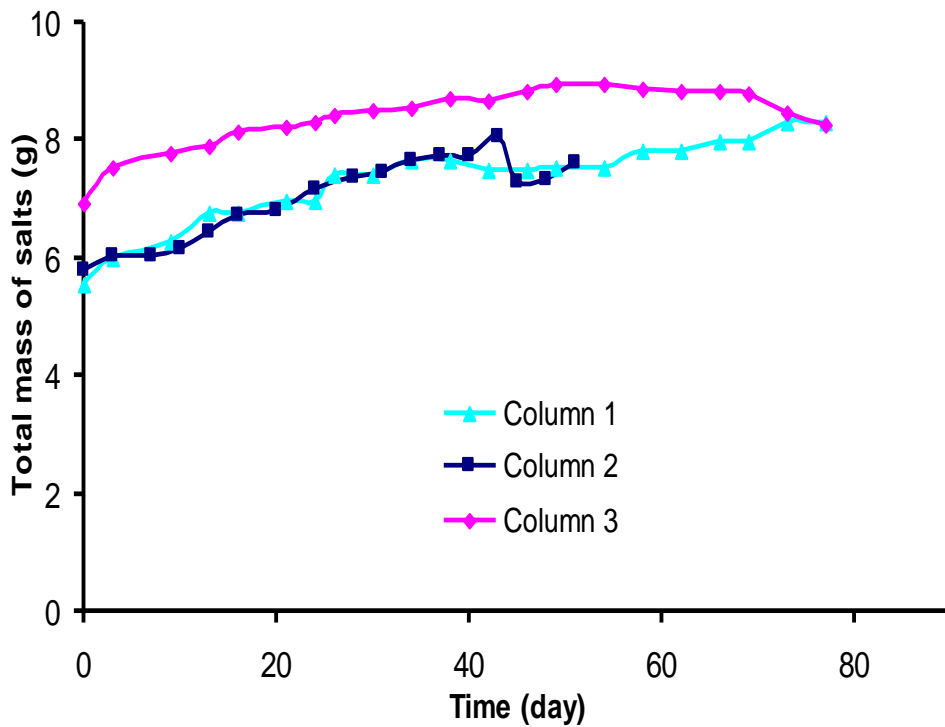


Figure 4.12: Total mass of dissolved salts as a function of time (cycles) for the three columns.

The upward and downward net movements can explain the slight variation of change of total mass of salts between columns 2 and 3 because the net movement in column 2 is

down while it is up in column 3. Therefore, it is expected that the loss of dissolved salt mass in column 2 is higher than it is in column 3 as it would have drained out the bottom. However, the total change of mass in column 1 was relatively high (2.8 g). Figure 4.12 also indicates that the total mass of dissolved salts in column 3 is higher than it is in columns 1 and 2, and columns 1 and 2 had similar values during the study period. These variations in total mass of salts might be due to differences of initial concentration and mass of salts between column 3 and the other columns (Table 4.9). Moreover, the total mass of dissolved salts increased with cycles (time) in the three sand columns during the first 40 days, then it started to decrease in the end of the experiment time in column 3 and it remained constant then increased again in column 1 (Figure 4.11). The increase of the total mass of salts in each column was because there was contribution of salts from the sand to the solution (Appendix E).

#### **4.3.2.4 Contribution of dissolved salts**

Although, not planned, it soon became evident that there were some salt precipitates (assumed to be primarily calcium carbonate) in the sand. With time, these salts dissolved and contributed to the dissolved salt concentration, thus resulting in an increase in EC with time. The rate and amount of dissolved salts contributed from the sand had to be determined because it could influence the evaluation of the concentration profile shape and position. Therefore, the EC data measured using the TDR had to be corrected by subtracting the dissolved salts contributed from the sand to the measured EC values. This is described in Appendix E. A general equation (model) was developed to describe the change in EC for each column as a function of time and depth (see section 3.10). This model enabled the subtraction of the soil contribution to EC for the experiment done under the cycling conditions of upward and downward seasonal flows. Both Wilson (1990) and Bruch (1993) used the same sand (Beaver Creek sand) for their experiment, but they did not report the problem of salt contribution from the sand. Acton and Ellis (1978) stated that soils from this location might contain moderate amounts of soluble lime-carbonate and salts.

### **4.3.3 Change of concentration profile shape and position under cycling conditions**

The second objective of this thesis was to investigate the effects of repeated cycles of directionally-varying flow upon solute profile shape and position used by tracer methods for estimation of soil water fluxes. The profile shape refers to the distribution of solute concentration with depth in the column (soil profile). The profile position refers to the peak location or “depth” in the column (soil profile). Three different conditions of directionally-varying flows of upward and downward directions were considered. The contribution of dissolved salts from the sand to the solution was subtracted from the TDR-measured EC data as it is discussed in details in Appendix E. There were some noise in the concentration profile because of instrument or experiment error. For example, in Figure 4.14 there is a peak at about 0.88 m that is due to instrument error or a sand layer. This noise influenced the accuracy of determining the change of the profile shape using the statistical parameters. Therefore, the profile shape was smoothed by correcting the concentration values in this noise on the profile (see Appendix H). After correction, the changes of the profile shape under cycling conditions of each flow regime were determined by comparing the profile shape for selected cycles (5, 10, 15, and 20) with the profile shape before start of the cycling. A number of apparent and statistical parameters were calculated and considered. Skewness and kurtosis were calculated using the TDR data from a depth of 0.18 m to near the bottom (1.025 m depth) to avoid the effects of the evaporation process at the top of the column, and that of the influence of drainage water at the bottom of the column. The ranges of normality of skewness and kurtosis were calculated (section 3.11), to investigate whether the profile shape is significant relative to the normal distribution. In the following sub-sections the change of the solute profile shape and position was determined under the three different regimes of directionally-varying flows. To date, no literature was found showing methods to describe the change of the solute profile shape and position under repeated cycles; therefore, the apparent and statistical methods mentioned early were developed and used in this thesis.

#### **4.3.3.1 The change of the solute profile shape and position under cycling of three different flow regimes**

The changes of the concentration profile shape and position were determined under the cycling conditions of three different seasonal flow regimes. The seasonal flow regime can be defined as a number of different climatic seasons that occur within one year or ‘cycle’. In this study, there are two different climatic seasons within each cycle, one of upward flow (caused by evaporation) and one of downward flow that occurs due to excess rain. These flow regimes were: 1) equal upward and downward soil water flows; 2) downward soil water flow being greater than upward flow; and 3) downward soil water flow being less than upward soil water flow. These three flow regimes were tested using sand columns 1, 2, and 3, respectively.

##### **4.3.3.1.1 Downward flow = upward flow**

In column 1 (downward flow was equal to upward flow), the profile shape changed under the cycling conditions (Table 4.12; Figure 4.13). The peak moved up during the first five cycles then it stayed at the same location during the following cycles. The peak concentration decreased by 47% after 20 cycles relative to the peak concentration before starting the cycles. The distance between the rising and the falling points increased by 0.44 m after 20 cycles. Also, the difference between the rising and falling points’ concentrations decreased by 0.07 g L<sup>-1</sup> after 20 cycles.

Calculations of total mass of salts above and below the peak depth show that there was change of the profile shape. The total mass of salts above the peak depth decreased by 0.83 g (15% relative to that before starting cycles) after 20 cycles. The total mass of salts below the peak depth increased by 0.31 g (8% relative to that before starting cycles) after 20 cycles. The calculated skewness values indicated that the distribution started with an asymmetric tail extending towards positive values (downward) and under the cycling conditions, it decreased to be about normal distribution (-0.09) after 20 cycles. The skewness range of normality varied between ±0.82 and ±0.87. The skewness values

indicate that just the first profile (before starting the cycles) was significantly skewed (non-normal). The change of skewness values from skewed (non-normal distribution) to normal distribution indicates that the profile shape changed under the cycling conditions of equal upward and downward soil water flows.

Table 4.12: Change of the profile shape at completion of cycles for column 1 (downward seasonal flow = upward seasonal flow).

Parameters	Number of cycles				
	0	5	10	15	20
Rising point	depth (m)	0.39	0.27	0.27	0.27
	conc. ( $\text{g L}^{-1}$ )	0.28	0.30	0.29	0.29
Peak	depth (m)	0.61	0.55	0.63	0.67
	conc. ( $\text{g L}^{-1}$ )	1.58	1.13	1.03	0.91
Falling point	depth (m)	0.71	0.75	1.03	1.03
	conc. ( $\text{g L}^{-1}$ )	0.43	0.42	0.39	0.37
Total mass above peak (g)	5.43	5.18	4.79	5.22	4.60
Total mass below peak (g)	3.89	4.42	4.58	3.99	4.20
Mean ( $\text{g L}^{-1}$ )	0.61	0.59	0.56	0.53	0.50
SD ( $\text{g L}^{-1}$ )	0.44	0.31	0.25	0.22	0.20
Skewness	1.06	0.45	0.35	0.02	-0.09
Kurtosis	-0.33	-1.46	-1.18	-1.35	-1.45

conc. = concentration

The mean and standard deviation decreased by 54% and 18%, respectively after 20 cycles relative to that before starting the cycles. Calculated kurtosis values show that the profile shape got flatter (platykurtic or more negative) after first five cycles. The kurtosis range of normality varied between  $\pm 1.6$  and  $\pm 1.7$ , and it showed that just the first profile (before starting cycles) was significantly non-normal relative to the normal distribution.

The regime of equal upward and downward seasonal flows simulates wet and dry seasons that might occur in the field. It was assumed that during these seasons, the lost water during the dry period is equal to the gained water during the wet period and there was soil water and solute fluctuation as a result of the climate effects (evapotranspiration and precipitation). All apparent and statistical parameters (Table 4.12) show that the solute profile shape for equal upward and downward flow changed with time, from initial

conditions. The solute profile shape got flatter with time, and it changed from skewed downward to normal distribution.

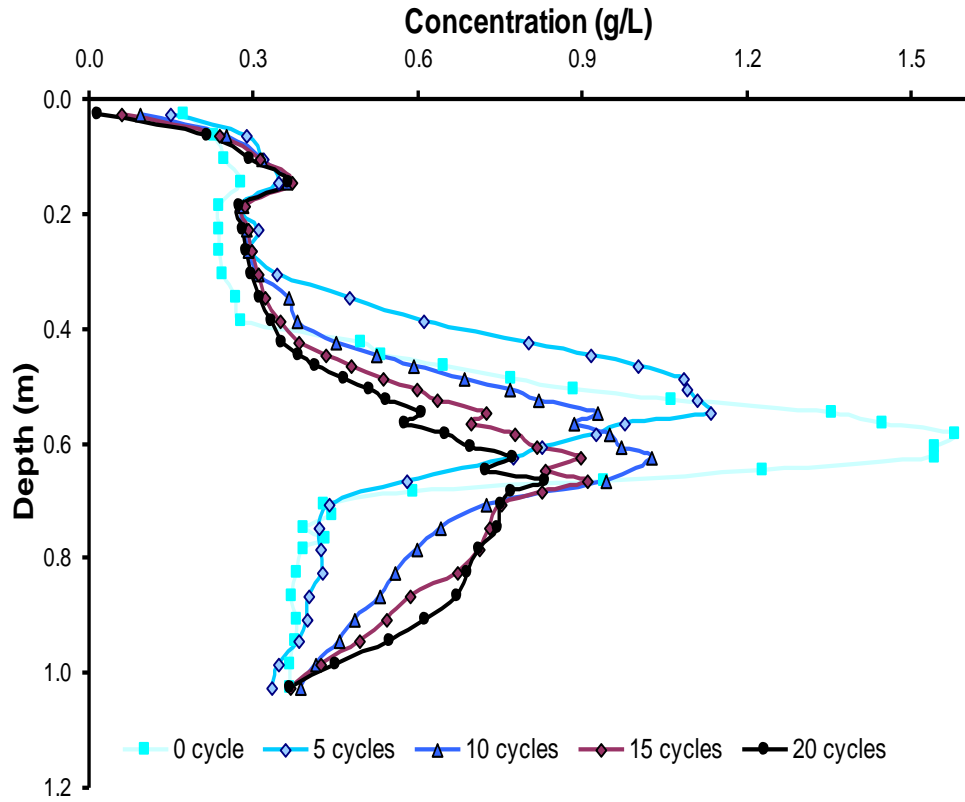


Figure 4.13: Shape of concentration profiles, corrected by subtracting the dissolved salts from soil, at different cycles for the regime of upward flow = downward flow (column 1).

#### 4.3.3.1.2 Downward flow > upward flow

Under conditions of downward flow being greater than upward flow (column 2), the concentration profile shape and position changed with time (Table 4.13; Figure 4.14). As the concentration peak moved down, its concentration decreased by  $0.28 \text{ g L}^{-1}$  (after 16 cycles). The distance between the rising and falling points did not change much (decreased by 0.04 m) after 16 cycles; however, the difference between the rising and falling points' concentrations increased by  $0.14 \text{ g L}^{-1}$  after 16 cycles.

Table 4.13: Change of the profile shape at completion of cycles for column 2 (downward seasonal flow > upward seasonal flow).

Parameters	Number of cycles				
	0	5	10	16	
Rising point	depth (m)	0.12	0.12	0.34	0.56
	conc. ( $\text{g L}^{-1}$ )	0.25	0.26	0.32	0.35
Peak	depth (m)	0.44	0.50	0.68	0.80
	conc. ( $\text{g L}^{-1}$ )	1.02	0.86	0.84	0.74
Falling point	depth (m)	0.56	0.64	0.76	0.96
	conc. ( $\text{g L}^{-1}$ )	0.35	0.52	0.56	0.59
Mean ( $\text{g L}^{-1}$ )	0.50	0.52	0.50	0.48	
SD ( $\text{g L}^{-1}$ )	0.24	0.17	0.17	0.18	
Skewness	1.02	0.29	0.43	0.08	
Kurtosis	-0.48	-0.61	-0.45	-1.65	

Skewness values decreased with time under the cycling conditions. They show that the concentration profile, at the start of cycling, was skewed to the right +1.02 (downward) and after 16 cycles it had a normal distribution (+0.08). The skewness range of normality, calculated using the standard error of skewness, was  $\pm 0.8$ , showing that just the first profile was significantly non-normal, and that there was a significant change of the profile shape under cycling conditions.

The mean did not change much under cycling conditions (between 0.48 and 0.52  $\text{g L}^{-1}$ , Table 4.13). The standard deviation decreased rapidly during the first five cycles then it remained relatively constant. Kurtosis decreased from -0.48 to -1.65 after 16 cycles. The kurtosis range of normality was  $\pm 1.58$  indicating that the profile shape is significantly non-normal after 16 cycles because kurtosis (-1.65) was out of the kurtosis range of normality. It indicates that the profile shape changed and became flatter (platykurtic) after 16 cycles.

Calculated statistical and apparent parameters show that under cycling conditions of downward flow being greater than upward flow, the solute profile shape and position changed as compared to the profile shape and position before cycling. The seasonal regime of downward flow is greater than upward flow simulates wet seasons in the field (net soil water movement is downward) assuming that the precipitation exceeds the evapotranspiration and there are vertical soil water and solute fluctuations. The result

shows that there is an effect of these fluctuations on the solute profile shape and position used by tracer methods for determining soil water fluxes. This effect is that the peak moved downward and the solute profile got flatter under the cycling conditions of this regime. Also, the solute profile changed from skewed downward to normally distributed after 16 cycles.

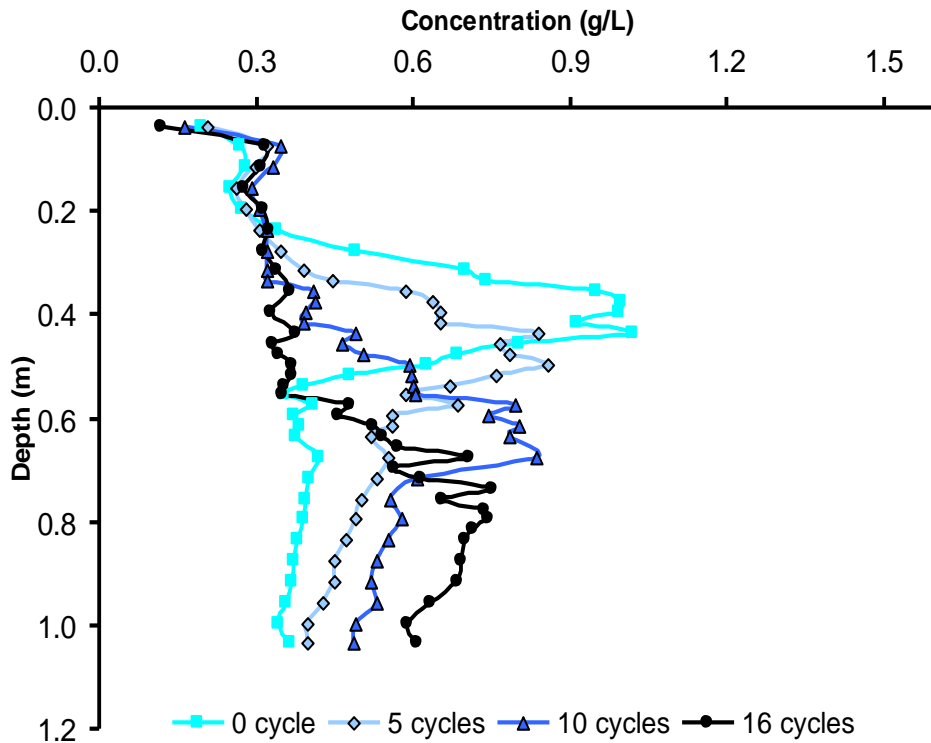


Figure 4.14: The change of the concentration profile shape under the cycling condition of upward flow < downward flow (column 2).

#### 4.3.3.1.3 Upward flow > downward flow

The third column focused on having a season of upward water flux greater than a season of downward water flux. The shape and position of the concentration profile changed under the repeated cycles of this regime (Table 4.14; Figure 4.15). The peak was difficult to determine at times and tended towards flatness after 15 cycles, then it was observed in the end of the cycling period. This could be due to instrument error and/or sand layers that were caused by packing. The peak concentration decreased with cycling, then increased slightly in the last five cycles as it neared the surface and became affected

by evaporation (that removes the water and leaves the salts behind). The distance between rising and falling points increased by 0.28 m after 20 cycles indicating that the solute profile became wider. The difference between the rising and falling points' concentrations decreased by 0.06 g L<sup>-1</sup> after 20 cycles.

Skewness values decreased with cycling during the first 15 cycles then increased at the end of the cycling. The profile was normally distributed during the first four cycles and then became skewed (tending towards upward or more negative). At the 10<sup>th</sup> and 15<sup>th</sup> cycles, the profile was significantly non-normal as indicated by the skewness range of normality ( $\pm 0.78$ ).

Table 4.14: Change of the profile shape at completion of cycles for column 3 (downward seasonal flow < upward seasonal flow).

Parameters	Number of cycles				
	0	5	10	15	20
Rising point	depth (m)	0.34	0.34	0.32	0.34
	conc. (g L <sup>-1</sup> )	0.34	0.41	0.46	0.60
Peak	depth (m)	0.68	0.68	0.50	0.40
	conc. (g L <sup>-1</sup> )	0.89	0.88	0.82	0.81
Falling point	depth (m)	1.00	1.06	1.06	1.06
	conc. (g L <sup>-1</sup> )	0.53	0.39	0.27	0.19
Mean (g L <sup>-1</sup> )	0.58	0.62	0.63	0.62	0.52
SD (g L <sup>-1</sup> )	0.18	0.16	0.16	0.18	0.25
Skewness	0.14	-0.08	-0.76	-1.36	-0.34
Kurtosis	-1.16	-1.24	-0.18	1.14	-0.83

conc. = concentration

The average concentration was relatively constant during the first 15 cycles and it decreased in the end of the cycling period. The calculated standard deviation also was relatively constant during the first 15 cycles and it increased in the end of the cycling period. Kurtosis values varied between -1.24 and +1.14, showing that the profile shape changed under the cycling conditions in term of peakedness (leptokurtic) and flatness (platykurtic). During the first 15 cycles, the profile was peaked (increase of kurtosis values) under the cycling condition. The kurtosis range of normality was  $\pm 1.52$  showing that there was no profile significantly non-normal because all calculated kurtosis values were within the kurtosis range of normality.

In conclusion, during the first 15 cycles, the width of the concentration profile was relatively constant under the cycling conditions; however, there was upward movement for the concentration peak. The concentration profile shape changed under the cycling conditions due to it being affected by evaporation (increase in concentration as it reached near the surface). These changes of the concentration distribution are a result of the upward movement, so distilled water entered from the bottom of the column and salts concentrated in the top part of the column.

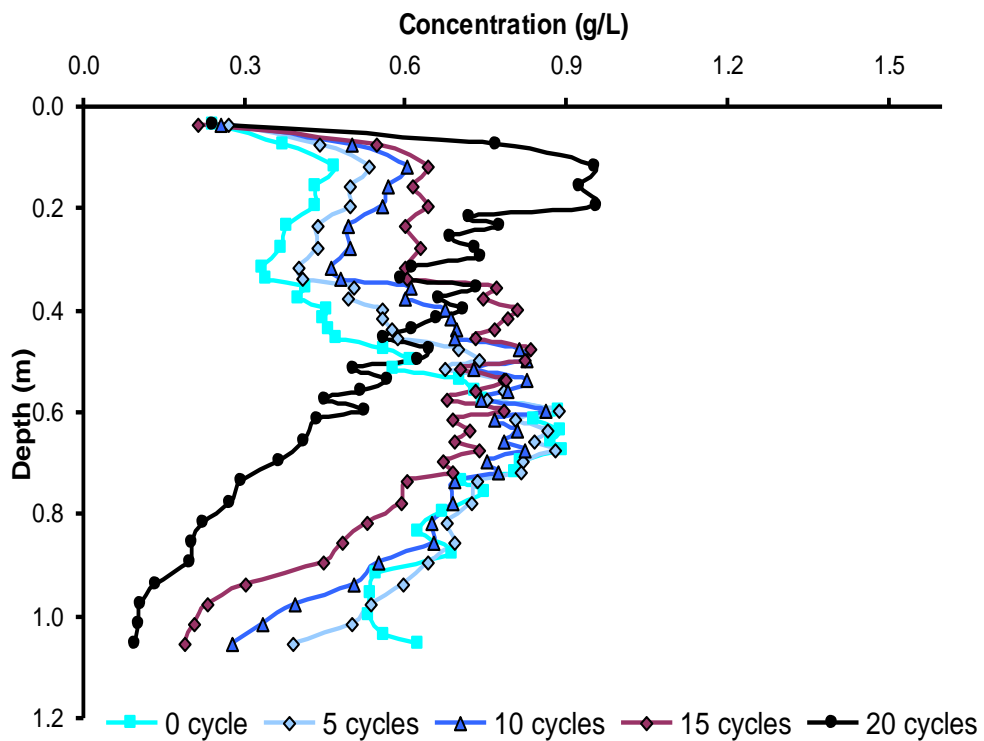


Figure 4.15: The change of the concentration profile shape under the cycling condition of upward flow > downward flow (column 3).

This flow regime (upward > downward flow) simulates a dry climate that might occur in the field. It was assumed that under the effect of climate, there was upward net movement for the concentration peak and vertical soil water fluctuations occurred. This simulation showed that soil water fluctuations affected the solute profile shape and position. These effects are that the peak moved upward and the solute profile got peaked under the cycling conditions of this regime. Also, the solute profile skewed upward after 15 cycles

of this regime. It indicates that these fluctuations can effect the calculations of soil water fluxes using the tracer profile methods because these methods are based on the solute profile shape and position.

#### **4.3.3.2 Comparing the change of profile shape among the three columns and summary**

The changes of the profile shape under cycling conditions of three directionally-varying flow regimes are compared in order to show and summarize the significance of simulating these regimes. The comparison was done by using a base measurement (Table 4.15) calculated as follows:

- The percentage of change of peak depths was calculated relative to the total sand column depth (1.05 m).
- The percentage of change of concentrations was calculated relative to the average concentration among the three columns ( $0.55 \text{ g L}^{-1}$ ).
- The percentage of change of the statistical parameters was calculated relative to the greatest change among the three columns.

The second objective of this thesis was to investigate the effect of cycling three different climatic regimes on solute profile shape and position. The profile shape refers to the distribution of solute concentration with depth in the column (soil profile). The profile position refers to the peak location or “depth” in the column (soil profile). Considering the effect of cycling climatic regimes on peak shape is also important. The peak shape is the solute distribution in the depth where the solute concentration increases from the baseline (Figure 3.2). The change of the peak shape is important because it shows the major change of the solute profile shape. However, the change of the peak shape under cycling the climatic flow regimes was not evaluated and discussed in this thesis because of the effect of column length limitations, so just the changes of the solute profile shape and position were discussed. The change of the peak depth under the cycling conditions was a result of the net movement in each column. For example, in column 2, the peak depth increased by 34% after 16 cycles because the net movement was downward. The

peak concentration, with time, decreased in columns 1 and 2, but it increased in column 3. The increase of the peak concentration in column 3 is likely due to the effect of evaporation in increasing the concentration of salt beneath the sand surface. The decrease of the peak concentration in columns 1 and 2 was due to the change of the profile shape (change of solute distribution with depth). The solute profile got wider under the cycling conditions in columns 1 and 3; however, there was not much change in the profile width in column 2 (movement dominantly downward). The difference in concentration between the rising and falling points decreased in columns 1 and 3, but it increased in column 2.

Table 4.15: Change\* of the profile shape at completion of cycles for the three columns (different regimes).

Parameters	Change* %		
	Column 1 Up=down	Column 2 Up<down	Column 3 Up>down
Rising point	depth (m)	-11	38
	conc. ( $\text{g L}^{-1}$ )	2	-18
Peak	depth (m)	6	34
	conc. ( $\text{g L}^{-1}$ )	-136	-50
Falling point	depth (m)	31	38
	conc. ( $\text{g L}^{-1}$ )	-11	-77
Width (m)	42	0	27
Mean ( $\text{g L}^{-1}$ )	18	3	11
SD ( $\text{g L}^{-1}$ )	82	23	23
Skewness	-47	-39	-20
Kurtosis	-40	-42	12

\* Change refers to the change between the last cycle and just before the first cycle.

Wideness refers to the distance between the rising point and the falling point depths.

The change of skewness with time shows that the profile in the three columns skewed upward in the column under the cycling conditions. Calculations of standard deviation showed that it increased under the three directionally-varying flow regimes. The change of kurtosis shows that the profiles in columns 1 and 2 got flatter (platykurtic) under the cycling conditions, but it peaked (leptokurtic) in column 3 after 20 cycles (it changed by 88% after 15 cycles). The profile became leptokurtic (peaked) in the end of the cycling period in column 3 because the peak was closer to the sand surface and salts concentrated at the top of the column. These results show that the limitation of the study was the

column length which affected the evaluation of the change of the profile shape and position under the cycling conditions.

Skewness, kurtosis, and the other statistical parameters used in this study have been used in different hydrological experiments. Farrell et al. (1994) used skewness, kurtosis, and other parameters to describe the solute distribution with depth in a plume when they computed the zeroth through the fourth spatial moments of a plume in a lower hydraulic conductivity zone (Ontario, Canada). Das et al. (2007) used skewness, kurtosis, and mean to describe a numerical solution of solute transport in a hypothetical, homogeneous, isotropic aquifer under constant seepage velocity. Alcolea et al. (2008) studied the effects of small scale variability of hydraulic conductivity on ground water contaminant transport and some of the subtle aspects of transport through heterogeneous media. They used skewness and kurtosis parameters to determine that the main difference between conditional estimation and simulation stems from the variability. However, no literature was found showing the evaluation and description of the change of solute profile shape and position under cycling conditions of different climatic regimes.

In this study, each regime simulated climatic seasons that might occur in the field. The regime of equal upward and downward flows simulated successive wet and dry seasons of equal intensity. These seasons assumed to have equal precipitation inputs to loss of water by evapotranspiration. The second regime of the downward flow season being greater than the upward flow simulated a wet climate, so precipitation exceeds evapotranspiration. The regime of the downward flow being less than the upward flow simulated a dry climate where evapotranspiration exceeds precipitation. Cycling the same climatic regime over years causes the vertical soil water fluctuation. These cycles occur in the field as a result of climatic effects. This investigation shows that the simulated vertical soil water fluctuations can affect the solute profile shape and position which are used commonly in the field for estimation of soil water and solute transport (tracer profile methods). The change of the solute profile shape might be a result of the change of the peak position (peak location), so when the concentration peak moves up or down, it might cause change of the solute distribution with depth. Also, these results show that the

profile shape and position after a number of cycles (years of fluctuations) can provide a description of the previous climatic effects on the concentration profile. For example, the solute profile shape after 20 cycles of the regime of upward greater than downward flow (Figure 4.15; ignoring the effect of the column length limitation) is different than the profile shape after 16 cycles of the regime of downward greater than upward flow (Figure 4.14). Under the cycling condition of upward flow being greater than downward flow, the peak moved upward, the solute profile got peaked, and the solute profile skewed upward after 15 cycles. However, the peak moved downward, the solute profile got flatter, and the solute profile changed from skewed downward to normally distributed after 16 cycles of downward flow being greater than upward flow. Therefore, the profile shapes determined in this study after a number of cycles of three different climatic regimes can be used as indicators of the flow regime that has affected the solute profile shape and position. That can be done by visually comparing a particular solute profile (solute profile that measured in the field) with solute profiles presented in this study or/and by considering parameters used in this study then comparing the numerical results with results showed in this thesis (Figures 4.13, 4.14, and 4.15; Tables 4.12, 4.13, and 4.14). For instance, if the profile is peaked, it indicates that the climatic regime that affected the solute profile is upward flow being greater than downward flow; however, if it is flat, it indicates that the regime is equal upward and downward flows or downward flow being greater than upward flow. Moreover, if a reference solute profile, from before the passage of many cycles, is available, it is easier to determine the flow regime by determining the change of the profile shape and position using the statistical methods. It can be done by comparing a particular solute profile with the initial solute profile that was measured before (determining the change of the solute profile after a period of time) using parameters used in this study (Table 4.15). For instance, if the solute profile is peaked (change of kurtosis value is positive) after a period of time, it indicates that the climatic flow regime that has affected the solute profile shape was dry (upward flow > downward flow). On the contrary, flatter solute profile (negative change of kurtosis) indicates that the climatic flow regime was wet (downward > upward) or wet and dry (downward = upward) (Table 4.15). Other parameters, such as width, can be used to determine if the regime is wet (downward > upward) or wet and dry (downward = upward). To determine

the effects of changing the profile shape on estimation of soil water fluxes using the tracer profiles, the soil water fluxes were determined under cycling conditions.

#### **4.3.4 Estimation of soil water fluxes under different regimes**

Solute concentrations and soil moisture data were used to calculate the soil water fluxes under different conditions of the three directionally-varying flow regimes using the peak migration method to the soil water balance method. The aim of estimating soil water fluxes under different conditions of the three regimes is to determine the effect of cycling these regimes on estimated soil water fluxes using tracer profile methods. Also, the comparison between the results from two methods (peak migration and soil water balance) will show the accuracy of estimating the soil water flux using concentration profile relative to that of the soil water balance method. The peak migration and the soil water balance methods were described in section 3.7. The contribution of dissolved salts from the sand was subtracted from the EC data measured by TDR, so there should be little effect of dissolved salts from the sand on the estimation of soil water fluxes.

Average net soil water flux in the column was estimated using both the peak migration and the soil water balance methods under each seasonal flow regime. The peak migration method used the average net peak movement after all the cycles were completed and the average soil moisture measured in the depth where the peak moved. The soil water balance method used the amount of water added and lost from the system and the change of moisture storage in the column after all cycles were completed. In the following subsections, the estimated average net, upward, and downward soil water fluxes will be discussed under each condition of directionally-varying flow regimes.

##### **4.3.4.1 Soil water fluxes in column 1 (downward flow = upward flow)**

The average net soil water flux after 20 cycles (77 days) of equal upward and downward flows was 0.38 and 0.48 mm d<sup>-1</sup> for the peak migration and the soil water balance methods, respectively. Note that the positive value indicates a net downward movement. Both the upward and downward fluxes estimated using the soil water balance

had smaller standard deviations than that using the peak migration method (Table 4.16; Figures 4.16 and 4.17).

Table 4.16: Average upward and downward flows estimated using the peak migration method and the water balance method under the regime of downward flow = upward flow (column 1).

Flow direction	Used method	Average Flux	Standard deviation
Upward flux (mm d <sup>-1</sup> )	Peak migration	-7.3	5.5
	Water balance	-5.2	1.5
Downward flux (mm d <sup>-1</sup> )	Peak migration	477.6	309
	Water balance	328.8	56

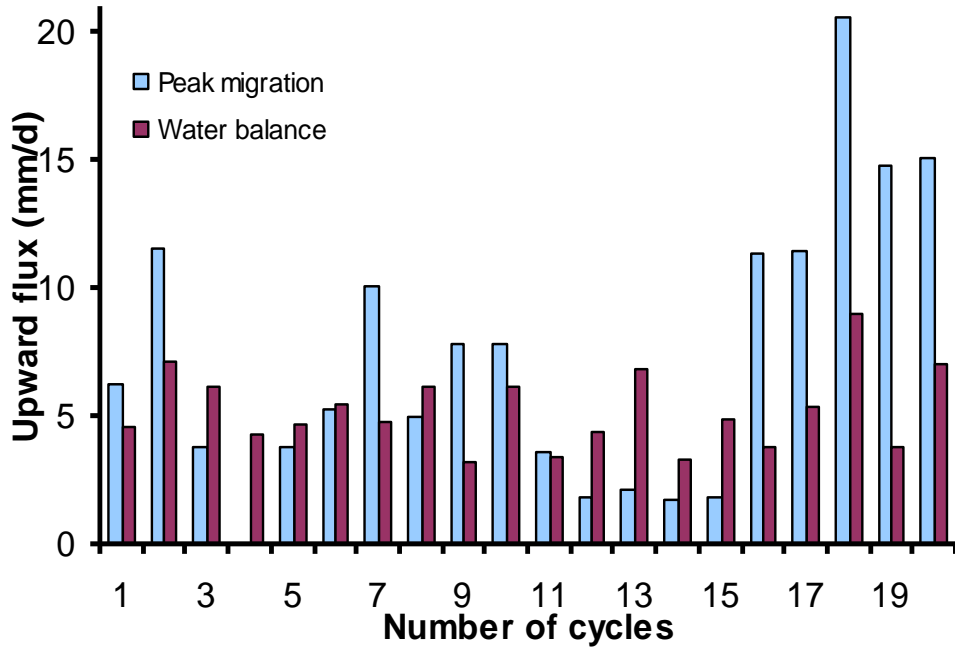


Figure 4.16: Upward soil water flux using peak migration method and soil water balance method under the cycling conditions of upward flow being equal to downward flow (column 1).

The upward and downward fluxes, estimated using the peak migration method, were relatively high in value near the end of the cycling period (Figures 4.16 and 4.17). The average estimated upward and downward soil water fluxes for each cycle using the peak migration method were higher by 29 and 31% relative to higher flux, respectively than that estimated using the soil water balance method. Data used for calculating the upward and downward fluxes show that the peak migration gave higher flux in the end of the

cycling period because the peak moved faster during this period compared to that at the beginning of the cycling period. No explanation for this is currently apparent.

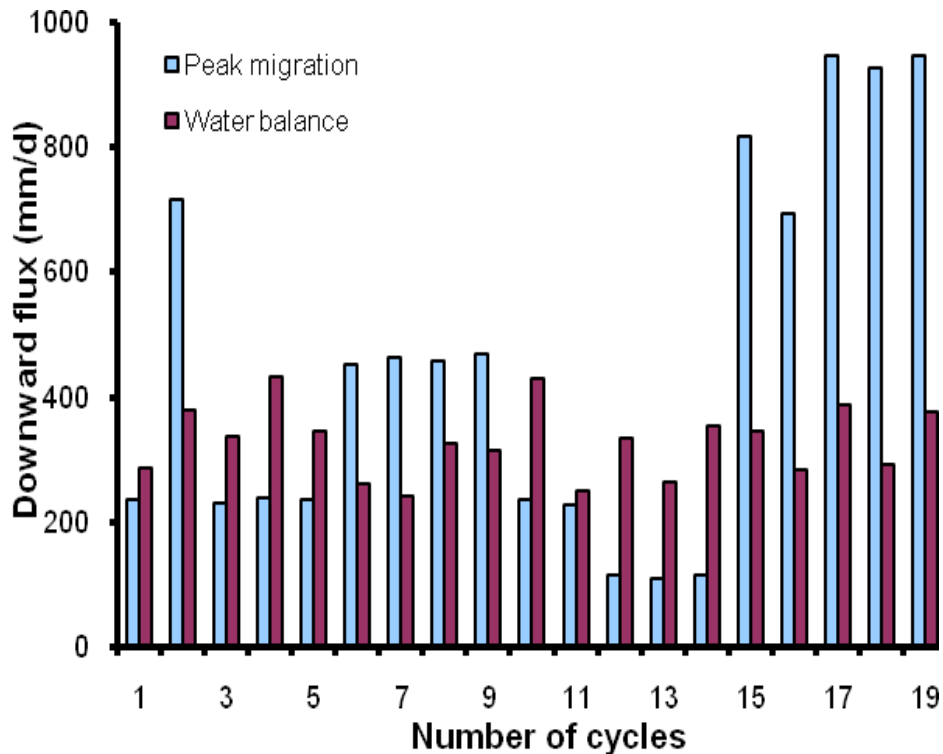


Figure 4.17: Downward soil water flux using peak migration method and soil water balance method under the cycling condition of upward flow being equal to downward flow (column 1).

#### 4.3.5.2 Soil water fluxes in column 2 (downward flow > upward flow)

The average net soil water flux for the study period (51 days) under the cycling conditions of downward flow is greater than upward flow, was  $3.41$  and  $1.42 \text{ mm d}^{-1}$  for the peak migration method and the soil water balance method, respectively. The average net flux for the peak migration method was higher (by 58% relative to the higher flux) than that estimated using the soil water balance method. Thus, the peak migration method overestimated the flux (by 140% relative to the water balance method) indicating that the peak migration method did not give the actual average net soil water flux under the cycling conditions of downward flow being greater than upward flow. The estimated upward and downward fluxes for each cycle using the water balance method were less

variable (lower standard deviation) than that estimated using the peak migration method (Table 4.17; Figures 4.18 and 4.19).

Table 4.17: The variation of upward and downward flows estimated using the peak migration method and the water balance method under the regime of downward flow > upward flow (column 2).

Flow direction	Used method	Average of flux	SD
Upward flux (mm d <sup>-1</sup> )	Peak migration	-4.3	4.8
	Water balance	-4.8	1.8
Downward flux (mm d <sup>-1</sup> )	Peak migration	377	279
	Water balance	329	64

Average flux and standard deviation were calculated including zero flux values.

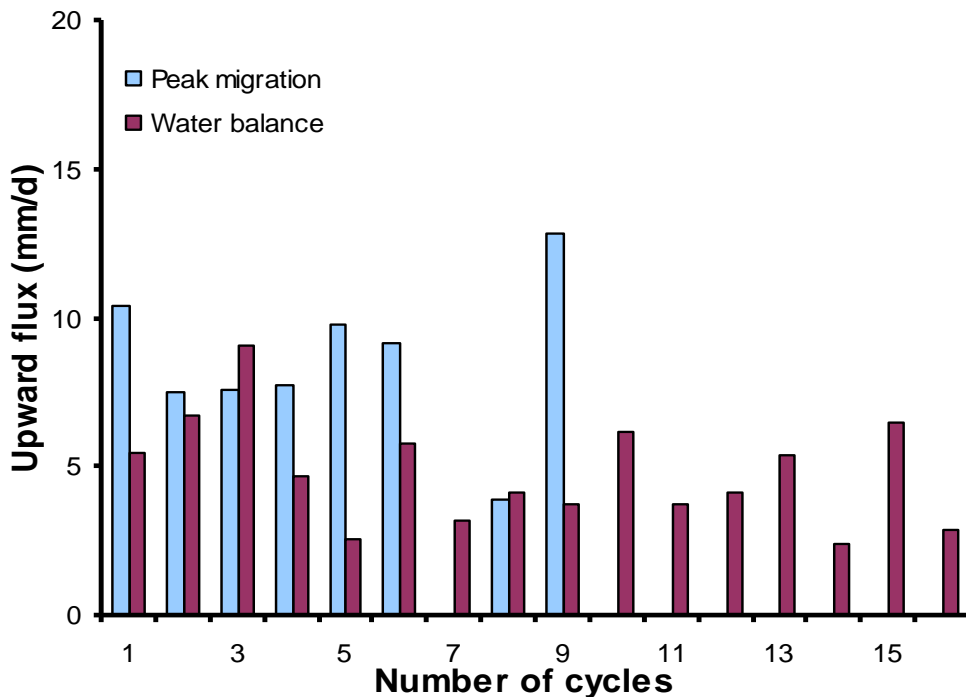


Figure 4.18: Upward soil water flux for each cycle under conditions of downward flow being greater than upward flow (column 2). The absence of values refers to zero flux.

However, both methods gave a similar average for upward soil water flux. Due to the lack of movement of the peak for numerous upward cycles (10<sup>th</sup> to 16<sup>th</sup>) and downward cycles (11<sup>th</sup>, 12<sup>th</sup>, 13<sup>th</sup>, and 15<sup>th</sup> cycles) zero flux occurred for these cycles. The fluxes in

these cycles can be low (but not zero) because the vertical distance between each two TDR probes in the column was 20 mm, and the peak might move within this depth without monitoring it. The reason, why the flux was low (or absent) in the end of the evaporation periods and some of the raining periods, is not clear.

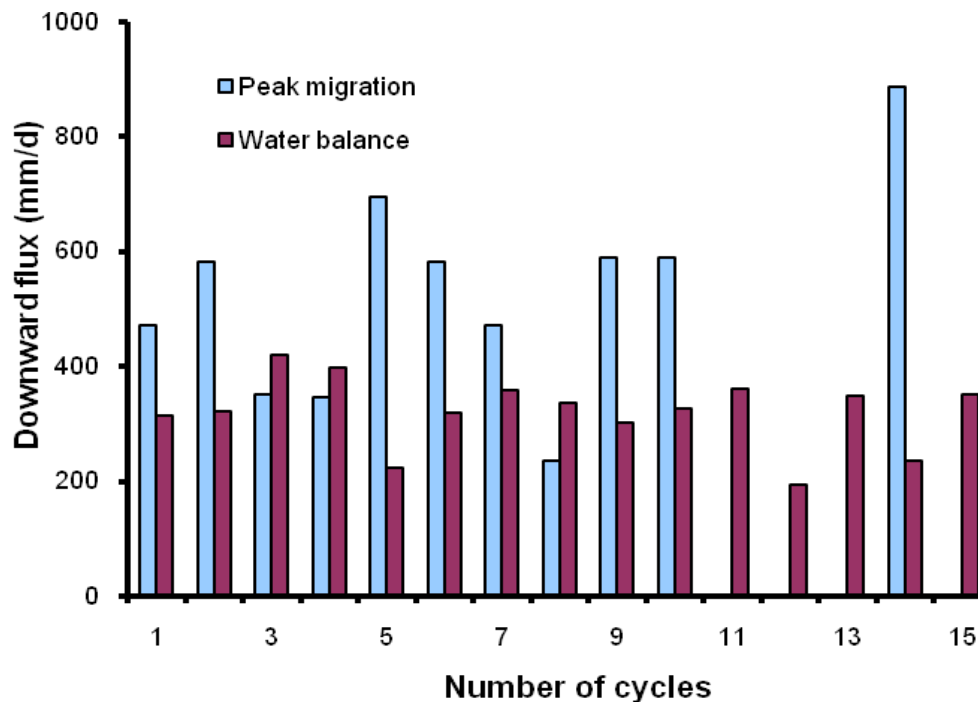


Figure 4.19: Downward soil water flux for each cycle under conditions of downward flow being greater than upward flow (column 2). The absence of values refers to zero flux.

#### 4.3.5.3 Soil water fluxes in column 3 (upward flow > downward flow)

The average net soil water flux for the study period (78 days) under the cycling conditions of upward flow being greater than downward flow was  $2.40$  and  $2.27 \text{ mm d}^{-1}$  for the peak migration and the soil water balance methods, respectively. The estimated soil water flux using the peak migration method was relatively similar (by 5% relative to higher flux) to that estimated using the soil water balance method. The water balance method gave less variable (lower standard deviation) results of upward and downward soil water fluxes than that from the peak migration method (Table 4.18; Figures 4.20 and 4.21).

Table 4.18: The variation of upward and downward flows estimated using the peak migration method and the water balance method under the conditions of upward flow > downward flow.

Flow direction	Used method	Average of flux	SD
Upward flux (mm d <sup>-1</sup> )	Peak migration	-5.5	3.7
	Water balance	-6.1	1.8
Downward flux (mm d <sup>-1</sup> )	Peak migration	242	205
	Water balance	314	112

Average flux and standard deviation were calculated including zero flux values.

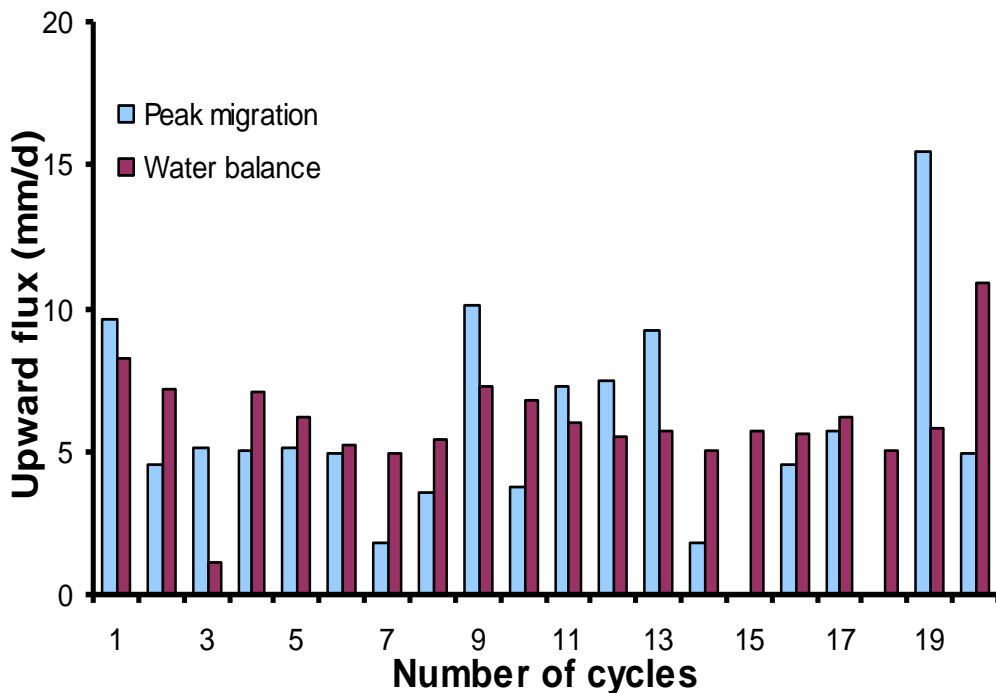


Figure 4.20: Upward soil water flux for each cycle under cycling conditions of upward flow being greater than downward flow (column 3). The absence of values refers to zero flux.

The estimated downward soil water flux shows that both methods had relatively similar behavior in the period between the fourth and thirteenth cycles (Figure 4.21). The peak migration method gave zero downward soil water flux at the end of the experiment period. This could be due to the peak moving to the region in the column where the sand is not saturated.

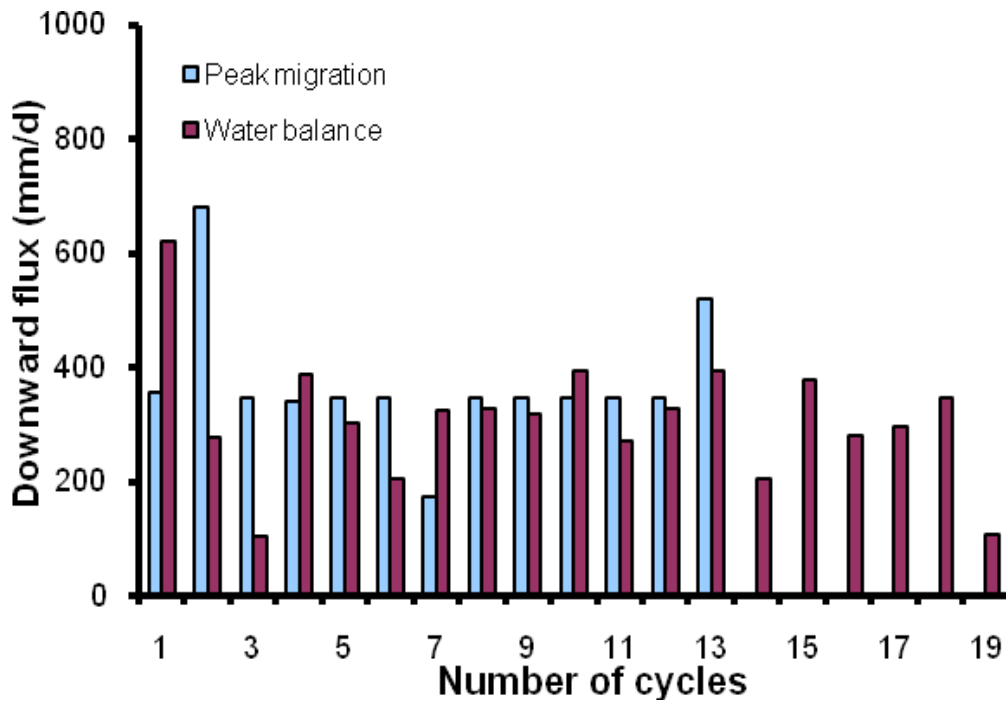


Figure 4.21: Estimated downward soil water flux for each cycle under cycling conditions of upward flow being greater than downward flow (column 3). The absence of values refers to zero flux.

#### 4.3.4.4 Comparison of estimated fluxes among the three regimes and summary

The average net soil water flux for conditions of downward flow being greater than upward flow (column 2) showed that the peak migration method gave a relatively higher average net soil water flux than that estimated using the water balance method. However, under the regime of equal upward and downward flows, the estimated average net flux using the water balance method was relatively higher. The estimated average net soil water flux using both methods was relatively similar under the regime of upward flow being greater than downward flow (Table 4.19). It indicates that the peak migration method did not give the actual average net soil water flux in the sand column under the cycling conditions of upward flow equal to downward flow (column 1) and downward flow being greater than upward flow (column 2) assuming that the soil water balance gives the actual flux. The differences of estimated average net soil water flux can be related to the accuracy of determining the water balance and the peak migration parameters (section 3.12). The average net estimated soil water flux in column 1 was low

relative to that in the other columns due to the simulated seasonal flow regime (equal upward and downward flows).

The soil water balance method gave more constant results of upward and downward fluxes for each cycle than that estimated using the peak migration method in the three columns. That can be because there is 20 mm vertical distance between each pair of TDR probes, so the peak depth can not be determined within this depth. Also, it can be because the soil water balance gives a total flux for the column each time it was calculated. There were no upward and downward peak movement in the end of the experiment time in columns 2 and 3, respectively (Figures 4.22 and 4.23).

Table 4.19: Average net soil water flux using the peak migration and the water balance methods in the three sand columns.

Method	Average net soil water flux ( $\text{mm d}^{-1}$ )		
	Column 1	Column 2	Column 3
	Up=down	Up<down	Up>down
Peak migration	0.38	3.41	-2.40
Soil water balance	0.48	1.92	-2.27

The column length might affect the peak migration calculations because the peak might be influenced by the column end (columns 2 and 3). The difference between estimated flux using the peak migration and the soil water balance methods might be because of the short cycling period (3 to 4 days), so estimated fluxes might be affected by switching flow direction and flux takes time to be established in the beginning of each flow period (rain and evaporation). Also, there is possibility of presence of layers caused by packing, which can hold the soil water movement, might cause variations of estimated fluxes using one of the methods. The three regimes represent three different seasonal flow regimes that might occur in the field. The result from this investigation was not compared with other results because no literature was found showing estimated soil water fluxes in a soil column using any tracer method and the soil water balance method. This investigation shows that under the conditions of cycling an equal flow regime (equal upward and downward flows, column 1) and a wet regime (downward flow season is greater than upward, column 2), the tracer method did not give an accurate flux assuming that the soil water balance gives the actual flux.

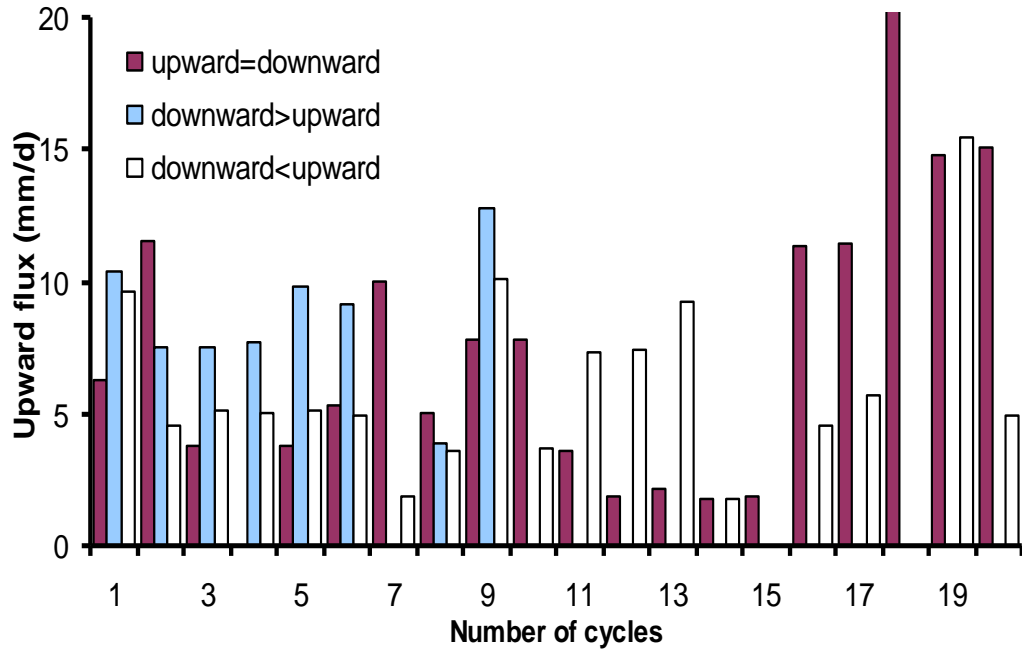


Figure 4.22: Estimated upward flux using the peak migration method under each regime of upward and downward flows (under the condition of downward flow > upward flow, only 16 cycles were done). The absence of values refers to “zero” flux.

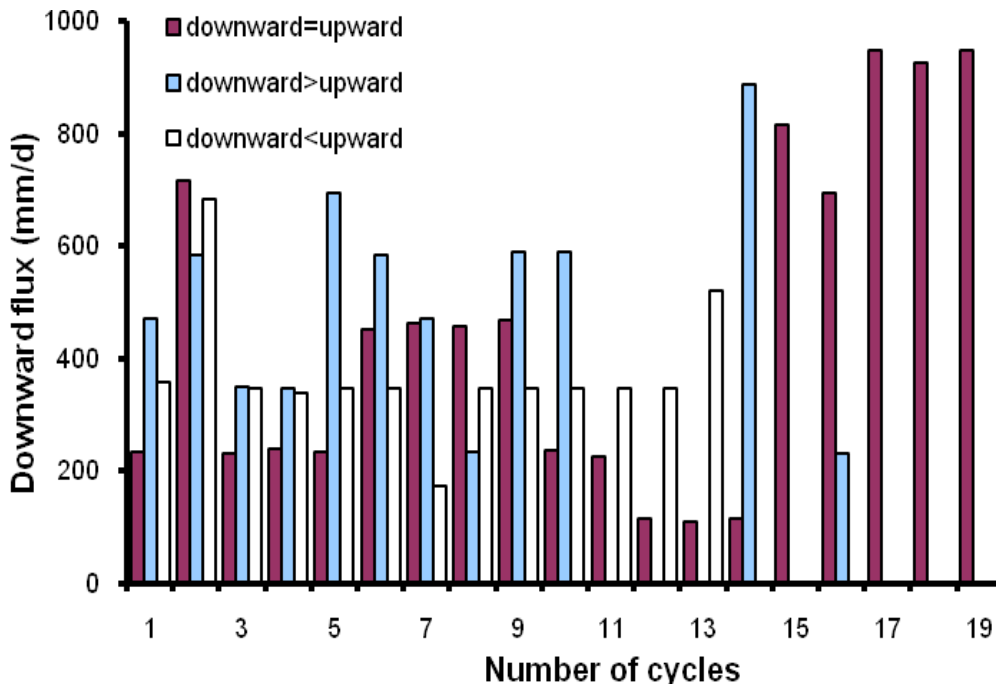


Figure 4.23: Estimated downward flux using the peak migration method under each regime of upward and downward flows (under the condition of downward flow > upward flow, only 16 cycles were done). The absence of values refers to “zero” flux.

However, under the cycling conditions of a dry regime (upward greater than downward, column 3) the peak migration gave a similar result of average net flux to that obtained using the soil water balance method. This result shows the effect of the change of the peak position, caused due to the effects of vertical soil water fluctuation (seasonality), on estimation of soil water fluxes using the tracer profile methods. Also, this investigation shows that under cycling conditions (vertical soil water fluctuation) the peak migration method gives more variable fluxes compared to the soil water balance method.

## CHAPTER 5: SUMMARY AND CONCLUSIONS

The first objective of this thesis was to show the capability of TDR for determination of soil water fluxes using tracer methods. The peak migration and the soil water balance methods gave similar average upward and downward soil water fluxes; however, individual fluxes did not always agree. The estimated upward soil water flux using both methods varied with time. The soil water balance method gave higher upward fluxes most of the time. This result of estimated upward and downward fluxes indicates that tracer methods using a TDR, can be recommended for determination of soil water fluxes in natural conditions or in laboratory studies for over adequate time periods and depth intervals. An advantage with the peak migration method is that it shows greater spatial and temporal resolution than that of the water balance method.

The second objective of this thesis was to investigate the effects of repeated cycles of directionally-varying flows upon solute profile shape and position used by tracer methods. The relevance of this objective is to determine the accuracy of the tracer method in determining long-term net flux values in deep unsaturated systems under directionally varying flows. The major result was that the solute profile shape and position clearly changed under the three repeated regimes of downward and upward seasonal flows. Several apparent and statistical parameters were calculated and considered to compare the change of the concentration profile shape and position under the cycling conditions among the three regimes. The distance between the rising and falling points got wider under the regimes of equal upward and downward flows (column 1) and greater upward flow than downward flow (column 3) after 20 cycles, but there was no change under the regime of greater downward flow than upward flow (column 2) up to 16 cycles. The regimes that had the greatest change in depth of rising point, peak, and falling point were those whose net movement was dominantly downward or upward (columns 2 and 3). Skewness of the profile shape changed with time under all three regimes with skew values becoming more negative (higher solute concentrations are in the upper part of the column). Kurtosis was used to measure the ‘peakedness’ of the profile shape. Kurtosis changed with time, showing that for regimes of equal upward and

downward flow and for greater downward flow than upper, that the profile shape got flatter (platykurtic). Under the regime of greater upward flow, the kurtosis indicated more peaked (leptokurtic) conditions with time. The profile for column 3 became leptokurtic at the end of the cycling period because the peak was closer to the sand surface and salts concentrated in the top of the column. In this study, three seasonal flow regimes simulated three natural climates that might occur beneath the root zone. The regime of equal upward and downward flows simulates wet and dry seasons of equal intensity. The regime of downward flow greater than upward flow simulates climatic conditions where wet season has a greater downward flow than the dry season. The regime of upward flow greater than downward flow simulates a dry climate where there is a greater amount of water removed (due to evapotranspiration) than that added through precipitation. It was concluded that climate that has such distinct seasons can have significant impacts on the estimation of soil water fluxes using tracer methods. Since tracer methods, based on solute profile shape and position, are commonly used for estimation of soil water fluxes, the change of the profile shape and position under the climatic effects (vertical soil water fluctuations) can affect the accuracy of these flux estimations. Under the flow regime of upward flow being greater than downward flow, the peak moved upward, the solute profile got peaked, and the solute profile skewed upward after a number of cycles. However, the solute profile got flatter and changed from skewed downward to normally distributed after a number of cycles of equal upward and downward flows and downward flow being greater than upward flow. The peak moved downward under the regime of downward being greater than upward and it remained relatively at the same depth under the regime of equal seasonal flows. The result from this investigation shows that the profile shape and position after a number of cycles (years of seasonally caused moisture flow fluctuations) can provide a description of the previous climatic effects on the concentration profile. Therefore, the profile shape can be used as an indicator of the flow regime that has affected the solute profile shape. That can be done by visually comparing a particular solute profile with concentration profiles presented in this study and/or by considering the parameters used in this study (e.g. peak position, skewness, kurtosis, and width) then comparing the numerical results with results showed in this thesis. The result from visual or calculation comparisons can be considered generally in term of

peakedness, skewed distribution, width, and the peak position. Moreover, if a reference of solute profile is available (a solute profile before a period of time), it is easier to determine whether the flow regime affected the profile shape and position by determining the change of the profile shape and position using the statistical parameters. It can be done by comparing a particular solute profile with the reference solute profile that was measured before (determining the change of the solute profile) using parameters used in this study, then comparing the result of the change of the profile shape and position with results found in this thesis.

The estimated average net soil water flux using the peak migration method was relatively higher than that estimated using the soil water balance method under the cycling conditions of downward flow being greater than upward flow (column 2). However, under the regime of equal upward and downward flows (column 1) the estimated average net flux using the water balance method was relatively higher. The average net soil water flux estimated using both methods was relatively similar under the regime of upward flow being greater than downward flow (column 3). The upward and downward fluxes were estimated using the peak migration and the water balance methods also in each cycle. The water balance method gave more constant results than that estimated using the peak migration method in the three columns during the study period. The results showed that the limitation of the column length and the vertical distance between each two TDR probes might have an effect on the estimated upward and downward fluxes using the peak migration method. Also, the short cycling period for each cycle (3 to 4 days) and the possibility of the presence of sand layers might have an effect on the upward and downward fluxes. Indeed, this investigation shows that under the condition of cycling wet and dry seasons (equal upward and downward flows) and wet seasons (downward greater than upward), the tracer method did not give the actual average net flux assuming that the soil water balance gives the actual flux. The difference between estimated flux by peak migration and soil water balance methods was 21 and 44% relative to higher flux, for regimes of equal upward and downward flows and greater downward flow, respectively. However, under the conditions of cycling dry seasons (upward greater than downward) the peak migration gave a similar result of the average net soil water flux to

the soil water balance. This result shows the effect of the change of the profile shape, caused by vertical soil water fluctuation (seasonality), on estimation of soil water fluxes using the tracer profile method. Also, this investigation shows that under cycling conditions (vertical soil water fluctuation), the peak migration method gives variable individual fluxes (greater standard deviation) compared to the soil water balance method under the three climatic regimes.

## 5.1 Recommendations for future work

Recommendations towards improving methods and thus confirming the results would be:

1. Using different soils: The Beaver Creek sand was used in this study to better control soil porosity and pore size distribution and to avoid cracks and aggregates such that would occur with soils with any clay content. For future work, and because of the difficulty of doing the same research in the field, the same objectives can be investigated using different soils such as clay or loam soils under controlled laboratory conditions. Using other soils also gives the opportunity of investigating the effects of soil texture on the capability of TDR with tracer methods of estimating solute and soil water fluxes, and on the effect of seasonality upon solute and soil water movement. Layered soils also can be used to investigate the same objectives.
2. Being able to verify packing homogeneity with depth: One of the difficulties in this study was the possibility of the presence of layers in the sand column caused by the packing method. These layers can affect the estimated soil water flows and the solute profile shape and position. Therefore, the packing method used in this study should be improved and that the soil column used is homogeneous. Another packing method also can be used.
3. Having sand with no precipitated salts: Contribution of salts from sand to the solution was monitored in the beginning of the study. This contribution effected the evaluation of the change of the solute profile shape, so it was simulated and

- subtracted from the measured EC data by TDR. As a recommendation, sand with no precipitated salts is preferred for similar studies in order to avoid the effect of the salt contribution on the change of the solute profile shape.
4. Having replicate regimes within different columns: In this study, the effects of three different directionally-varying flow regimes of upward and downward flows on the solute profile shape and position were investigated using three sand columns. Each sand column represented one of the flow regimes. However, replication for each regime should be done using different sand columns to evaluate the accuracy and the significance of reached results. We were unable to do regime replications because of time limitations.
  5. Increasing the length of the sand column: Several apparent and statistical parameters were used in this study to evaluate the change of the solute profile shape and position in the sand column under different cycling conditions. One of these parameters was the depth and concentration of the rising and falling points of the solute profile. In some of the concentration profiles, and when the solute profile gets closer to the upper end or the bottom end of the sand column, it was difficult to observe the depth and concentration of the rising and the falling points. Also, the limitation of the sand column length might have an effect on the estimation of the soil water fluxes. Therefore, longer sand columns are recommended for similar studies, so the rising and falling points are not affected by the column ends. Also, the change of the peak shape can be evaluated instead of evaluating the solute profile shape if longer columns are used.
  6. Investigating the accuracy of using other tracer methods such as the mass balance method for determination of soil water fluxes in field and laboratory studies: The first objective of this thesis was to investigate the capability of TDR for estimation of soil water fluxes using tracer methods, and to investigate the accuracy of a tracer method used for estimation of soil water fluxes. The tracer method used in this study was the peak migration method and its performance was tested by comparing the results of upward and downward fluxes with the results from the soil water balance method assuming that the soil water balance method gives the actual soil water fluxes. The accuracy of other tracer methods

such as the tracer mass balance method can also be evaluated using the same methods used in this study. The accuracy of the tracer mass balance method was not investigated in this study because distilled water was used for “rain” and the tracer mass balance method requires known additional concentration to the system.

7. Investigating the same objectives using unsaturated sand columns: Although, the main objective of this thesis was investigating the effects of seasonality upon water and solute movement in the unsaturated zone, the sand columns used in this study were not unsaturated. The water table was raised to 0.32 m beneath the sand surface in order to enhance the evaporation rate from the sand surface, and to develop sufficient upward soil water flux in the sand column such that the project could be completed within the required time frame. For future work, unsaturated sand columns should be used to investigate the same objectives and to simulate the field conditions of the semiarid and arid environments.
8. Investigating the effects of the water table fluctuations on the tracer profile used for estimation of soil water fluxes: The water table and the capillary fringe in natural environments fluctuate at different time scales ranging from hours to years (Freeze and Cherry 1979). Moreover, the water table may affect the solute profile shape and position. Hinz (1998), Yang and Yanful (2002), and others assessed the general behavior of water flow near a fluctuating water table; however, the effect of the water table fluctuating on the solute profile shape and position used for estimating soil water fluxes needs to be investigated.

## REFERENCES

- Acton, D.F. and J.G. Ellis. 1978. *Soil of the Saskatoon Map Area 73-B Saskatchewan.* Saskatoon, SK: Extension Division, University of Saskatchewan.
- Alcolea, A., J. Carrera and A. Medina. 2008. Regularized pilot points method for reproducing the effect of small scale variability: Application to simulations of contaminant transport. *Journal of Hydrology* 355: 76-90.
- Allison, G. and M. Hughes. 1974. Environmental tritium in the unsaturated zone: Estimation of recharge to an unconfined aquifer. pp. 57-72. Isotope techniques in groundwater hydrology. IAEA, Vienna.
- Allison, G. and M. Hughes. 1978. The use of environmental chloride and tritium to estimate total recharge to an unconfined aquifer. *Australian Journal of Soil Research* 16: 181-195.
- Allison, G. and M. Hughes. 1983. The use of natural tracer as indicators of soil water movement in temperate semiarid region. *Journal of Hydrology* 60: 157-173.
- Allison, G. 1987. A review of some physical chemical and isotopic techniques available for estimating groundwater recharge. In *Estimation of Natural Groundwater Recharge* 222: 49-72. Editor I. Simmers, NATO ASI Series C.
- Allison, G., G. Gee and S. Tyler. 1994. Vadose-zone techniques for estimating groundwater recharge in arid and semiarid regions. *Soil Science Society of America Journal* 58: 6-14.
- Amente, G., J. Baker and C. Reece. 2000. Estimation of soil solution electrical conductivity from bulk soil electrical conductivity in sandy soils. *Soil Science Society of America Journal* 64: 1931-1939.
- Armstrong, A., D. Rycroft and T. Tanton. 1996. Seasonal movement of salts in naturally structured saline-sodic clay soils. *Agricultural Water Management* 32: 15-27.
- Balasubramanian, V., L. Ahuja, Y. Kanehiro and R. Green. 1976. Movement of water and nitrate in an unsaturated aggerated soil during non-steady infiltration-a simplified solution for solute flow. *Soil Science* 122: 245-255.
- Bekele, E., R. Salama and D. Commander. 2006. Impact of change in vegetation cover on groundwater recharge to a phreatic aquifer in Western Australia:

- assessment of several recharge estimation techniques. *Australian Journal of Earth Sciences* 53: 905-917.
- Bonsal, B., X. Zhang and W. Hogg. 1999. Canadian Prairie growing season Precipitation variability and associated atmospheric circulation. *Climate Research* 11: 191-208.
- Brown, S. 2008. Skewness and kurtosis on the T1-83/84.  
<http://www.tc3.edu/instruct/sbrown/ti83/skurt.htm>. June 14, 2008.
- Bruch, P.G. 1993. A laboratory study of evaporative fluxes in homogeneous and layered Soils. Unpublished M.Sc. thesis. Saskatoon, SK: Department of Civil Engineering, University of Saskatchewan.
- Burford, R.L. 1968. *Statistics: A Computer Approach*. Columbus, Ohio: Charles E. Merrill Publishing Company.
- Buttle, J. and D. Leigh. 1995. Isotopic and chemical tracing of macropore flow in laboratory columns under simulated snowmelt conditions. Tracer Technologies for Hydrological Systems. Proceedings of a Boulder Symposium, July 1995. IAHS Publ. no. 229, pp. 67-76.
- Champion, D.J. 1970. *Basic Statistics for Social Research*. Scranton, Pennsylvania: Chandler Publishing Company.
- Chen, Y., M. Shi and X. Li. 2006. Experimental investigation on heat, moisture and salt transfer in soil. *International Communications in Heat and Mass Transfer* 33: 1122-1129.
- Christie, H.W., D. Graveland and C. Palmer. 1985. Soil and subsoil moisture accumulation due to dryland agriculture in southern Alberta. *Canadian Journal of Soil Science* 65: 801-810.
- Dahiya, I.S., M. Singh, J. Richter and M. Singh. 1984. Leaching of soluble salt during infiltration and redistribution. *Irrigation Science* 5: 15-24.
- Daniels, D., S. Fritz and D. Leap. 1991. Estimating recharge rates through unsaturated glacial till by tritium tracing. *Groundwater Journal* 29: 26-34.
- Danquigny, C., P. Ackerer and J. Carlier. 2004. Laboratory tracer tests on three-

- dimensional reconstructed heterogeneous porous media. *Journal of Hydrology* 294: 196-212.
- Das, S., A. Warke and R. Gorla. 2007. Qualitative study to assess the effect of a subsurface barrier on contaminant transport in groundwater: computation of moments. *International Journal of Fluid Mechanics Research* 34: 210-223.
- Derby, N. and R. Knighton. 2001. Field preferential transport of water and chloride tracer by depression-focused recharge. *Journal of Environmental Quality* 30: 194-199.
- Dey, B. 1982. Nature and possible causes of droughts on the Canadian Prairies-case studies. *Journal of Climatology* 2: 233–249.
- Dregne, H.E. and W. Willis. (Eds.). 1983. *Dryland Agriculture*. Madison, Wisconsin: Soil Science Society of America, Inc., Publishers.
- Dyck, M., R. Kachanoski and E. de Jong. 2003. Long-term movement of a chloride tracer under transint, sime-arid conditions. *Soil Science Society of America Journal* 67: 471-477.
- Ebramimi-Birang, N., C. Maule and W. Morley. 2006. Calibration of a TDR instrument for simultaneous measurements of soil water and soil electrical conductivity. *American Society of Agriculture and Biological Engineering* 49: 75-82.
- Edmunds, W., E. Fellman, J. Goni and C. Prudhomme. 2002. Spatial and temporal distribution of groundwater recharge in northern Nigeria. *Hydrogeology Journal* 10: 205-215.
- Farrell, D., A. Woodbury and E. Sudicky. 1994. The 1978 Borden tracer experiment: Analysis of the spatial moments. *Water Resources Research* 30: 3213-3223.
- Ferre, P., J. Redman, D. Rudolph and R. Kachanoski. 1998. The dependence of the electrical conductivity measured by time domain reflectometry on the water content of a sand. *Water Resources Research* 34: 1207-1213.
- Freeze, R.A. and J.A. Cherry. 1979. *Groundwater*. Englewood Cliffs, NJ: Prentice-Hall.
- Fullerton, S. and S. Pawluk. 1987. The role of seasonal salt and water fluxes in the

- genesis of solonetzic B horizons. *Canadian Journal of Soil Science* 67: 719-730.
- Gardner, W.R. 1958. Some steady-state solutions of the unsaturated flow equation with application to evaporation from a water table. *Soil Science* 85: 228-232.
- Gaye, C. and A. Editor. 2001. Isotope techniques for monitoring groundwater salinization. *Hydrogeology Journal* 9: 217-218.
- Gaye, C. and W. Edmunds. 1996. Groundwater recharge estimation using chloride, stable isotopes and tritium profiles in the sands of northwestern Senegal. *Environmental Geology* 27: 246-251.
- Gee, G. and D. Hillel. 1988. Groundwater recharge in arid regions: review and critique of estimation methods. *Hydrological Processes* 2: 255-266.
- Ghuman B.S. and S. Prihar. 1980. Chloride displacement by water in homogeneous columns of three soils. *Soil Science Society of America Journal* 44: 17-21.
- Ghuman, B.S., S. Verma and S. Prihar. 1975. Effect of application rate, initial soil wetness, and redistribution time on salt displacement by water. *Soil Science Society of America Journal* 39: 7-10.
- Granger, R., D. Gary and G. Dyck. 1984. Snowmelt infiltration to frozen prairie soils. *Canadian Journal of Earth Science* 21(6): 669-677.
- Gray, D. 1986. Snow hydrology of the prairie environment. Snow Hydrology. Canadian National Committee; The International Hydrological Decade. Proceedings of the Workshop Seminar, University of New Brunswick, Feb. 28 and 29: 21-33.
- Hart, G. and B. Lowery. 1998. Measuring instantaneous solute flux and loading with time domain reflectometry. *Soil Science Society of America Journal* 62: 23-35.
- Harvey, F. 2001. Use of NADP archive samples to determine the isotope composition of precipitation: Characterizing the meteoric input function for use in groundwater studies. *Ground Water* 39(3): 380-390.
- Healy, R. and P. Cook. 2002. Using groundwater levels to estimate recharge. *Hydrogeology Journal* 10(1): 91-109.

Heimovaara, T. 1995. Assessing temporal variation in soil water composition with time domain reflectometry. *Soil Science Society of America Journal* 59: 689-698.

Hillel, D. 1980. *Applications of Soil Physics*. New York: Academic Press.

Hillel, D. 1998. *Environmental Soil Physics*. New York: Academic Press.

Hinz, C. 1998. Analysis of unsaturated/saturated water flow near a fluctuating water table. *Journal of Contaminant Hydrology* 33: 59-80.

Hook, W. and N. Livingston. 1995. Errors in converting time domain reflectometry measurements of propagation velocity to estimates of soil water content. *Soil Science Society of America Journal* 60(1): 35-41.

Hsieh, J., O. Chadwick, E. Kelly and S. Savin. 1998. Oxygen isotopic composition of soil water: Quantifying evaporation and transpiration. *Geoderma* 82: 269-293.

Idso, S., R.J. Reginato, R.D. Jackson, B.A. Kimball and F.S. Nakayama. 1974. The three stages of drying of a field soil. *Soil Science Society of America* 38(5): 831-837.

Johnston, M. 1994. An evaluation of the four-electrode and electromagnetic induction techniques of soil salinity measurement. Water Research Commission Report No. 269/1/94, South Africa, p. 191.

Joshi, B. and C. Maule. 2000. Simple analytical model for interpretation of environmental tracer profiles in the vadose zone. *Hydrological Process* 14: 1503-1521.

Joshi, B. 1997. Estimation of diffuse vadose zone soil-water flux in a semi-arid region. Unpublished Ph.D. thesis. Saskatoon, SK: Department of Agricultural and Bioresource Engineering, University of Saskatchewan.

Jury, W. and K. Roth. 1990. *Transfer functions and solute movement through soil: Theory and application*. Birkhauser. Basel and Boston.

Jury, W., W.R. Gardner and W.H. Gardner. 1991. *Soil Physics*. New York: John Wiley and Sons, Inc.

Kirda, C., D.R. Nielsen and J.W. Biggar. 1973. Simultaneous transport of chloride and water during infiltration. *Soil Science Society of America Journal* 37: 339-345.

- Kirkham, D. and W. Powers. 1972. *Advanced Soil Physics*. New York: Wiley-interscience, John Wiley and Sons, Inc.
- Konukcu, F., A. Istanbulluoglu and I. Kocaman. 2004. Determination of water content in drying soils: incorporating transition from liquid phase. *Australian Journal of Soil Research* 42: 1-8.
- Kowalik, P.J. 2006. Drainage and capillary rise components in water balance of alluvial soils. *Agricultural Water Management* 86: 206-211.
- Landon, M., G. Delin, S. Komor and C. Regan. 1999. Comparison of stable-isotopic composition of soil water collected from suction lysimeters, wick samplers, and cores in a sandy unsaturated zone. *Journal of Hydrology* 224: 45-54.
- Lee, J., R. Horton, K. Noborio and D. Jaynes. 2001. Characterization of preferential flow in undisturbed, structured soil columns using a vertical TDR probe. *Journal of Contaminant Hydrology* 51: 131-144.
- Lehmann, P., F. Stauffer, C. Hinz, O. Dury and H. Fluhler. 1998. Effect of hysteresis on water flow in a sand column with a fluctuating capillary fringe. *Journal of Contaminant Hydrology* 33: 81-100.
- Lloyd, J. 1986. A review of aridity and groundwater. *Hydrological Process* 1: 63-78.
- Maclean, A. 1974. Soil genesis in relation to groundwater and soil moisture regimes near Vegreville, Alberta. Unpublished Ph.D. thesis. Edmonton, AB: Department of Soil Science, University of Alberta.
- Magesan, G., B. Vogeler, B. Clothier, S. Green and R. Lee. 2003. Solute movement through an allophonic soil. *Journal of Environmental Quality* 32: 2325-2333.
- Maidment, D. 1993. *Handbook of Hydrology*. New York: McGraw-Hill.
- Marshall, T. and C. Gurr. 1954. Movement of water and chlorides in relatively dry soil. *Soil Science* 77: 147-152.
- Marshall, T. and J. Holmes. 1979. *Soil Physics*. London: Cambridge University Press.

- Maule, C., D. Chanasyk and K. Muehlenbachs. 1993. Finite difference model for seasonal vadose zone flow. American Society of Agricultural Engineers. Winter Meeting, Chicago, Dec 13-17, 1993. Paper No. 933582.
- Maule, C., D. Chanasyk and K. Muehlenbachs. 1992. The contribution of snow to soil water and shallow groundwater as determined by stable isotopes. *Soil Moisture Modelling*. Proceeding of the NHRC workshop held March 9-10.
- Mckenzie, R., W. Chomistek and N. Clark. 1989. Conversion of electromagnetic inductance readings. *Canadian Journal of Soil Science* 69: 25-32.
- Nadler, A., S. Dasberg and I. Lapid. 1991. Time domain reflectometry measurements of water content and electrical conductivity of layered soil columns. *Soil Science Society of America Journal* 55: 938-943.
- Nakayama, F., R. Jackson, B. Kimball and R. Reginato. 1973. Diurnal soil-water evaporation: Chloride movement and Accumulation near the soil surface. *Soil Science Society of American Process* 37: 509-513.
- Noborio, K., R. Kachanoski and C. Tan. 2006. Solute transport measurement under transient field conditions using Time Domain Reflectometry. *Vadose Zone Journal* 5: 412-418.
- Onodera, S. and M. Kobayashi. 1995. Evaluation of seasonal variation in bypass flow and matrix flow in a forest soil layer using bromide ion. Tracer Technologies for Hydrological Systems. Proceedings of a Boulder Symposium, July 1995. IAHS Publ. no. 229, pp. 99-107.
- Phillips, I.R. 2004. Measurement and prediction of potassium chloride movement in an unsaturated sand. *Communications in Soil Science and Plant Analysis* 35: 1663-1679.
- Potter, L. 1992. *Desert characteristics as related to waste disposal, in Deserts as dumps? The Disposal of Hazardous Materials in Arid Ecosystems*, edited by C. C. Reith and B. M. Thomson. Albuquerque, University of New Mexico Press.
- Price, I. 2000. Determining if skewness and kurtosis are significantly non-normal. <http://salises.uwimona.edu.jm:1104/sa63c/Determining%20skewness%20and%20kurtosis.htm>. June 14, 2008.

- Rhoades, J., F. Chanduvi and S. Lesch. 1999. Soil salinity assessment; methods and interpretation of electrical conductivity measurements. FAO Irrigation and Drainage Paper No. 57.
- Ripley, E. 1988. Drought prediction on the Canadian prairies. Saskatoon: The Canadian Climate Program.
- Ritter, A., R. Munoz-Carpena, C. Regaldo, M. Javaux and M. Vanclooster. 2005. Using TDR and inverse modeling to characterize solute transport in a layered agricultural volcanic soil. *Soil Science Society of America Journal* 4: 300-309.
- Robinson, D., S. Jones, J. Wraith and S. Friedman. 2003. A review of advance in dielectric and electrical conductivity measurement in soils using time domain reflectometry. *Soil Science Society of America Journal* 2: 444-475.
- Sabburg, J., J. Ball and N. Hancock. 1997. Dielectric behavior of moist swelling clay soils at microwave frequencies. *IEEE Trans. Geosci. Remote Sensing* 35: 784-787.
- Salle, C., C. Marlin, C. Leduc, J. Taupin, M. Massault and G. Favreau. 2001. Renewal rate estimation of groundwater based on radioactive tracers( $^3\text{H}$ ,  $^{14}\text{C}$ ) in an unconfined aquifer in a semi-arid area, Iullemeden Basin, Niger. *Journal of Hydrology* 254: 145-156.
- Scanlon, B., S. Tyler and P. Wierenga. 1997. Hydrologic issues in arid, unsaturated systems and implications for contaminant transport. *Reviews of Geophysics* 34(4): 461-490.
- Si, B. and R. Kachanoski. 2003. Measurement of local soil water flux during field solute transport experiments. *Soil Science Society of America Journal* 67: 730-736.
- Si, B., R. Kachanoski, F. Zhang, G. Parkin and D. Elrick. 1999. Measurement of hydraulic properties during constant flux infiltration: Field average. *Soil Science Society of American Journal* 63: 793-799.
- Smiles, D.E. and J.R. Philip. 1978. Solute transport during absorption of water by soil: Laboratory studies and their practical implications. *Soil Science Society of America Journal* 42: 537-544.
- Smiles, D.E., J.R. Philip, J.H. Knight and D.E. Elrick. 1978. Hydrodynamic dispersion

- during absorption of water by soil. *Soil Science Society of America Journal* 42: 229-234.
- Smiles, D.E., K.M. Perroux, S.J. Zegelin and P. Raats. 1981. Hydrodynamic dispersion during constant rate absorption of water by soil. *Soil Science Society of America Journal* 45: 453-458.
- Smith, D., H. Wearn, H. Richards and P. Rowe. 1970. Water movement in the unsaturated zone of high and low permeability strata by measuring natural tritium. p. 73-87. In Isotope hydrology. IAEA, Vienna.
- Soil Classification Working Group. 1998. The Canadian System of Soil Classification (Third Edition). Agriculture and Agri-Food Canada Publication 1646, 187 pp. Table 4 <http://sis.agr.gc.ca/cansis/taxa/cssc3/table4.jpg>
- Stephen, D. 1993. A perspective on diffuse natural recharge mechanisms in areas of low precipitation. *Soil Science Society of America Journal* 58: 40-48.
- Steppuhn, H. 1980. Snow management for crop production on the Canadian Prairies. 48<sup>th</sup> Annual Western Snow Management Conf. pp. 50-61.
- Topp, G., J. Davis and A. Annan. 1980. Electromagnetic determination of soil water content: measurements in coaxial transmission lines. *Water Resource Research* 16: 574-582.
- United States Salinity Laboratory Staff. 1954. Saline and alkali soils. Agriculture Handbook No. 60. Riverside, California: Washington, D.C.
- Vanclooster, M., P. Viaene, K. Christiaens and S. Ducheyne. 1996. WAVE: A mathematical model for simulating water and agrochemicals in the soil and vadose environment. Reference and user's manual. Release 2.1. Institute for Land and Water Management, Katholieke Universiteit Leuven, Leuven, Belgium.
- van der Kamp, G. and H. Maathuis. 1991. Annual fluctuations of groundwater levels as a result of loading by surface moisture. *Journal of Hydrology* 127: 137-152.
- Vogeler, I., C. Duwig, B. Clothier and S. Green. 2000. A simple approach to determine reactive solute transport using time domain reflectometry. *Soil Science Society of America Journal* 64: 12-18.
- Wang, D., S. Yates and F. Ernst. 1998. Determining soil hydraulic properties using

- tension infiltrometers, time domain reflectometry, and tensiometers. *Soil Science Society of America Journal* 62: 318-325.
- Ward, A., R. Kachanoski and D. Elrick. 1994. Laboratory measurements of solute transport using time domain reflectometry. *Soil Science Society of America Journal* 58: 1031-1039.
- Ward, B.N. 2003. Recharge rate estimation and environmental tracers in a semi-arid environment. Unpublished M.Sc. thesis. Saskatoon, SK: Department of Division of Environmental Engineering, University of Saskatchewan.
- Warner, G., M. Colombo and K. Guillard. 1997. Field estimation of upward capillary flux into a shallow root zone using TDR. ASAE Annual International Meeting, held in Minneapolis, Minnesota in August 10-14, 1997, pp. 129-132.
- Warrick, A.W., J.W. Biggar and D.R. Nielsen. 1971. Simultaneous solute and water transfer in an unsaturated soil. *Water Resources Research* 7: 1216-1225.
- Weast, R., ed. 1986. *Handbook of Physics and Chemistry*. 67<sup>th</sup> ed. Boca Raton, Fla.: CRC Press.
- Wilson, G.W. 1990. Soil evaporative fluxes for geotechnical engineering problems. Unpublished Ph.D. thesis. Saskatoon, SK: Department of Civil Engineering, University of Saskatchewan.
- Wood, W., K. Rainwater and D. Thompson. 1997. Quantifying macropore recharge: examples from a semi-arid area. *Groundwater Journal* 35: 1097-1106.
- Wraith, J. and J. Baker. 1991. High-resolution measurement of root water uptake using automated time domain reflectometry. *Soil Science Society of America Journal* 55: 928-932.
- Yang, M. and E. Yanful. 2002. Water balance during evaporation and drainage in cover soils under different water table conditions. *Advances in Environmental Research* 6: 505-521.
- ZebARTH, B., E. de Jong and J. Henry. 1989. Water flow in a hummocky landscape in central Saskatchewan, Canada, II. Saturated flow and groundwater recharge. *Journal of Hydrology* 110: 181-198.
- ZebARTH, B. and E. de Jong. 1989. Water flow in a hummocky landscape in central

Saskatchewan, Canada, III. Unsaturated flow in relation to topography and land use. *Journal of Hydrology* 110: 199-218.

Zhang, X. and P. van Geel. 2007. Development of a vertical TDR probe to evaluate the vertical moisture profile in peat columns to assess biological clogging. *Journal of Environmental Engineering and Science* 6(6): 629-642.

## APPENDIX A: CALIBRATION AND SIMULATION CURVES

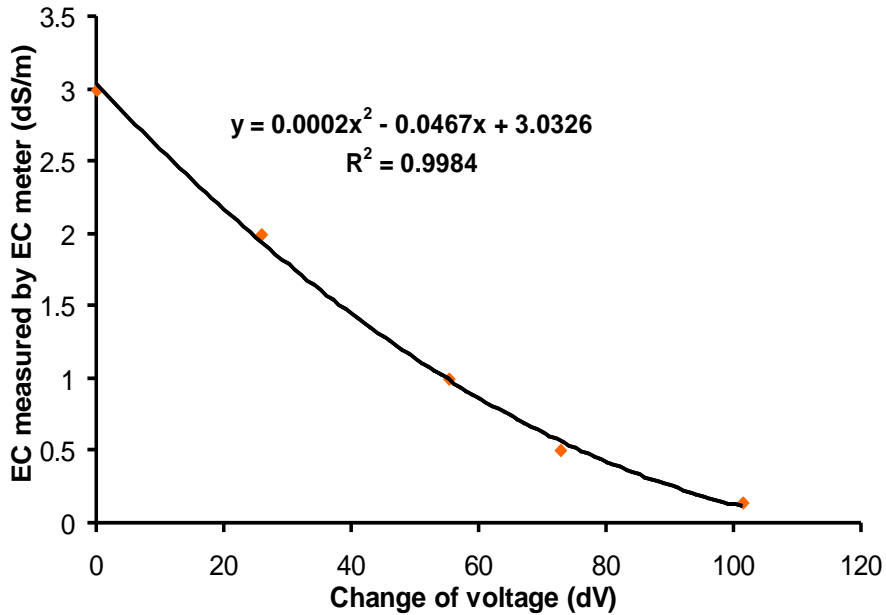


Figure A.1: Calibration curve obtained using EC meter and TDR readings in order to calibrate the TDR readings.

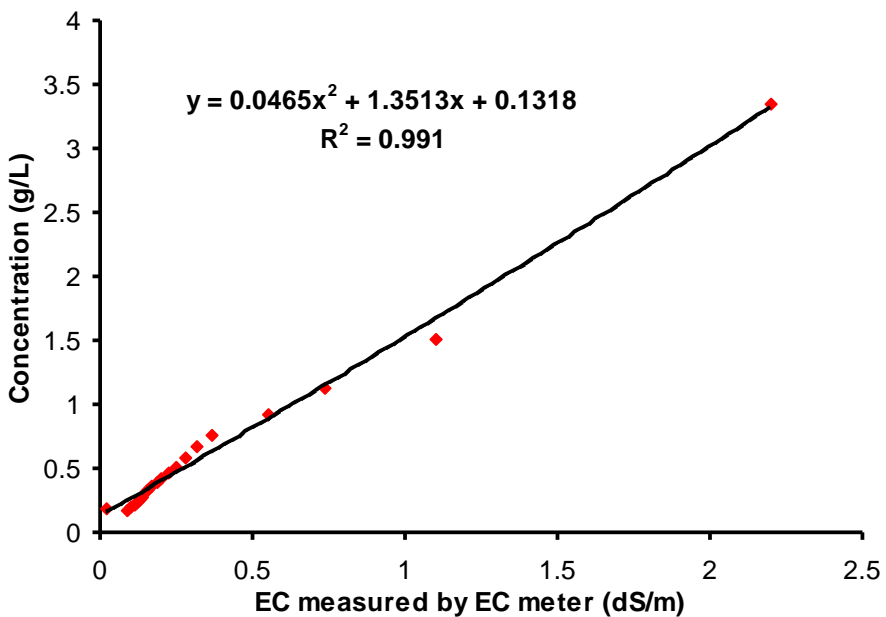


Figure A.2: Calibration curve obtained using EC meter and concentrations in order to calibrate the EC meter readings.

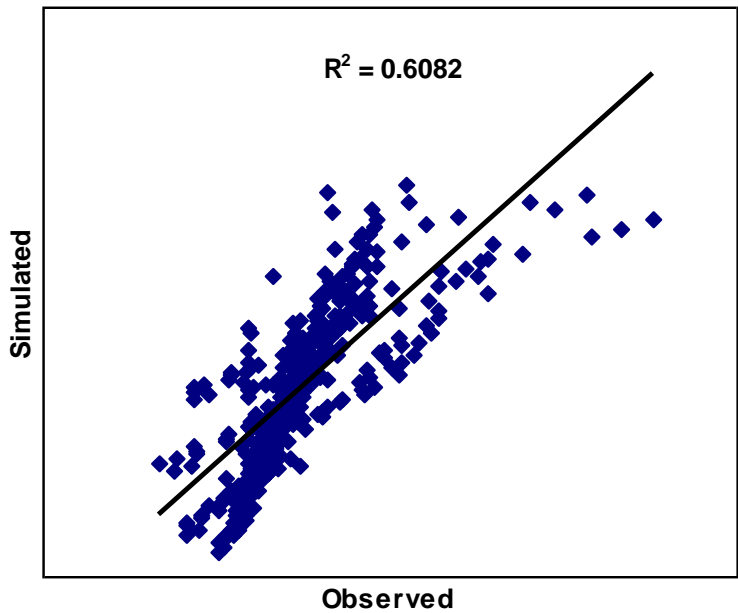


Figure A.3: Observed and simulated change of concentration obtained using the SPSS.

## APPENDIX B: ESTIMATING POROSITY UNDER FLOW CONDITIONS

### B.1 Estimating porosity under upward flow conditions

Porosity was estimated from the concentration data collected during the study of the first objective, under the evaporative conditions in column 1. Equation 3.1 was used to determine the porosity using the concentration peak location method. The concentration peak moved 0.36 m (from 0.51 to 0.15 m depth “Figure C.3”) during the evaporation period (13 days) under the upward flow conditions, and there was 133.9 mm (depth in soil) of water evaporated from the sand column during this period. Therefore, the average estimated porosity using the peak location method was  $0.372 \text{ m m}^{-1}$  which is same as the measured porosity from the soil moisture data ( $0.37 \text{ m}^3 \text{ m}^{-3}$ ) (Table 4.3). However, the estimated porosity varied when smaller time steps were used. Table B.1 shows the variation of estimated porosity under the upward flow conditions using the peak location method. It can be indicated that the estimated porosity for the depth between 0.51 and 0.39 m was relatively high ( $0.515 \text{ m m}^{-1}$ ). The estimated porosity in the depths between 0.39 and 0.23 m decreased to  $0.258 \text{ m m}^{-1}$  then it was  $0.386 \text{ m m}^{-1}$  for the last three days of evaporation. The low value of the estimated porosity using the peak location method in the depth between 0.39 and 0.23 m indicates that there might be affects of the water table on the peak shape or the peak movement because the water table was located in depth of 0.32 m from the sand surface. Therefore, this method can be recommended to estimate the porosity for saturated sand if the upward movement of the peak is equilibrium under the upward flow (evaporative) conditions.

Table B.1: The variation of estimated porosity under the upward flow conditions.

Days of evaporation	Upward peak movement (m)	Evaporated water (mm)	Estimated porosity ( $\text{m m}^{-1}$ )
0-6	0.51-0.39	61.8	0.515
6-10	0.39-0.23	41.2	0.258
10-13	0.23-0.15	30.9	0.386
0-13	0.15-0.51	133.9	0.372

## B.2 Estimating porosity under downward flow conditions

The concentration peak moved down by 0.76 m during the raining period (three days). The raining rate was constant in  $89.6 \text{ mm d}^{-1}$ , so there was 268.8 mm of water added to the column during the raining period. Therefore, the estimated porosity was  $0.354 \text{ m m}^{-1}$  which is lower than the measured porosity from the soil moisture data ( $0.37 \text{ m}^3 \text{ m}^{-3}$ ). However, if the porosity calculated using the concentration movement for just two last days of raining, the estimated porosity is  $0.37 \text{ m m}^{-1}$  which maintains the same result was measured using the soil moisture data. Table B.2 shows the estimated porosity using the downward peak movement under the downward flow conditions. It seems that the concentration peak for the last day of evaporation does not represent the start peak depth for the downward flow (zero day of raining) because the column was left covered for two days between the evaporation period and the rain period and the sand was relatively dry in the depth between the sand surface and the water table after the evaporation period. Also, it seems that the system took one day to be established under the rain conditions.

Table B.2: The estimated porosity under the downward flow conditions using the peak location method.

Raining period (day)	Downward peak movement (m)	Rain rate (mm d <sup>-1</sup> )	Estimated porosity (m m <sup>-1</sup> )
1-2	0.43-0.67	89.6	0.373
2-3	0.67-0.91	89.6	0.373
1-3	0.43-0.91	89.6	0.373

**APPENDIX C: CHANGE OF SOME SOIL WATER PROPERTIES UNDER UPWARD AND DOWNWARD FLOW CONDITIONS**

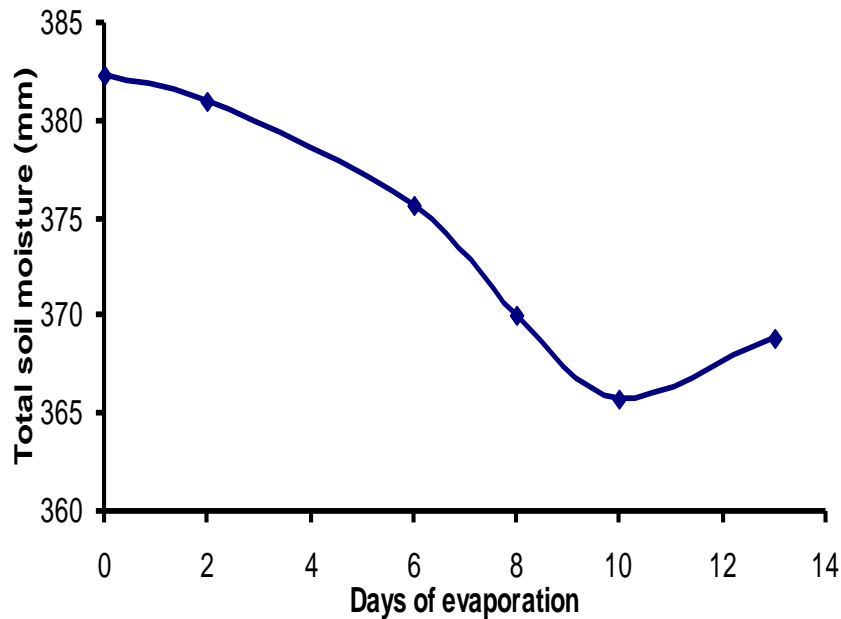


Figure C.1: The change of total soil moisture as a function of time in column 1 under the evaporation conditions (first objective).

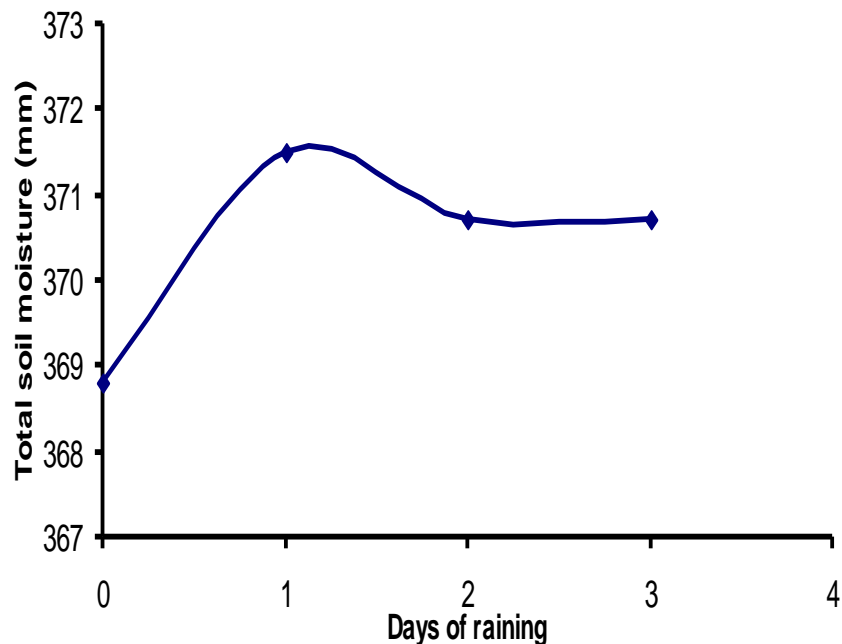


Figure C.2: The change of total soil moisture with time in column 1 under the raining condition (first objective).

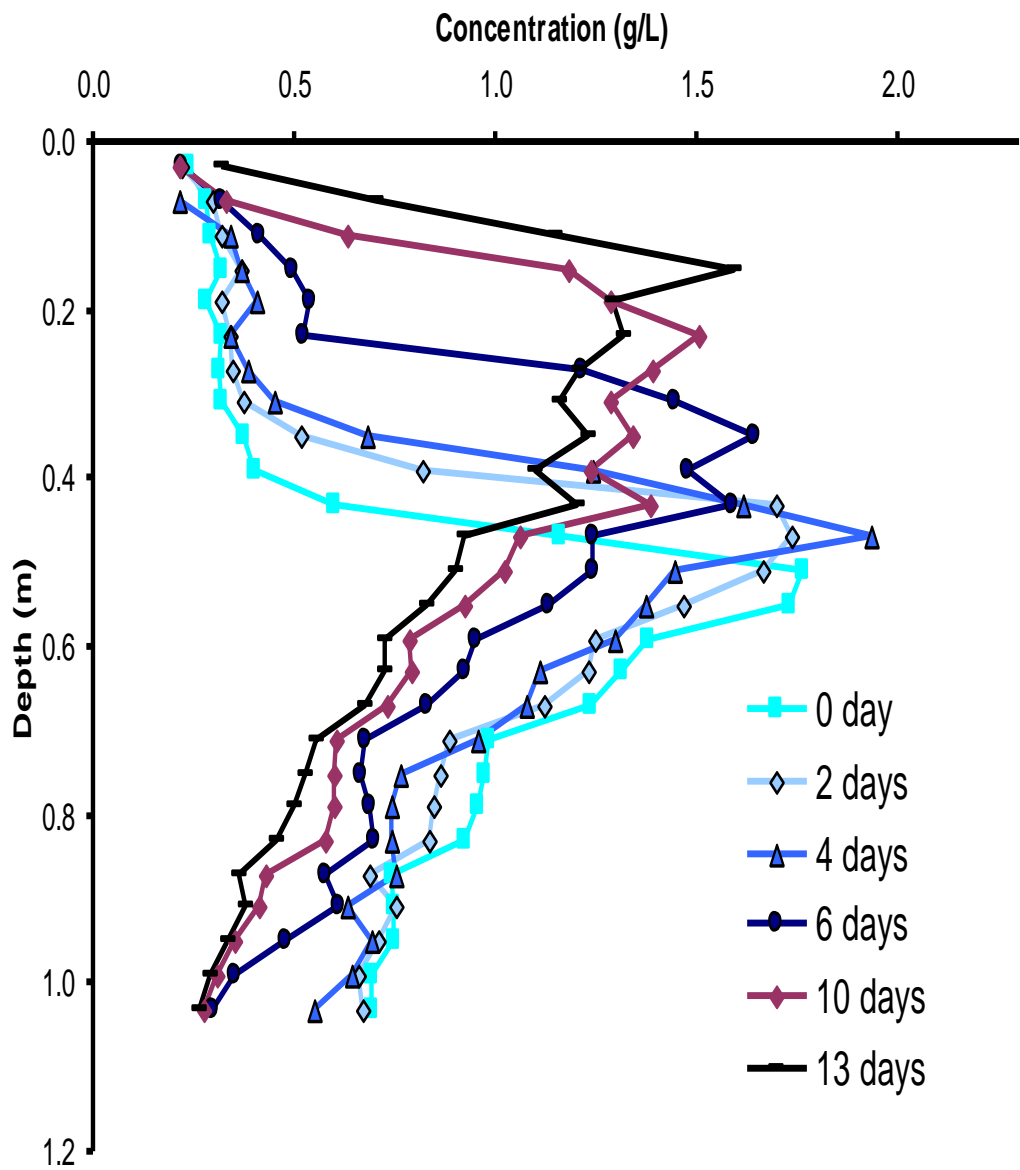


Figure C.3: Concentration profiles under the evaporation conditions in column 1 used to estimate the upward flux in the first objective.

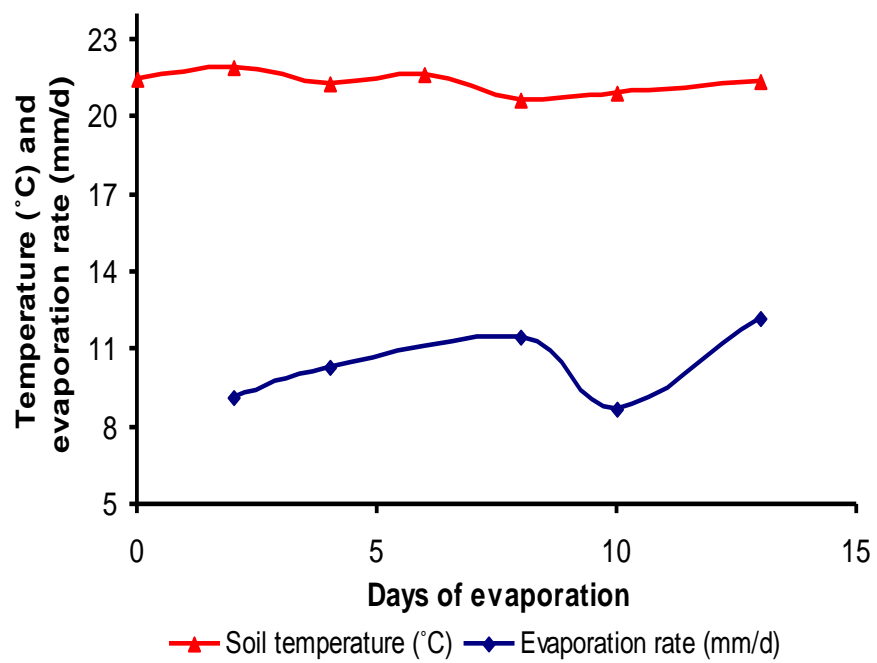


Figure C.4: The soil temperature (0.02 m depth) and evaporation rate as a function of evaporation time in column1 (first objective).

**APPENDIX D: CHANGE OF SOIL TEMPERATURE, ROOM TEMPERATURE, AND HUMIDITY DURING THE CYCLING PERIOD**

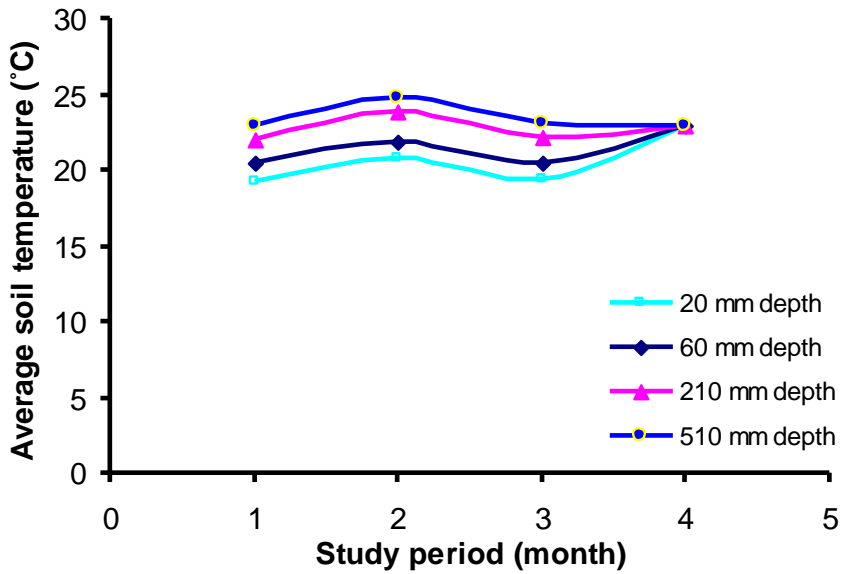


Figure D.1: Average soil temperature in different depths from the sand surface during the study period in column 1.

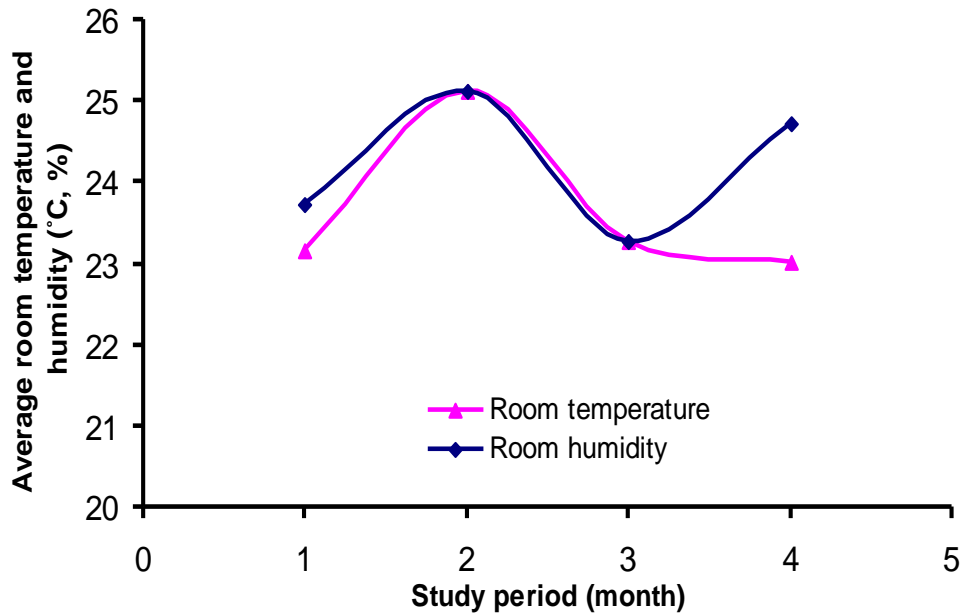


Figure D.2: Average room temperature and humidity during the study period.

## **APPENDIX E: THE CONTRIBUTION OF SALT FROM THE SAND**

There was evidence of salt precipitates (assumed to be primarily calcium carbonate) in the sand. This was indicated by light to moderate fizzing (Personal Communication Charles Maule, Professor, Department of Agricultural and Bioresource Engineering, University of Saskatchewan, Canada) when a 7% HCl solution was applied and by the presence of inorganic carbon. These salts dissolved and contributed to the dissolved salt concentration resulting in an increase in EC with time. The rate and amount of dissolved salts contributed from the sand had to be determined because it could influence the evaluation of the concentration profile shape.

At the end of the experiment, when the cycles were done, the three columns were flushed by distilled water (one pore volume), and then TDR measurements were taken for each column. In columns 1, 2, and 3 the total mass of dissolved salt was 3.7, 3.8, and 3.9 g, respectively after flushing with distilled water. After flushing, the three columns had similar concentration distributions with depth between the sand surface and 0.83 m (Figure E.1).

The columns then were covered preventing drainage and evaporation and EC was monitored weekly for 100, 94, and 96 days for columns 1, 2, and 3, respectively. Monitoring showed that dissolved salts increased with time with a greater increase in the top half of the column (Figures E.1 and E.2). The contribution of dissolved salts from the sand was similar for all three columns, varying between 3.0 and 3.8 g over 94 to 100 days (Table E.1). The rate of increase in dissolved contribution was thus similar, varying between 0.8 and 1.1 mg d<sup>-1</sup> (Table E.1; Figure E.3), however was greater in shallower depths. In the top half of all three columns, the increase was between 0.7 and 2.6 mg d<sup>-1</sup>, whereas below 0.65 m, it was lower, at between 0.07 and 1.06 mg d<sup>-1</sup>. Currently, it is not clear why there is such a difference in rates between the bottom and top halves of the columns. The rate of salts becoming dissolved in column 1 was lower than the other columns (Table E.1, Figure E.3), perhaps because it had been flushed more in conjunction with the first objective.

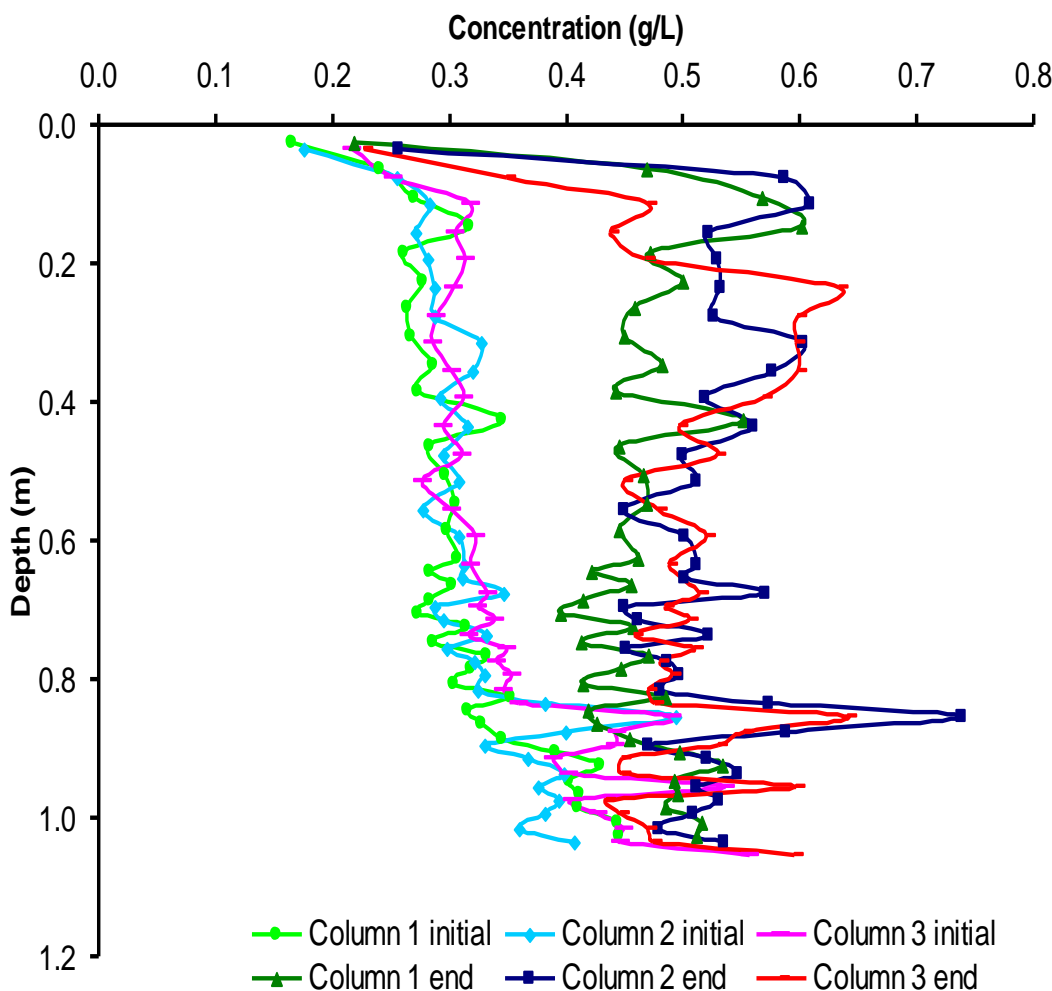


Figure E.1: Concentration in columns 1, 2 and 3 as a function of depth before (initial) and after (end) leaving the columns stagnant for 100, 94 and 96 days respectively.

Table E.1: Total dissolved salts and the daily contribution rate of dissolved salts in each sand column.

Columns	Period of time <sup>1</sup> (day)	Total dissolved salts <sup>2</sup> (g)	Min <sup>3</sup> . rate of dissolved salts (mg d <sup>-1</sup> )	Max <sup>4</sup> . rate of dissolved salts (mg d <sup>-1</sup> )	Average rate of dissolved salts (mg d <sup>-1</sup> )
C1	100	3.02	0.19	2.20	0.84
C2	94	3.79	0.45	2.61	1.12
C3	96	2.95	0.05	2.44	0.85

<sup>1</sup> Time which the column was remained covered with no losses by evaporation or drainage.

<sup>2</sup> Total dissolved salt refers to total mass of dissolved salts in each column that contributed by the soil during the period of time.

<sup>3</sup> Min. rate of dissolved salts refers to the minimum rate of dissolved salt contributed by soil.

<sup>4</sup> Max. rate of dissolved salts refers to the maximum rate of dissolved salt contributed by soil.

A general equation (model) was developed to describe the change in EC for each column as a function of time and depth (see section 3.10). This model enabled the subtraction of the soil contribution to EC for the experiments done under the cycling conditions of upward and downward seasonal flows.

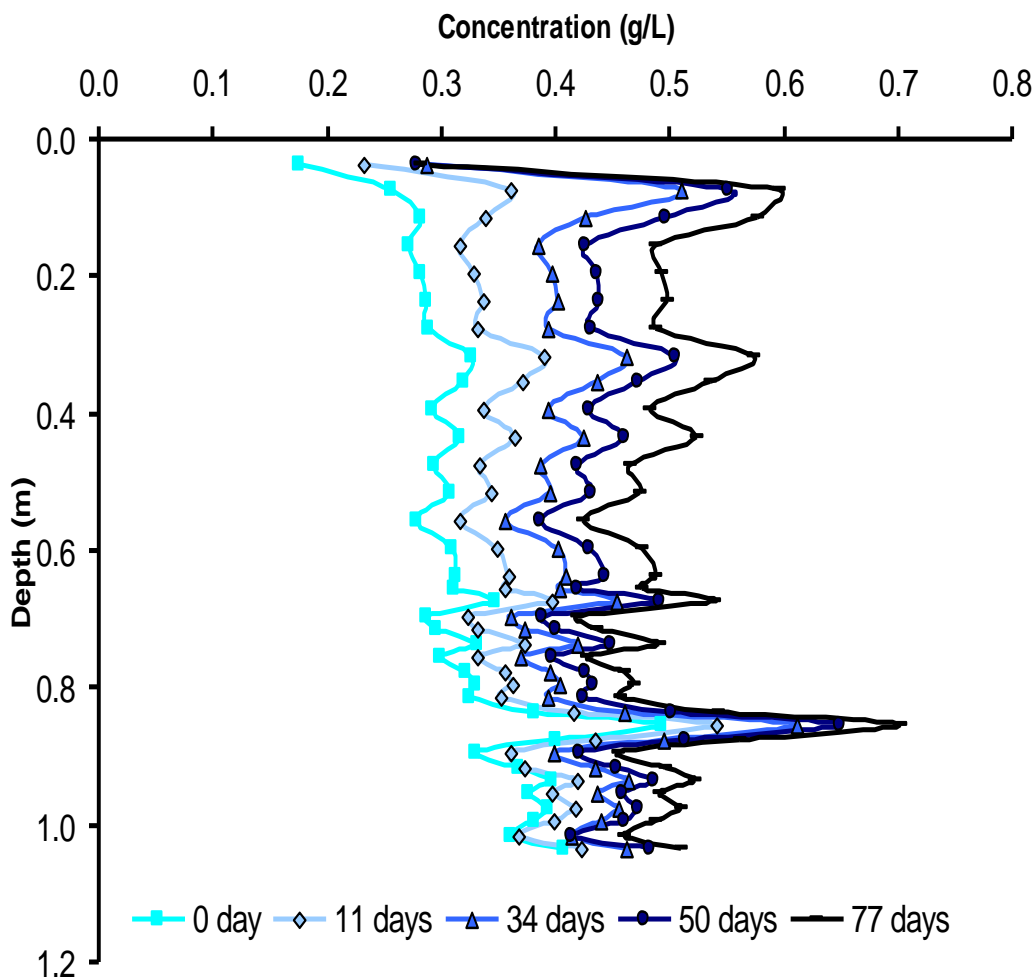


Figure E.2: Dissolved salt concentration as a function of time and depth in column 2 during 77 days of stagnant conditions.

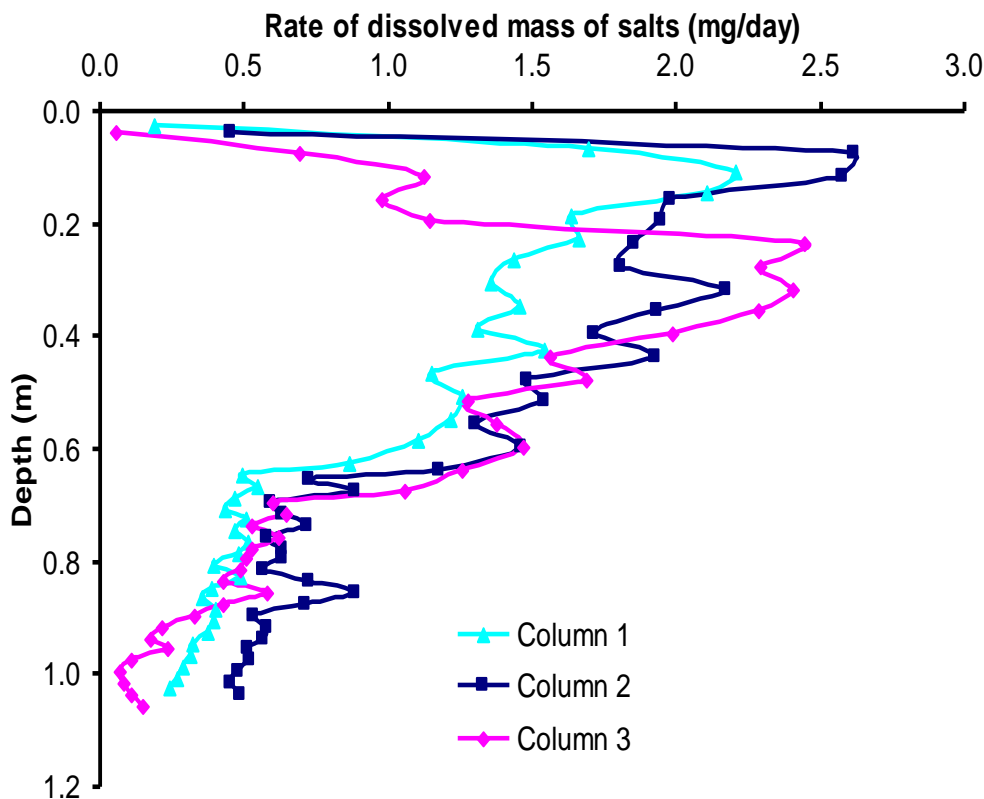


Figure E.3: The rate of dissolved mass of salts contributed by soil to the solution as a function of depth in the three columns.

Table E.2: The contribution of salts from sand to the solution measured in column 1 when it was left covered (no loss by evaporation or drainage) for a period of time.

Time (day)	Total mass of salts (g)	Change of total mass of salts (g)	Rate of change of total mass of salts ( $\text{g d}^{-1}$ )
7	6.26	0.68	0.097
15	6.46	0.88	0.059
23	6.73	1.16	0.050
32	6.92	1.34	0.042
42	7.48	1.91	0.045
51	7.74	2.16	0.042
61	8.06	2.48	0.041
68	8.29	2.71	0.040
79	8.39	2.81	0.036
91	8.52	2.94	0.032
100	8.74	3.17	0.032

Table E.3: The contribution of salts from sand to the solution measured in column 2 when it was left covered (no loss by evaporation or drainage) for a period of time.

Time (day)	Total mass of salts (g)	Change of total mass of salts (g)	Rate of change of total mass of salts ( $\text{g d}^{-1}$ )
4	6.13	0.32	0.079
11	6.59	0.78	0.071
18	6.86	1.04	0.058
27	7.29	1.48	0.055
34	7.66	1.85	0.054
42	7.96	2.15	0.051
50	8.26	2.44	0.049
59	8.29	2.48	0.042
68	9.05	3.23	0.048
77	9.14	3.33	0.043
87	9.47	3.66	0.042
94	9.54	3.72	0.040

Table E.4: The contribution of salts from sand to the solution measured in column 3 when it was left covered (no loss by evaporation or drainage) for a period of time.

Time (day)	Total mass of salts (g)	Change of total mass of salts (g)	Rate of change of total mass of salts ( $\text{g d}^{-1}$ )
7	6.70	0.50	0.072
16	7.07	0.87	0.055
26	7.53	1.33	0.051
33	7.68	1.48	0.045
34	7.96	1.76	0.052
46	8.11	1.91	0.042
55	8.00	1.80	0.033
62	8.22	2.02	0.033
96	9.09	2.90	0.030

## APPENDIX F: THE CHANGE OF SOME SOIL WATER PROPERTIES UNDER CYCLING CONDITIONS

Table F.1: The change of total soil moisture, average concentration, and total mass of salts during the cycling period (taken after the evaporation period of each cycle) in column 1 (upward flow = downward flow).

Number of cycles	Total moisture <sup>1</sup> (mm)	Average <sup>2</sup> concentration (g L <sup>-1</sup> )	Total mass of salts <sup>3</sup> (g)
1	372.3	0.62	5.5
2	380.8	0.59	6.0
3	382.2	0.58	6.3
4	378.7	0.62	6.8
5	377.4	0.62	6.8
6	383.9	0.64	7.0
7	383.1	0.64	7.0
8	377.2	0.65	7.4
9	370.1	0.65	7.4
10	375.7	0.67	7.7
11	369.3	0.67	7.7
12	378.5	0.65	7.5
13	375.9	0.65	7.5
14	376.0	0.64	7.5
15	377.3	0.64	7.5
16	376.9	0.65	7.8
17	382.4	0.65	7.8
18	377.1	0.66	8.0
19	374.6	0.66	8.0
20	376.4	0.65	8.3

<sup>1</sup> Total moisture refers to total soil moisture in the column measured by TDR.

<sup>2</sup> Aver. concen. refers to the average concentration in the column measured by TDR and corrected to 25°C.

<sup>3</sup> Total mass of salt refers to total mass of salts in the column calculated using soil moisture and concentration data.

Table F.2: The change of total soil moisture, average concentration, and total mass of salts during the cycling period (taken after the evaporation period of each cycle) in column 2 (upward flow < downward flow).

Number of cycles	Total moisture <sup>1</sup> (mm)	Average <sup>2</sup> concentration (g L <sup>-1</sup> )	Total mass of salts <sup>3</sup> (g)
1	386.5	0.52	5.8
2	387.0	0.53	6.0
3	384.0	0.54	6.1
4	380.7	0.55	6.2
5	386.7	0.56	6.4
6	387.7	0.57	6.7
7	382.2	0.58	6.8
8	386.5	0.58	7.2
9	385.1	0.59	7.4
10	385.2	0.58	7.4
11	379.2	0.60	7.6
12	382.8	0.58	7.8
13	374.6	0.58	7.7
14	374.1	0.60	8.1
15	378.9	0.63	7.3
16	376.3	0.63	7.3

<sup>1</sup> Total moisture refers to total soil moisture in the column measured by TDR.

<sup>2</sup> Aver. concen. refers to the average concentration in the column measured by TDR and corrected to 25°C.

<sup>3</sup> Total mass of salt refers to total mass of salts in the column calculated using soil moisture and concentration data.

Table F.3: The change of total soil moisture, average concentration, and total mass of salts during the cycling period (taken after the evaporation period of each cycle) in column 3 (upward flow > downward flow).

Number of cycles	Total moisture <sup>1</sup> (mm)	Average <sup>2</sup> concentration (g L <sup>-1</sup> )	Total mass of salts <sup>3</sup> (g)
1	380.1	0.60	6.9
2	383.6	0.62	7.6
3	378.2	0.63	7.8
4	383.5	0.64	7.9
5	384.2	0.65	8.2
6	387.5	0.67	8.2
7	384.7	0.68	8.3
8	386.6	0.69	8.4
9	385.4	0.71	8.5
10	388.1	0.72	8.5
11	387.1	0.74	8.7
12	388.3	0.73	8.7
13	386.0	0.74	8.8
14	389.3	0.75	9.0
15	387.5	0.76	9.0
16	389.4	0.76	8.9
17	389.0	0.77	8.8
18	387.9	0.76	8.8
19	391.2	0.75	8.8
20	385.7	0.76	8.5

<sup>1</sup> Total moisture refers to total soil moisture in the column measured by TDR.

<sup>2</sup> Aver. concen. refers to the average concentration in the column measured by TDR and corrected to 25°C.

<sup>3</sup> Total mass of salt refers to total mass of salts in the column calculated using soil moisture and concentration data.

**APPENDIX G: THE CHANGE OF THE CONCENTRATION PROFILE SHAPE AND POSITION UNDER CYCLING CONDITIONS**

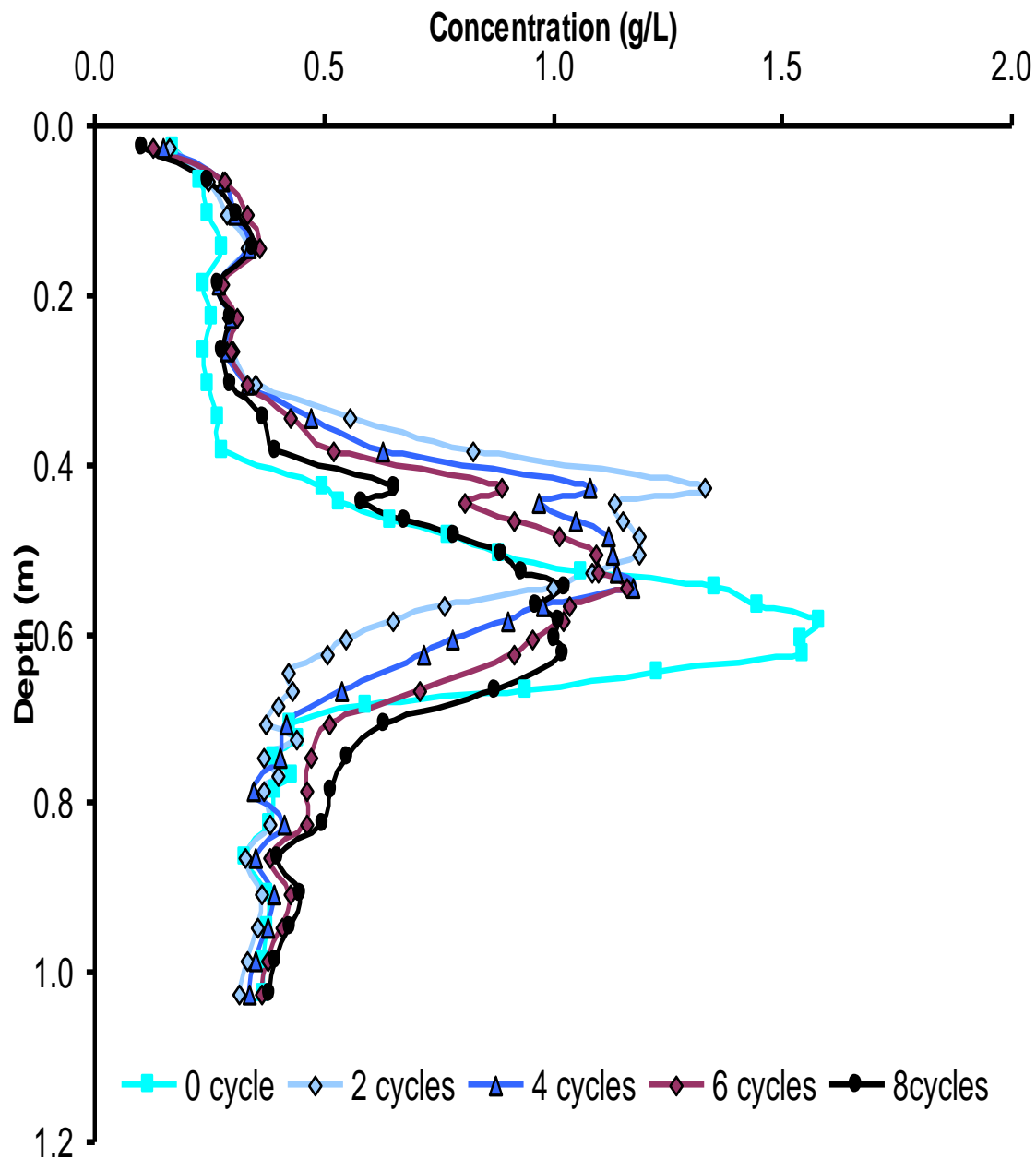


Figure G.1: The change of the solute profile shape under the cycling conditions of equal upward and downward flows (column 1).

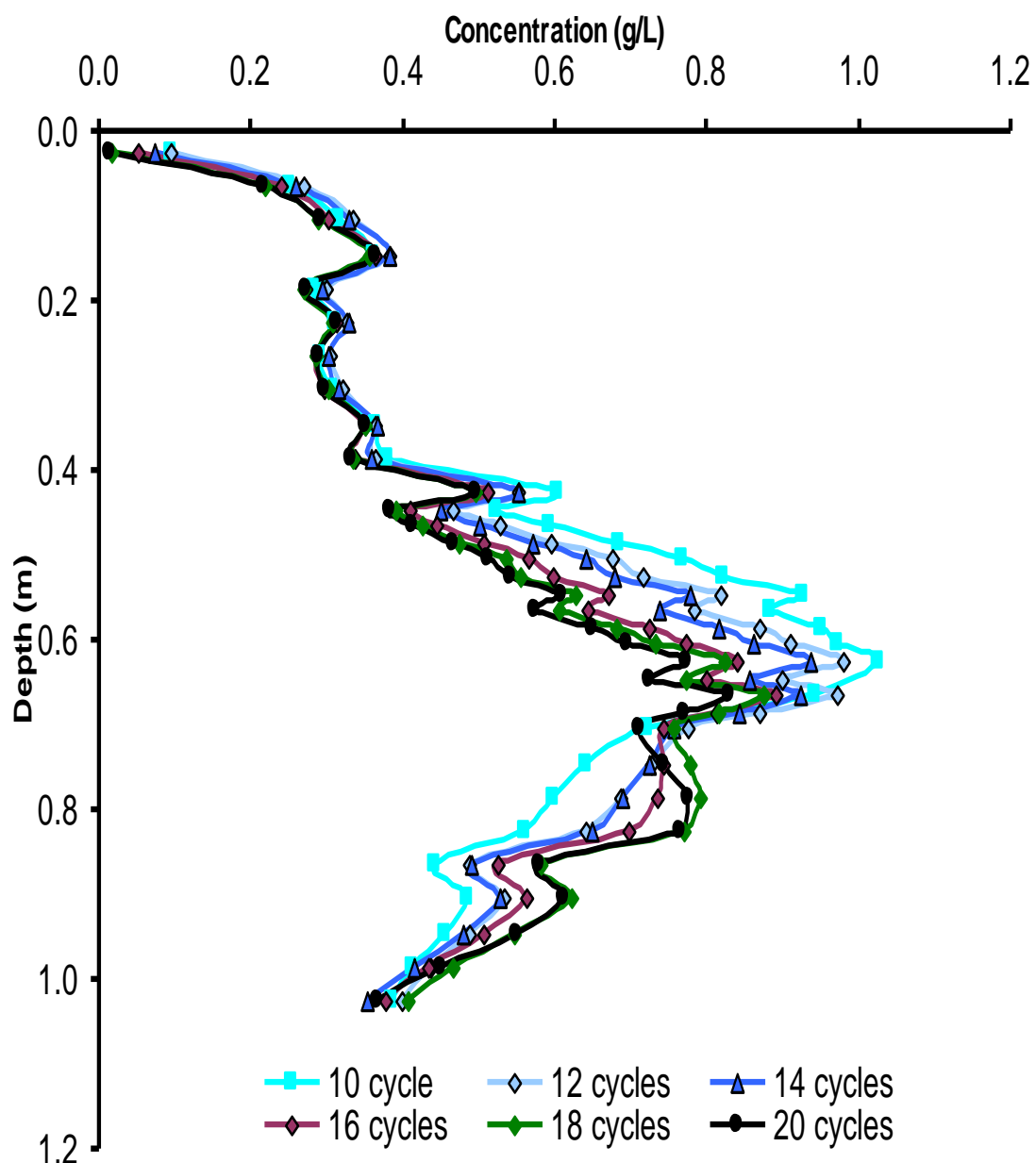


Figure G.2: The change of the solute profile shape under the cycling conditions of equal upward and downward flows (column 1).

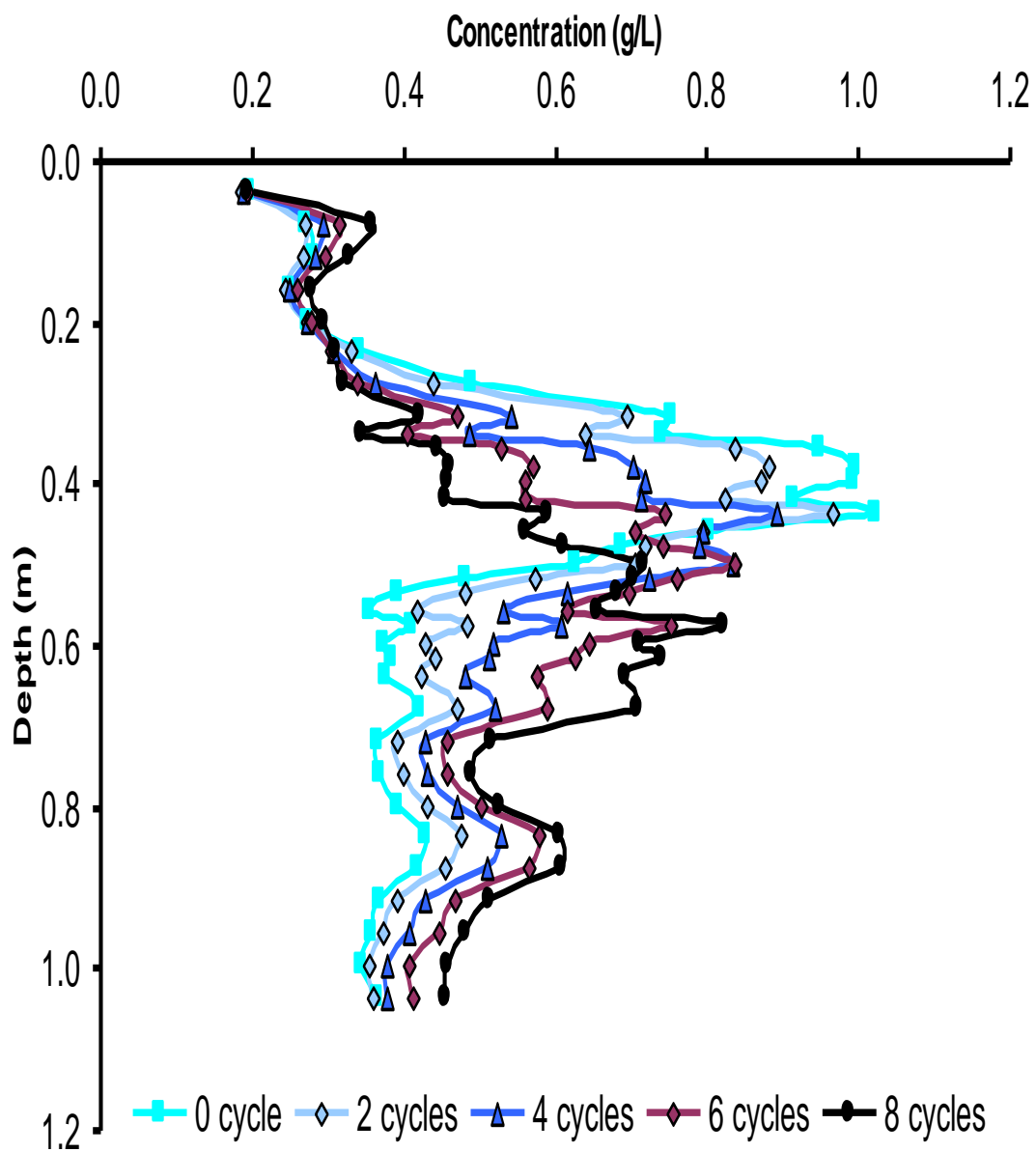


Figure G.3: The change of the solute profile shape under the cycling conditions of downward flow is greater than upward flow (column 2).

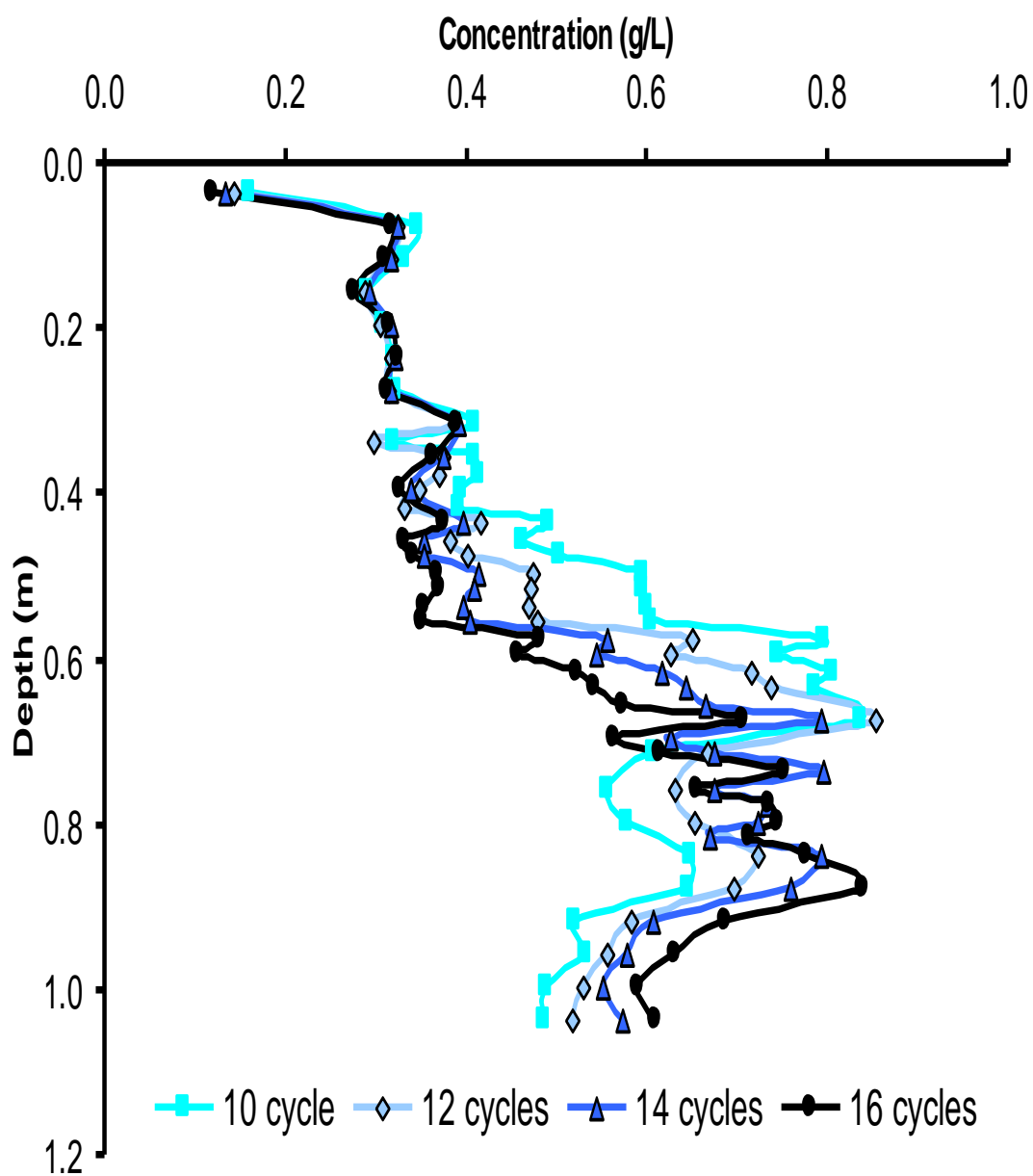


Figure G.4: The change of the solute profile shape under the cycling conditions of downward flow is greater than upward flow (column 2).

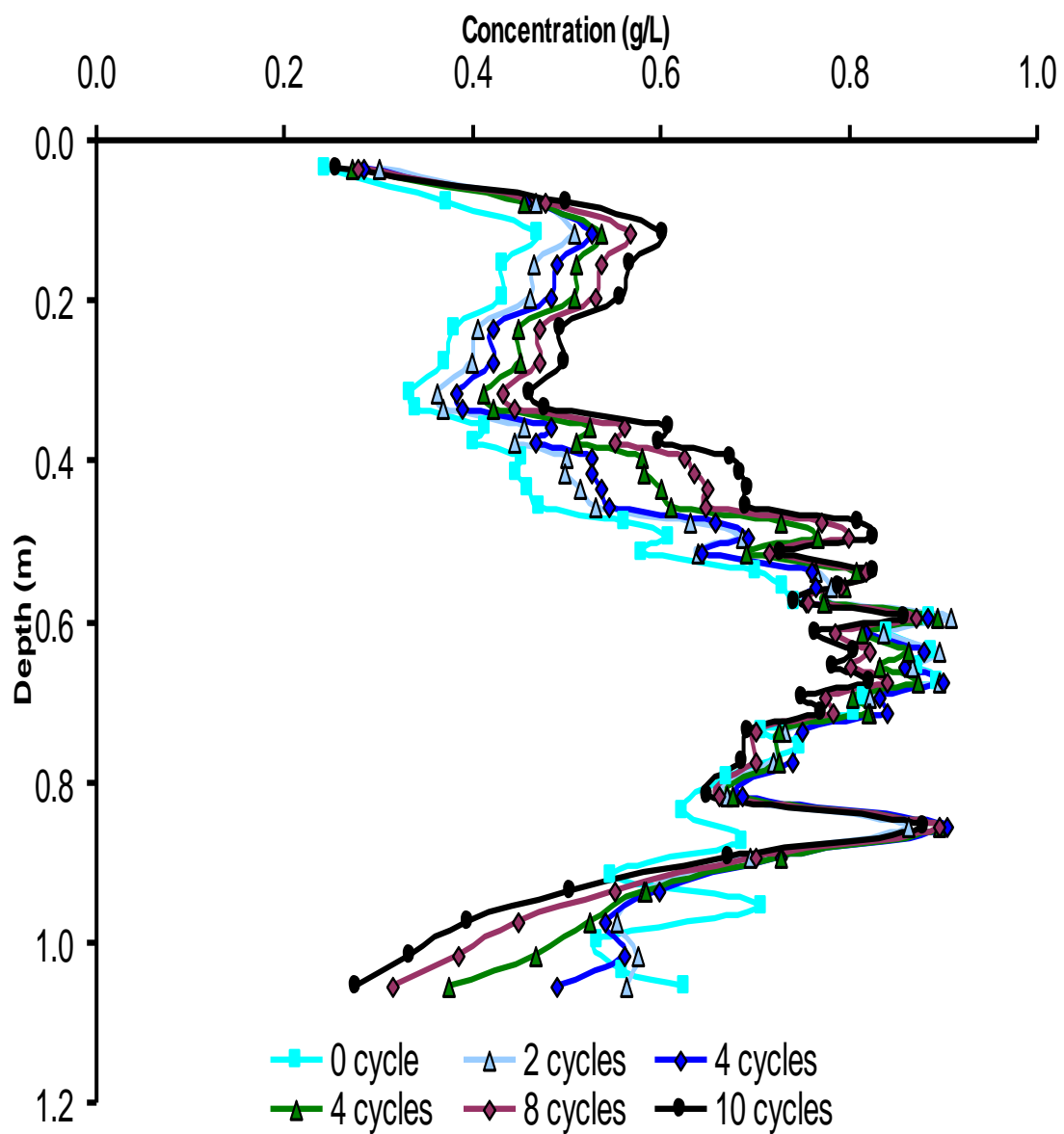


Figure G.5: The change of the solute profile shape under the cycling conditions of upward flow being greater than downward flow (column 3).

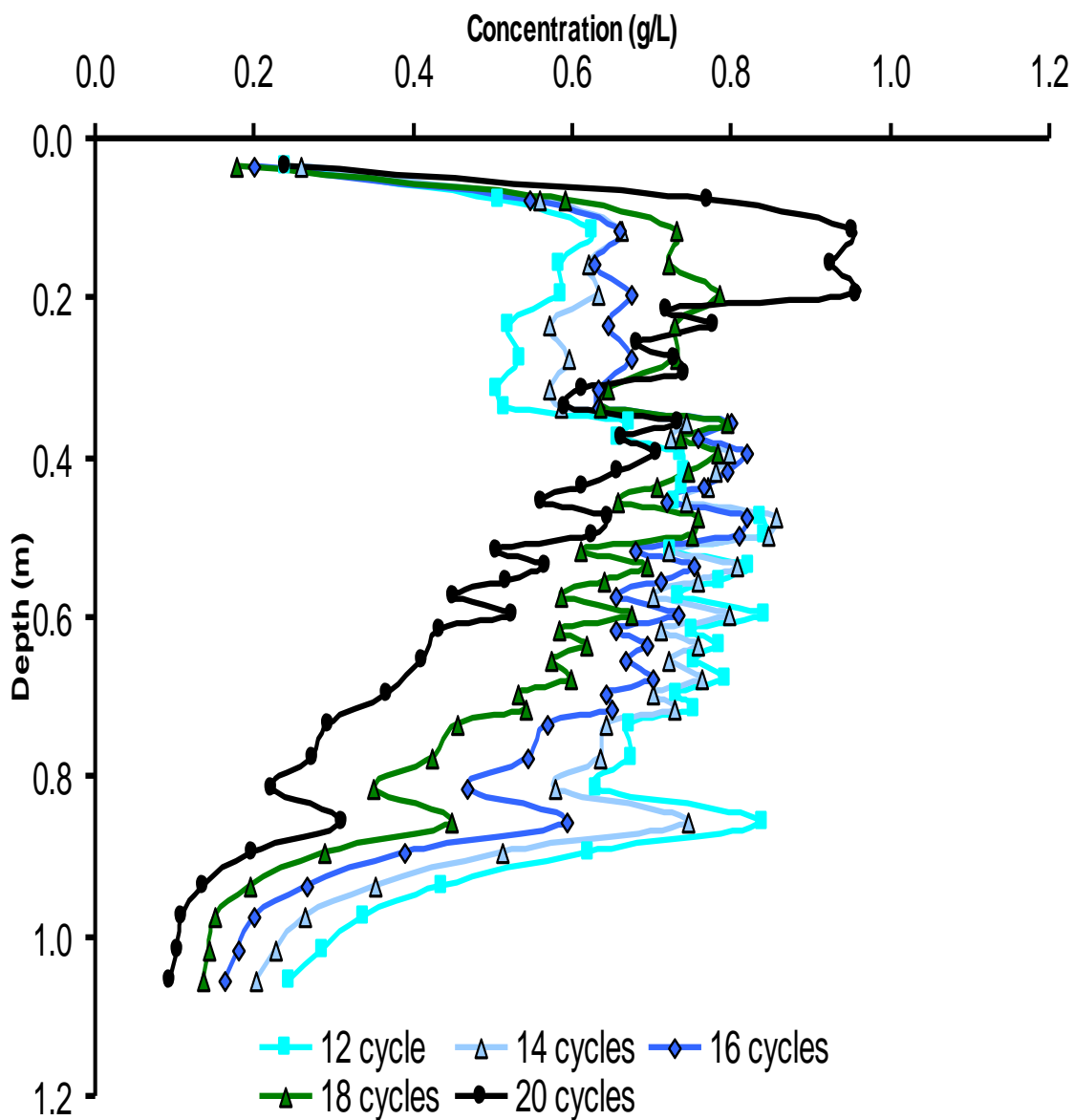


Figure G.6: The change of the solute profile shape under the cycling conditions of upward flow being greater than downward flow (column 3).

## APPENDIX H: CORRECTING THE SOLUTE PROFILE SHAPE

Some noise were observed on the solute profile in each column. Some of these noise observed on the solute profile in the same depth in the column under the cycling conditions. The cause of these noise can be because of instrumental error or because there might be layers in the sand column caused by the packing method. These noise had to be corrected because they influenced the accuracy of using statistical methods such as skewness and kurtosis. The corrected concentration values were selected randomly depending on the solute profile shape. Table shows the corrected values and depths in each column.

Table H.1: The observed and corrected concentration values in different depths in each column.

Column	Depth (m)	Concentration ( $\text{g L}^{-1}$ ) in each cycles (observed/corrected)				
		0	5	10	15	20
C1	0.225	0.76/0.24	0.31/0.39	0.31/0.29	0.32/0.29	0.31/0.28
	0.425	nc	1.03/0.80	0.60/0.45	0.53/0.38	0.50/0.35
	0.865	0.33/0.37	0.35/0.40	0.44/0.53	0.50/0.67	0.58/0.67
C2	0.315	0.75/0.70	0.50/0.39	0.41/0.32	0.39/0.34	-
	0.715	0.36/0.40	0.49/0.53	nc	nc	-
	0.755	0.37/0.40	0.44/0.50	nc	nc	-
	0.835	0.43/0.38	0.56/0.47	0.65/0.55	0.78/0.70	-
	0.875	0.47/0.37	0.54/0.45	0.64/0.53	0.84/0.69	-
C3	0.855	nc	0.90/0.69	0.88/0.65	0.67/0.48	0.31/0.20
	0.895	nc	0.72/0.64	0.67/0.55	nc	nc

nc = not corrected, (-) = not available

**APPENDIX I: ESTIMATED UPWARD AND DOWNWARD FLUXES UNDER  
DIFFERENT FLOW REGIMES**

Table I.1: The estimated upward fluxes (in each cycle) using the peak migration and soil water balance methods under the regime of equal upward and downward flows (column 1).

Cycle	Upward flow						
	Peak migration method			Soil water balance method			
	Peak movement (mm)	Aver. soil moisture <sup>1</sup> (m <sup>3</sup> m <sup>-3</sup> )	Time <sup>2</sup> (h)	Flux (mm h <sup>-1</sup> )	Evapo. rate <sup>3</sup> (mm h <sup>-1</sup> )	Storage change <sup>4</sup> (mm h <sup>-1</sup> )	Flux (mm h <sup>-1</sup> )
1	-80	0.37	114	-0.26	-0.27	0.08	-0.19
2	-120	0.38	93	-0.48	-0.36	0.06	-0.30
3	-40	0.36	91	-0.16	-0.20	-0.06	-0.26
4	0	0.37	78	0.00	-0.17	-0.01	-0.18
5	-40	0.37	93	-0.16	-0.21	0.02	-0.20
6	-40	0.38	69	-0.22	-0.22	-0.01	-0.23
7	-80	0.36	69	-0.42	-0.20	0.00	-0.20
8	-40	0.36	69	-0.21	-0.26	0.00	-0.26
9	-80	0.37	90	-0.33	-0.21	0.08	-0.13
10	-40	0.36	95	-0.15	-0.21	-0.04	-0.26
11	-40	0.36	96	-0.15	-0.19	0.04	-0.14
12	-20	0.36	93	-0.08	-0.23	0.04	-0.18
13	-20	0.36	79	-0.09	-0.30	0.01	-0.29
14	-20	0.35	94	-0.08	-0.21	0.07	-0.14
15	-20	0.37	95	-0.08	-0.20	0.00	-0.20
16	-120	0.37	94	-0.47	-0.22	0.06	-0.16
17	-120	0.37	92	-0.48	-0.21	-0.01	-0.23
18	-160	0.37	69	-0.86	-0.31	-0.07	-0.38
19	-160	0.37	96	-0.62	-0.21	0.06	-0.16
20	-160	0.37	93	-0.63	-0.25	-0.05	-0.29

Table I.2: The estimated downward fluxes (in each cycle) using the peak migration and soil water balance methods under the regime of equal upward and downward flows (column 1).

Cycle	Downward flow						
	Peak migration method			Soil water balance method			
	peak movement (mm)	Aver. soil moisture ( $\text{m}^3 \text{ m}^{-3}$ )	Time (h)	Flux ( $\text{mm h}^{-1}$ )	Rain rate ( $\text{mm h}^{-1}$ )	Storage change ( $\text{mm h}^{-1}$ )	Flux ( $\text{mm h}^{-1}$ )
1	40	0.37	1.5	9.8	14.7	-2.8	11.9
2	120	0.37	1.5	29.9	14.7	1.2	15.8
3	40	0.36	1.5	9.7	14.7	-0.6	14.0
4	40	0.37	1.5	9.9	14.7	3.4	18.1
5	40	0.37	1.5	9.8	14.7	-0.3	14.4
6	80	0.35	1.5	18.8	14.7	-3.8	10.8
7	80	0.36	1.5	19.3	14.7	-4.6	10.0
8	80	0.36	1.5	19.1	14.7	-1.0	13.6
9	80	0.37	1.5	19.5	14.7	-1.6	13.1
10	40	0.37	1.5	9.9	14.7	3.3	17.9
11	40	0.35	1.5	9.4	14.7	-4.2	10.4
12	20	0.36	1.5	4.8	14.7	-0.7	14.0
13	20	0.35	1.5	4.6	14.7	-3.6	11.0
14	20	0.36	1.5	4.8	14.7	0.1	14.7
15	140	0.36	1.5	34.0	14.7	-0.3	14.4
16	120	0.36	1.5	29.0	14.7	-2.8	11.8
17	160	0.37	1.5	39.4	14.7	1.5	16.1
18	160	0.36	1.5	38.6	14.7	-2.5	12.1
19	160	0.37	1.5	39.4	14.7	1.0	15.7
20	160	0.36	1.5	38.6	14.7	0.0	14.7

Table I.3: The estimated upward fluxes (in each cycle) using the peak migration and soil water balance methods under the regime of downward flow greater than upward flow (column 2).

Cycle	<b>Upward flow</b>							
	<b>Peak migration method</b>				<b>Soil water balance method</b>			
	Peak movement (mm)	Aver. soil Moisture ( $\text{m}^3 \text{ m}^{-3}$ )	Time (h)	Flux ( $\text{mm h}^{-1}$ )	Evapo. Rate ( $\text{mm h}^{-1}$ )	Rate of storage change ( $\text{mm h}^{-1}$ )	Flux ( $\text{mm h}^{-1}$ )	
1	-80	0.37	67	-0.4	-0.27	0.04	-0.23	
2	-60	0.36	69	-0.3	-0.26	-0.02	-0.28	
3	-60	0.37	71	-0.3	-0.27	-0.11	-0.38	
4	-60	0.37	69	-0.3	-0.24	0.04	-0.20	
5	-80	0.37	72	-0.4	-0.23	0.13	-0.11	
6	-80	0.36	76	-0.4	-0.20	-0.05	-0.24	
7	0	0.36	69	0.0	-0.19	0.05	-0.13	
8	-40	0.37	92	-0.2	-0.17	0.00	-0.17	
9	-100	0.37	70	-0.5	-0.20	0.05	-0.16	
10	0	0.38	70	0.0	-0.20	-0.06	-0.26	
11	0	0.36	68	0.0	-0.20	0.04	-0.16	
12	0	0.36	71	0.0	-0.20	0.02	-0.17	
13	0	0.36	66	0.0	-0.22	-0.01	-0.23	
14	0	0.36	47	0.0	-0.36	0.26	-0.10	
15	0	0.35	72	0.0	-0.23	-0.04	-0.27	
16	0	0.36	81	0.0	-0.22	0.09	-0.12	

Table I.4: The estimated downward fluxes (in each cycle) using the peak migration and soil water balance methods under the regime of downward flow greater than upward flow (column 2).

Cycle	Downward flow						
	Peak migration method			Soil water balance method			
	Peak movement (mm)	Aver. soil moisture ( $\text{m}^3 \text{ m}^{-3}$ )	Time (h)	Flux ( $\text{mm h}^{-1}$ )	Evapo. rate ( $\text{mm h}^{-1}$ )	Rate of storage change ( $\text{mm h}^{-1}$ )	Flux ( $\text{mm h}^{-1}$ )
1	80	0.37	1.5	19.6	14.7	-1.5	13.1
2	100	0.36	1.5	24.3	14.7	-1.2	13.5
3	60	0.37	1.5	14.6	14.7	2.8	17.5
4	60	0.36	1.5	14.5	14.7	1.9	16.6
5	120	0.36	1.5	29.0	14.7	-5.4	9.3
6	100	0.36	1.5	24.3	14.7	-1.3	13.4
7	80	0.37	1.5	19.6	14.7	0.3	15.0
8	40	0.37	1.5	9.8	14.7	-0.7	14.0
9	100	0.37	1.5	24.5	14.7	-2.1	12.6
10	100	0.37	1.5	24.5	14.7	-1.0	13.6
11	0	0.36	1.5	0.0	14.7	0.4	15.0
12	0	0.35	1.5	0.0	14.7	-6.6	8.1
13	0	0.38	1.5	0.0	14.7	-0.1	14.6
14	160	0.35	1.5	36.9	14.7	-4.8	9.8
15	0	0.36	1.5	0.0	14.7	0.0	14.7
16	40	0.36	1.5	9.7	14.7	2.3	17.0

Table I.5: The estimated upward fluxes (in each cycle) using the peak migration and soil water balance methods under the regime of upward flow greater than downward flow (column 3).

Cycle	Upward flow						
	Peak migration method			Soil water balance method			
	Peak movement (mm)	Aver. soil moisture ( $\text{m}^3 \text{ m}^{-3}$ )	Time (h)	Flux ( $\text{mm h}^{-1}$ )	Evapo. rate ( $\text{mm h}^{-1}$ )	Rate of storage change ( $\text{mm h}^{-1}$ )	Flux ( $\text{mm h}^{-1}$ )
1	-80	0.36	72	-0.4	-0.2	-0.1	-0.3
2	-40	0.35	72	-0.2	-0.3	0.0	-0.3
3	-40	0.36	67	-0.2	-0.3	0.2	-0.1
4	-40	0.36	68	-0.2	-0.3	0.0	-0.3
5	-40	0.37	69	-0.2	-0.3	0.1	-0.3
6	-40	0.36	70	-0.2	-0.3	0.0	-0.2
7	-20	0.36	93	-0.1	-0.2	0.0	-0.2
8	-40	0.36	96	-0.2	-0.2	0.0	-0.2
9	-80	0.37	69	-0.4	-0.4	0.1	-0.3
10	-40	0.35	90	-0.2	-0.3	0.0	-0.3
11	-60	0.36	71	-0.3	-0.3	0.1	-0.3
12	-80	0.36	93	-0.3	-0.2	0.0	-0.2
13	-100	0.36	94	-0.4	-0.3	0.0	-0.2
14	-20	0.36	96	-0.1	-0.3	0.0	-0.2
15	0	0.38	117	0.0	-0.2	0.0	-0.2
16	-60	0.37	115	-0.2	-0.3	0.0	-0.2
17	-60	0.37	93	-0.2	-0.3	0.0	-0.3
18	0	0.38	119	0.0	-0.2	0.0	-0.2
19	-200	0.37	115	-0.6	-0.3	0.0	-0.2
20	-40	0.36	70	-0.2	-0.4	0.0	-0.5

Table I.6: The estimated downward fluxes (in each cycle) using the peak migration and soil water balance methods under the regime of upward flow greater than downward flow (column 3).

Cycle	Downward flow							
	Peak migration method				Soil water balance method			
	Peak movement (mm)	Aver. soil moisture ( $\text{m}^3 \text{ m}^{-3}$ )	Time (h)	Flux ( $\text{mm h}^{-1}$ )	Rain rate ( $\text{mm h}^{-1}$ )	Rate of storage change ( $\text{mm h}^{-1}$ )	Flux ( $\text{mm h}^{-1}$ )	
1	40	0.37	1	14.9	14.7	11.2	25.9	
2	80	0.36	1	28.4	14.7	-3.2	11.5	
3	40	0.36	1	14.5	14.7	-10.3	4.4	
4	40	0.35	1	14.2	14.7	1.5	16.2	
5	40	0.36	1	14.5	14.7	-2.0	12.6	
6	40	0.36	1	14.5	14.7	-6.1	8.6	
7	20	0.36	1	7.2	14.7	-1.1	13.6	
8	40	0.36	1	14.5	14.7	-0.9	13.7	
9	40	0.36	1	14.5	14.7	-1.3	13.3	
10	40	0.36	1	14.5	14.7	1.8	16.5	
11	40	0.36	1	14.5	14.7	-3.4	11.3	
12	40	0.36	1	14.5	14.7	-1.0	13.6	
13	60	0.36	1	21.7	14.7	1.8	16.5	
14	0	0.36	1	0.0	14.7	-6.1	8.6	
15	0	0.38	1	0.0	14.7	1.1	15.8	
16	0	0.38	1	0.0	14.7	-3.0	11.7	
17	0	0.36	1	0.0	14.7	-2.4	12.3	
18	0	0.38	1	0.0	14.7	-0.2	14.5	
19	0	0.38	1	0.0	14.7	-10.2	4.4	
20	0	0.36	1	0.0	14.7	1.6	16.2	